Technische Universität München

Wissenschaftszentrum Weihenstephan für Ernährung, Landnutzung und Umwelt

Experimentelle Radioonkologie und Strahlentherapie

The effect of heat shock factor 1 (HSF-1) and heat shock proteins Hsp70 and Hsp27 on radiosensitivity and immunogenicity

Annett Kühnel

Vollständiger Abdruck der von der Fakultät Wissenschaftszentrum Weihenstephan für Ernährung, Landnutzung und Umwelt der Technischen Universität München zur Erlangung des akademischen Grades eines

Doktors der Naturwissenschaften

genehmigten Dissertation.

Vorsitzender: Prof. Dr. Johann J. Hauner

Prüfer der Dissertation: 1. Prof. Dr. Gabriele Multhoff

2. Prof. Dr. Agnes Görlach

3. Prof. Dr. Johannes Buchner

Die Dissertation wurde am 12. Mai 2016 bei der Technischen Universität München eingereicht und durch die Fakultät Wissenschaftszentrum Weihenstephan für Ernährung, Landnutzung und Umwelt am 6. Juli 2016 angenommen.

TABLE OF CONTENTS

This cumulative thesis is based on the following publications that refer to the role of heat shock response in radiosensitivity and immunogenicity of tumor cells. Original publications are included in the appendix.

A) Murakami N*, **Kühnel A***, Schmid TE*, Ilicic K, Stangl S, Braun IS, Gehrmann M, Molls M, Itami J, Multhoff G. Role of membrane Hsp70 in radiation sensitivity of tumor cells. Radiation Oncology 2015
    Ref. [1]

B) Schilling D*, **Kühnel A***, Tetzlaff F, Konrad S, Multhoff G. NZ28-induced inhibition of HSF1, SP1 and NF-kB triggers the loss of the NK cell activating ligands MICA/B on tumor cells. Cancer Immunology, Immunotherapy 2015
    Ref. [2]

C) Schilling D, **Kühnel A**, Konrad S, Tetzlaff F, Bayer C, Yaglom J, Multhoff G. Sensitizing tumor cells to radiation by targeting the heat shock response. Cancer Letters 2015
    Ref. [3]

*Authors contributed equally to this work

SUMMARY

Heat shock factor 1 (HSF-1) is a powerful, multifaceted modifier of carcinogenesis and cancer progression. HSF-1 activates the heat shock response following stress and is frequently upregulated in many tumor cell types already under physiological conditions. As HSF-1 is a key transcription factor for heat shock protein 70 (Hsp70) and 27 (Hsp27), protein levels of these HSPs are increased in numerous tumor cell types. Elevated HSP levels contribute to a malignant tumor phenotype and mediate resistance to chemo- and radiotherapy.

Apart from the blockage of HSF-1, the inhibition of Hsp90 is considered as a promising concept to overcome radioresistance. However, most Hsp90 inhibitors induce the release of HSF-1 from the Hsp90 complex and therefore HSF-1 becomes activated. Active HSF-1 induces the transcription of Hsp70 and Hsp27 that are known to promote tumor cell survival by interfering with anti-apoptotic pathways.

A dual targeting of the heat shock response with NZ28 and Hsp90 with NVP-AUY922 potentiates the radiation sensitivity of tumor cells that are otherwise resistant to ionizing radiation. NZ28 is known to interfere with the heat shock response by inhibiting not only HSF-1 but also several other transcription factors. Therefore, I wanted to study the combined effects of a specific HSF-1 and Hsp90 inhibition on the sensitivity of tumor cells to ionizing irradiation.

In addition to its cytoprotective properties when located intracellular, Hsp70 is also present on the plasma membrane (mHsp70) of many different tumor cell types. Membrane-bound Hsp70 exerts a dual function as it also mediates protection against ionizing irradiation but also plays a role in NK (natural killer) cell-mediated anti-cancer immunity, *in vitro and in vivo*. Besides Hsp70, MICA and B (major histocompatibility class I chain-related proteins A and B) are also important recognition structures (ligands) on tumor cells for activated NK cells.

As HSF-1 is not only known to regulate Hsp27 and Hsp70, but also the MICA/B expression, the effects of a specific HSF-1 knockdown were analyzed with respect to radiation sensitivity and NK cell-mediated tumor cell killing in two different lung carcinoma cell lines (H1339, EPLC-272H).

The depletion of HSF-1 resulted in a strong reduction of cytosolic Hsp70 levels, whereas the density of membrane-bound Hsp70 remained unchanged. Since mHsp70 also is involved in mediating radioresistance, a knockdown of HSF-1 alone was unable to increase radiosensitivity in H1339 and EPLC-272H cancer cell lines. Due to an HSF-1-mediated downregulation of MICB on the membrane of H1339 cells, NK cell-mediated lysis of these tumor cells was reduced. In contrast, the combined inhibition of HSF-1 and Hsp90 resulted in an increased radiosensitivity of H1339 cells. With respect to EPLC-272H ctrl and EPLC-272H HSF-1 knockdown sublines a combined treatment regimen did not induce an increased radiosensitivity. This finding might be due to the high basal Hsp27 levels in EPLC-272H cells which were not affected by an HSF-1

knockdown. Surprisingly, an Hsp27 knockdown promotes the transition from G2 to M phase after ionizing irradiation. A shorter G2 phase in which the DNA damage repair occurs presumably increases the number of chromosomal aberrations. Further studies are ongoing to fully understand the role of Hsp27 in DNA damage/cell cycle signaling pathways.

ZUSAMMENFASSUNG

Hitzeschockproteine (HSPs), auch Stressproteine genannt, wie z.B. Hsp90, Hsp70 und Hsp27 sowie deren Transkriptionsfaktor Hitzeschock Faktor 1 (HSF-1) können die Tumorprogression und die Strahlenresistenz auf vielfältige Weise unterstützen. Als Haupttranskriptionsfaktor für Hsp27 und Hsp70 aktiviert der HSF-1 die Stressantwort sowohl in Normal- als auch in Tumorzellen nach Stresseinwirkung (z.B. erhöhte Temperatur, Strahlentherapie, Toxine/Chemotherapeutika etc.). Im Gegensatz zu Normalzellen ist die Expression des HSF-1 in vielen Tumorzellarten bereits unter physiologischen Bedingungen hochreguliert. Aus diesem Grund ist die Expression der Stressproteine Hsp70 und Hsp27 in Tumorzellen unterschiedlicher Entitäten häufig ebenfalls erhöht. Ein hoher intrazellulärer HSP Gehalt trägt zu einem malignen Phänotyp des Tumors bei und kann außerdem Resistenzmechanismen gegen Chemo- und Strahlentherapie aktivieren, indem apoptotische Signaltransduktionswege gehemmt werden.

Neben Hsp70 und Hsp27 spielt auch Hsp90 eine wichtige Rolle in der Tumorgenese. In jüngster Zeit gilt die Hemmung von Hsp90 als ein vielversprechendes Konzept zur Erhöhung der Strahlenempfindlichkeit. Hsp90 wird in vielen Tumorzellarten ebenfalls vermehrt produziert und dient der Stabilisierung onkogener Zielproteine und den entsprechenden Signalwegen. Eine Inhibition von Hsp90 setzt jedoch HSF-1 aus dem Komplex mit Hsp90 frei und fördert somit dessen Aktivierung. Der freie aktivierte HSF-1 induziert daraufhin die Expression der anti-apoptotisch wirkenden Hitzeschockproteine Hsp70 und Hsp27.

Die simultane Inhibition der Stressantwort durch NZ28 und von Hsp90 durch NVP-AUY922 konnte die Strahlensensitivität in Tumorzellen, die bisher als radioresistent galten, signifikant erhöhen. NZ28 hemmt allerdings die Funktion von verschiedenen anderen Transkriptionsfaktoren und ist somit kein spezifischer Inhibitor für HSF-1. Deshalb wurden in der vorliegenden Arbeit die Effekte einer gezielten Herabregulation von HSF-1 untersucht.

Hsp70 wird nicht nur im Zellinneren, sondern auch auf der Membran von Tumorzellen exprimiert und dient dem Schutz der Zellen vor Bestrahlung. Neben dieser Funktion agiert Membran-gebundenes Hsp70 auch als Tumor-spezifische Zielstruktur für aktivierte NK (Natürliche Killer) Zellen. Neben Hsp70 fungieren auch MICA und MICB (major histocompatibility class I chain-related proteins A and B) auf der Oberfläche von Tumorzellen als wichtige NK Zell-spezifische Liganden.

Da der HSF-1 nicht nur die Expression von Hsp27 und Hsp70, sondern auch von MICA und MICB induziert, wurde von mir der Effekt eines HSF-1 Knockdown auf die intrazelluläre und Membran-Expression von Hsp27, Hsp70 und MICA/B in Bezug auf Radiosensitivität und die NK Zell-vermittelte Lyse von H1339 und EPLC-272H Lungenkrebszelllinien untersucht.

Ergebnisse: Die Herabregulation von HSF-1 führt zu einer starken Reduktion des zytosolischen Hsp70 in beiden Tumorzelltypen, beeinflusste jedoch nicht den Membranstatus von Hsp70. Ein alleiniger HSF-1 knockdown führte daher nicht zu der gewünschten Radiosensitivierung in den beiden Tumorzelllinien. Eine HSF-1 vermittelte Herabregulation von MICB auf der Zelloberfläche von H1339 Zellen führte überdies zu einer reduzierten NK Zell-vermittelten Tumorzelllyse von H1339 Zellen. Lediglich eine kombinierte Inhibition von HSF-1 und Hsp90 konnte die Radiosensitivität von H1339 Zellen signifikant erhöhen. Im Gegensatz zu H1339 Zellen konnten EPLC-272H Zellen durch eine Kombinationsbehandlung mit Hsp90 Inhibitor und HSF-1 Knockdown nicht strahlenempfindlicher gemacht werden. Ein Grund dafür könnte die hohe basale Expression von Hsp27 sein, die durch eine Herabregulation von HSF-1 nicht signifikant erniedrigt werden konnte.

Allerdings beschleunigt die Eliminierung von Hsp27 nach Bestrahlung den Übergang der Zellen von der G2 Phase in die Mitosephase. Diese Erniedrigung der G2 Phase, in der normalerweise die DNA Reparatur erfolgt, könnte dazu führen, dass Zellen mit einer erhöhten Anzahl an chromosomalen Aberrationen in den Zellzyklus gehen.

Weitere Untersuchungen sind derzeit in Bearbeitung, um die molekularen Mechanismen aufzuklären wie Hsp27 in die DNA Reparatur bzw. den Zellzyklus eingreift.

I. INTRODUCTION

Lung cancer

Lung cancer is one of the most common diagnosed tumors and a leading cause of cancer-related death in males and females worldwide [4, 5]. Lung cancers are classified as either small cell lung cancer (SCLC, 15%) or non-small cell lung cancer (NSCLC, 85%) [6].

Despite novel therapeutic concepts the 5-year survival rate of late stage tumor diseases remains poor with about 15% [7, 8]. Radiotherapy plays a central role in the therapy of many solid tumors, including lung cancer, either as a single treatment modality or in combination with surgery or systemic chemotherapy. However, radio- and chemoresistance of pulmonary tumor cells is a major problem that limits the therapeutic outcome. Therefore, there is a high medical need for well-tolerated new therapeutic compounds that significantly improve radiosensitivity of lung cancer cells. In addition, a better understanding of the biological mechanisms which are involved in radiation resistance of tumor cells might result in the development of novel therapeutic concepts.

Heat shock response and Hsp90 inhibition

Heat shock factor 1 (HSF-1) is a ubiquitously expressed transcription factor that plays a fundamental role in tumor biology (e.g. malignant transformation, carcinogenesis, and metastasis) [9-12]. As a key transcription factor of heat shock proteins (HSPs), heat shock factor 1 activates the heat shock response in normal and tumor cells following stress [13-15]. In contrast to normal cells, HSF-1 is frequently upregulated in human cancer cells already under physiological conditions and thus the protein levels of Hsp27, Hsp70 and Hsp90 are increased in many tumor types [16-18], including lung carcinoma. Elevated HSP levels contribute to a malignant tumor phenotype and mediate resistance to chemo- and radiotherapy by inhibiting apoptotic signaling pathways [17, 19, 20].

The inhibition of Hsp90 is also considered as a promising concept to improve radiotherapy [21-25]. Previous studies have shown that Hsp90 inhibition enhances the radiosensitivity of different human tumor entities [26-33] although the exact molecular mechanisms of the interaction of irradiation and Hsp90 inhibition are not fully understood. However, many studies have shown that inhibition of Hsp90 leads to the degradation of several different oncogenic client proteins that in turn results in an inactivation of their corresponding oncogenic pathways [22-24, 34, 35].

The naturally occurring Hsp90 inhibitor geldanamycin and its derivates 17-AAG and 17-DMAG were shown to elicit radiosensitizing effects [26, 27, 29, 31, 36-38], but these Hsp90 inhibitors have several limitations for clinical practice because of their poor water solubility, bad biodistribution and hepatotoxicity [34, 39-41]. These results initiated large research projects with

the aim to design small synthetic Hsp90 inhibitors with improved bioavailability and lower toxicity. The isoxazole resorcinol NVP-AUY922 meets these requirements and shows good pharmaceutical and pharmacological properties referring to the well-tolerable toxicity against different tumor cell types *in vitro* and *in vivo* [34, 42].

It was shown that the Hsp90 inhibitor NVP-AUY922 either alone or in combination with radiation affects cell cycle, apoptosis and DNA repair mechanisms [43-45] and thus might increase radiosensitivity of tumor cells [25, 46].

However, NVP-AUY922 as well as most Hsp90 inhibitors induce the release of HSF-1 from the Hsp90 complex. As a result, HSF-1 trimerizes, translocates from the cytoplasm to the nucleus, gets hyperphosphorylated and binds to the heat shock elements (HSE) in *hsp* promoters, and thereby induces the transcription of Hsp70 and Hsp27 (Fig.1) [13-15, 47-53]. Hsp70 and Hsp27 are anti-apoptotic molecules that promote tumor cell survival. Furthermore, Hsp70 is also present on the plasma membrane (mHsp70) of many different tumor types [54-56] where it mediates protection against ionizing irradiation [1, 57].

Herein, I aimed to study the effects of a combined HSF-1 knockdown (HSF-1 k.d.) and Hsp90 inhibition on the expression of different HSPs, and on radiosensitivity of different lung cancer cell lines.

NK cell cytotoxicity

Evidence is accumulating that the host's immune system is an important factor that determines the outcome of different cancer therapies such as radio- and chemotherapy [58].

Natural killer (NK) cells that belong to the innate immune system are the first line of defense to fight cancer and infectious diseases. NK cells have the ability to kill their target cells without prior antigen-specific immune stimulation. The cytolytic activity of NK cells is regulated by a fine balance of activating and inhibitory NK cell receptors. Among others, the C-type lectin natural killer group 2D receptor (NKG2D) acts as an activating receptor which recognizes the major histocompatibility class I chain-related proteins A and B (MICA/B). An enhanced sensitivity of tumor cells to NK cell-mediated lysis has been attributed to an increased membrane expression density of the NKG2D ligands MICA and MICB [59-62]. Vice versa, a reduced MICA/B membrane expression on tumor cells impairs the recognition by NK cells and promotes tumor immune escape [63]. While absent on most normal tissues, MICA/B is expressed on the cell surface of various tumor cells of different entities.

Membrane-bound Hsp70 (mHsp70) also plays a role in NK cell-mediated anti-cancer immune response [64-66]. Our group has demonstrated that the pro-inflammatory IL-2 in combination with the Hsp70-derived peptide TKD increases the cytotoxicity of NK cells against Hsp70-membrane

positive tumors *in vitro* and *in vivo*. In detail, the transfer of IL-2/TKD activated human NK cells into xenograft tumor-bearing SCID/beige mice, lacking functional T, B, and NK cells, reduced tumor weight, delayed metastasis and prolonged their overall survival [67].

HSF-1 not only up-regulates the transcription of HSPs but also increases the transcription of MICA and MICB genes (Fig. 1) [68]. In the promoter regions of MICA and MICB, heat shock elements (HSE) which are similar to those of the *hsp* genes have been found [69].

As Hsp70 and MICA/B on tumor cells are important recognition structures (ligands) for activated NK cells, I was interested to analyze the effects of an HSF-1 knockdown on the membrane and intracellular expression of Hsp70 and MICA/B and its consequences on NK cell-mediated lysis in human lung cancer cell lines.
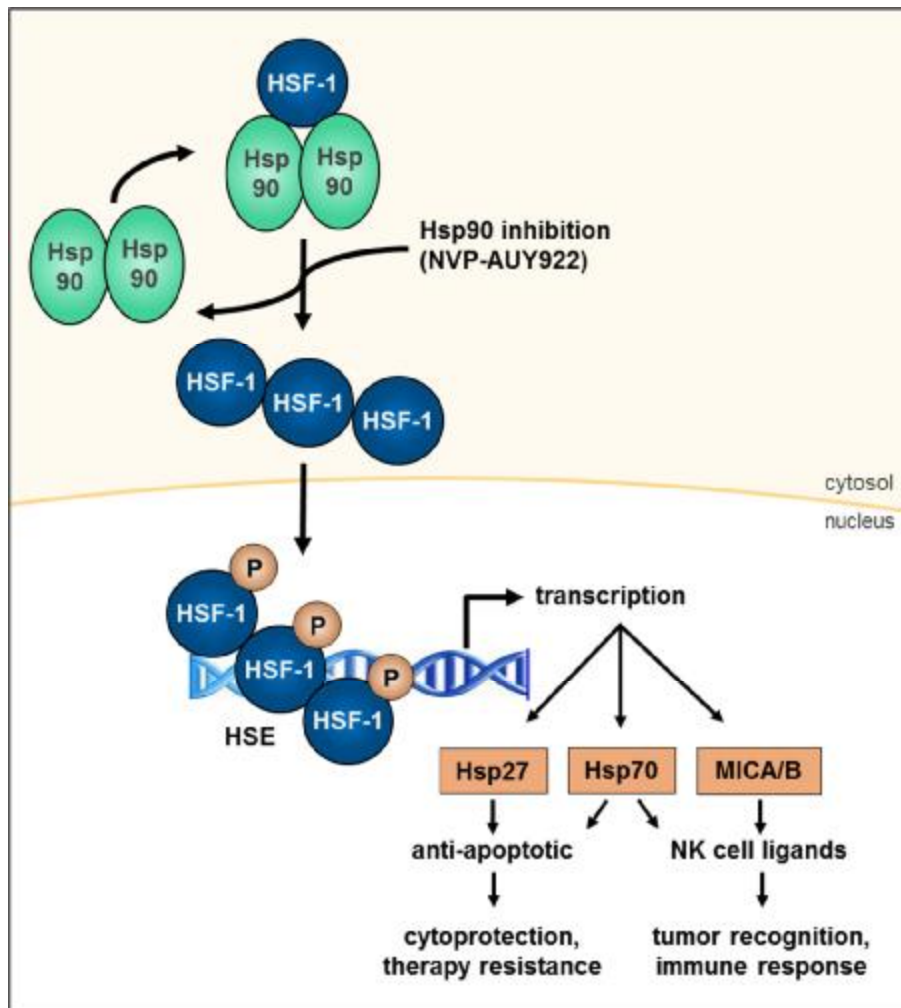
Fig.1 Diagram of HSF-1 activation and induction of HSPs and MICA/B after Hsp90 inhibition (adapted from Trepel et al. [50])

II. AIMS

In my thesis, I aimed to study the effects of an HSF-1 knockdown on the human lung cancer cell lines H1339 and EPLC-272H with respect to:

1. Hsp90 inhibition-mediated induction of the anti-apoptotic molecules Hsp70 and Hsp27 and radiosensitivity.
2. the expression of the NK cell ligands Hsp70 and MICA/B with regard to NK cell-mediated tumor cell killing.

III. MATERIAL AND METHODS

Reagents and treatment

10 mM stock solution of NVP-AUY922 (Novartis) was prepared in 100 % DMSO. Dilutions were performed in PBS. A vehicle control with the respective amount of DMSO diluted in PBS was used in all experiments to exclude an effect of DMSO itself. If not indicated otherwise, cells were incubated for 24 h with NVP-AUY922.

Cells and cell culture

The human lung cancer cell lines H1339 (SCLC) and EPLC-272H (NSCLC) were cultured as described previously [25, 70]. The authenticity of the tumor cell lines was tested by the DSMZ (German Collection of Microorganisms and Cell Cultures). Cells were routinely checked and determined as negative for mycoplasma contamination.

Retroviral vectors and transfection

For knockdown of HSF-1 in the lung carcinoma cell lines H1339 and EPLC-272H HSF-1 RNAi-Ready pSIRENRetroQ vectors with a puromycin resistance were used. Target sequence for HSF-1 short hairpin RNA was 5'-TATGGACTCCAACCTGGATAA-3' [71]. Retroviruses were produced by transfection of Phoenix cells with pSIREN-RetroQ/HSF-1 shRNA (HSF-1 k.d.) or pSIREN-RetroQ (ctrl) (kindly provided by J. Yaglom and M. Sherman, Boston University School of Medicine, USA) using Ca-phosphate. Tumor cells were infected with virus containing supernatants in the presence of 10 µg/ml polybrene. Selection was performed with 2 µg/ml puromycin.

For knockdown of Hsp27, pRS vectors (OriGene; control: TR30012; Hsp27 k.d.: TR320383D) with a puromycin resistance were used. Target sequence for Hsp27 short hairpin RNA was 5'-AAATCCGATGAGACTGCCGCCAAGTAAAG-3'. Stable Hsp27 knockdown cell lines were produced by transfection of tumor cells with pRS vector plasmids, either containing a non-effective 29-mer scrambled shRNA cassette (ctrl) or a gene specific shRNA cassette (Hsp27 k.d.) using Ca-phosphate.

HSF-1 and Hsp27 double knockdown cells (HSF-1/Hsp27 k.d.) were obtained by single cell cloning as both plasmids carry a puromycin resistance.

Western blot analysis and ELISA

Cells were lysed in TBST buffer as described previously [72]. The protein content in the cell lysates was determined using the BCA™ Protein Assay Kit (Pierce). On PVDF immunoblots, non-specific binding of the membranes was blocked with 5 % skim milk in PBS supplemented with 1 % Tween-

20. Proteins were detected with antibodies (4 °C, overnight) against HSF-1 (ADI-SPA-901; Enzo Life Sciences), HSF-1 phospho S326 (pHSF-1) (ab76076; abcam), Hsp70 (ADI-SPA-810; Enzo Life Sciences), Hsp27 (ADI-SPA-800; Enzo Life Sciences), Hsp27 phospho Ser82 (9709; Cell Signaling), ATM phospho Ser1981 (ab81292; abcam), MK2 phospho Thr334 (3007; Cell Signaling), Cdc2 phospho Tyr15 (9111; Cell Signaling) and β-actin (A5316; Sigma-Aldrich). Horseradish-peroxidase (HRP)-conjugated anti-rabbit/anti-mouse antibodies (Promega, W401B/W402B) were used as secondary antibodies. Immune complexes were detected using the ECL detection system (Amersham Biosciences). Blots were imaged digitally (ChemiDoc Touch Imaging System, Biorad). Total Hsp70 and Hsp27 protein amounts were verified by ELISA (R&D systems) in cell lysates following the manufacturer's recommendations.

HSE luciferase assay

In order to determine the HSF-1 transcriptional activity, cells were transfected with a heat shock element (HSE) reporter plasmid that contains a HSF-1 responsive firefly luciferase construct (Qiagen). One day after transfection, cells were treated with 100 nM NVP-AUY922 for 24 h. The luciferase activity was measured using the Dual Glo Luciferase assay system (Promega). A constitutive Renilla luciferase construct served as an internal control for normalizing transfection efficiencies, cell viability and cell numbers.

Flow cytometry of mHsp70, MICA/B

Single cell suspensions of untreated and treated H1339 and EPLC-272H sublines were collected. Cells were washed once with 10 % FCS in phosphate-buffered saline (PBS) and incubated with fluorescein isothiocyanate (FITC)-conjugated mouse monoclonal antibody specific for mHsp70 (cmHsp70.1, IgG1; multimmune GmbH, Munich, Germany), a FITC-labeled isotype matched IgG-negative control antibody (code 345815; BD Biosciences, NJ, USA), APC-conjugated MICA (clone 159227, FAB1300A, R&D Systems) and MICB antibodies (clone 236511, FAB1599A, R&D Systems) or the corresponding isotype-matched control antibody (clone 133303, IC0041A, R&D Systems) on ice in the dark for 30 min. Dead cells were stained with propidium iodide (PI), and only viable cells were analyzed on a FACSCalibur flow cytometer (BD Biosciences). Fluorescence data were plotted by using CellQuest software (Becton Dickinson, Heidelberg, Germany).

NK cell isolation

NK cells were generated of PBMCs from healthy human volunteers by a standard magnetic bead separation method (Miltenyi Biotec) using beads coupled with antibodies directed against CD3 (T cells) and CD19 (B cells). The purity of NK cells (89.9 % of lymphocytes) was determined by flow cytometry on a FACSCalibur flow cytometer (BD Biosciences) with antibodies against CD19 (#555413, BD Biosciences), CD3 (#345766, BD Biosciences) and CD56 (#345811, BD Biosciences).

NK cell cytotoxicity

NK cells were stimulated with 100 IU/ml IL-2 (Novartis) for 4 days. Activation of NK cells was checked by flow cytometry with antibodies against CD94 (#555888, BD Biosciences), NKG2D (FAB139P, R&D Systems) and CD56 (#345811, BD Biosciences). Their cytotoxic activity against tumor cells was determined either by europium or by CD107 degranulation assay.

For the europium assay, the tumor cells were labeled with BATDA (Perkin Elmer) and then co-incubated with NK cells at different ratios in a V-bottom 96-well plate in 200 µl medium. After a 4 h co-incubation period at 37 °C, 25 µl of supernatants were transferred into ELISA plates containing 200 µl europium solution (Perkin Elmer). The time-resolved fluorescence was measured using a Victor X4 plate reader (Perkin Elmer).

In the degranulation assay, the cytotoxicity of NK cells was determined by measuring the cell surface expression of the lysosomal marker, CD107a, which is associated with NK cell cytotoxicity [73]. Tumor cells were mixed with NK cells at a ratio of 1:1 in a U-bottom 96-well tissue culture plate. Anti-CD107a-FITC (#555800, BD Biosciences) or the isotype-matched control antibody (#555748, BD Biosciences) was added. After 1 h, GolgiStop™ (BD Biosciences) was added and after a co-incubation period of 3 h, the cells were stained with anti-CD3-PerCP (#345766, BD Biosciences) and anti-CD56-APC (#555518, BD Biosciences) antibodies. The CD107a expression on the CD3⁻CD56⁺ NK cell population was determined by flow cytometry on a FACSCalibur flow cytometer (BD Biosciences).

Proliferation assay

Cells were seeded in 96-well plates (4000 cells/well) and allowed to attach overnight. Cells were treated with various concentrations of NVP-AUY922 (2, 5, 10, 20, 50, 75, 100 nM) and incubated under standard conditions for 24 h and 48 h. As a control, the same volume of PBS was added. The proliferation was measured using the MTT-like colorimetric alamarBlue assay, according to the manufacturer's instructions (Biosource-Invitrogen, Germany). Briefly, alamarBlue was added, and 4 h after incubation at 37 °C, the absorption at 570 and 630 nm (reference wavelength) was

measured using an absorbance microplate reader (ELx808; BioTek, Germany). The proliferation of untreated cells incubated with PBS was set to 100 % in each experiment.

Cell death and apoptosis

Cells were stained with propidium iodide (PI) to determine cell death after treatment with NVP-AUY922. Apoptosis of the cells was assessed by FITC Active Caspase-3 Apoptosis Kit (BD Pharmingen) and Annexin V-FITC staining (Roche Diagnostics, Mannheim, Germany). Cells were collected 24 h after treatment with 100 nM NVP-AUY922 or 24 h after irradiation. The single cell suspension containing 1.5×10^5 cells were stained according to the manufacturer's instructions. Then cells were analyzed on a FACSCalibur flow cytometer (BD Biosciences).

Clonogenic assay and irradiation

To measure the radiosensitivity, clonogenic assays were performed. The cells were seeded in 12-well plates, one day later treated with NVP-AUY922 and 24 h later irradiated using the RS225A irradiation device (GulmayMedical Ltd) at a dose rate of 1 Gy/min (70 keV, 10 mA). Cells were irradiated with a single dose of 0, 2, 4 or 6 Gy, if not indicated otherwise. 1 h after irradiation the medium was exchanged by a drug-free medium. On day 7-9 after irradiation, colonies were fixed in ice cold methanol, stained with 0.1 % crystal violet and counted. All colonies with more than 50 cells were counted automatically using a Bioreader® (Bio-Sys GmbH, Karben, Germany). Survival curves were fitted to the linear quadratic model using Sigmaplot (Systat Software Inc).

Cell cycle analysis

To analyze the cell cycle distribution, cells were treated with 10 nM NVP-AUY922 for 24 h following irradiation with 6 Gy. 24 h after irradiation cells were harvested. After washing in PBS and fixation (70 % ethanol over night; -20 °C), cells were incubated in PI staining solution (PBS containing 0.1 % Triton X-100, 0.2 mg/ml RNase A, 0.02 mg/ml PI) for 1 h at room temperature and analyzed on a FACSCalibur flow cytometer (BD Biosciences). Cell cycle distribution was determined using ModFit LT (Verity Software House, Topsham, ME).

Alkaline comet assay

DNA damage was assessed using the alkaline comet assay. The protocol is based on a publication of Singh et al. [74], was modified according to the protocol of Sipinen et al. [75]. Briefly, cells were seeded into 6 cm petri dishes (4×10^5 cells) and allowed to attach overnight. Cells were treated with 10 nM NVP-AUY922 for 24 h following irradiation with 6 Gy. 24 h after irradiation, cells were harvested, resuspended (5×10^4 cells/100 µl) in cold phosphate-buffered saline (PBS)

and kept on ice until they were mixed 1:1 with 1 % low melting point agarose. The samples were subsequently casted onto standard glass slides pre-coated with 2 % normal melting point agarose and top-layered with 0.5 % low melting point agarose. Cell lysis was achieved through submerging the slides in lysis buffer (2.5 M NaCl, 100 mM Na_2EDTA, 10 mM Trizma base, and 1 % Triton X-100, pH 10) for 60 min at 4 °C. After lysis, the slides were incubated in electrophoresis buffer (300 mM NaOH and 1 mM Na_2EDTA, pH 13.2) at 4 °C for 20 min to unwind DNA and then subjected to electrophoresis at 25 V (0.8 V/cm on platform, 300 mA) for 20 min. Before staining with SYBR Gold (Invitrogen) slides were neutralized (0.4 M Trizma base, pH 7.5) 3 times for 5 min each. Comet visualization and scoring were performed with an epifluorescence microscope equipped with a charge-coupled device camera from Leica (Wetzlar, Germany) using the image analysis software Komet 6.0 (Andor, Belfast, UK). For each individual sample, 3 independent experiments were performed, and for each experiment, 100 cells were scored in a blinded assay.

Flow cytometry of γH2AX

DNA double strand breaks (DBSs) were measured by using γH2AX (phosphorylated Histone H2AX) antibody which is a marker of radiation induced DNA double strand breaks (DSBs). The single cell suspensions of untreated and treated cells were collected 24 h after irradiation using trypsin. Single cell suspensions were washed in 0.5 ml PBS and fixed with 70 % ethanol. Fixed cells were kept at -20 °C for up to two weeks before analysis. After removal of the fixative, cell pellets were resuspended in 1 ml 0.15 % Triton X-100 solution and incubated on ice with anti-phospho Histone H2AX, Alexa Fluor 488 conjugate (Novus Biologicals). The MFI (mean fluorescence intensity) of cells that bound the antibody was analyzed by flow cytometry.

Immunostaining for 53BP1 and Rad51 foci

Cells were seeded into 2-well chamber slides (Nunc, LabTek) and allowed to attach overnight. Cells were treated with 10 nM NVP-AUY922 for 24 h following irradiation with 2, 4 or 6 Gy. 4 h or 24 h after irradiation, cells were fixed in 2 % paraformaldehyde and dissolved in PBS for 15 min at room temperature. Cells were subsequently washed twice with PBS. Cell lysis was achieved through submerging the slides in lysis buffer (0.15 % Triton X-100 in PBS) for 3 x 5 min. After lysis, slides were submerged in blocking buffer (1 % BSA, 0.15 % glycine in PBS) for 3 x 10 min. Then, 53BP1 antibody (1:300 in blocking buffer; Novus) or Rad51 antibody (1:300 in blocking buffer, Merck) was applied, and slides were incubated overnight at 4 °C. Slides were subsequently washed three times for 5 min each with PBS, followed by incubation with Alexa Fluor 555 secondary antibody (1:500 in blocking buffer; Invitrogen, Carlsbad, CA, USA) overnight at 4 °C. Finally, unbound antibody was washed off with PBS (3 x 5min), and the cells were embedded in

4′,6-diamidino-2-phenylindole (DAPI)/Vectashield (Vector Laboratories, Burlingame, CA, USA) solution. Foci were counted throughout the whole nucleus.

Statistics

Statistical analysis was performed using SPSS 18.0.2 software (IBM). The Student's t-test was used to evaluate significant differences (*$p \leq 0.05$, **$p \leq 0.01$, ***$p \leq 0.001$).

Graphs represent mean values of at least 3 independent experiments ± SD (standard deviation).

IV. RESULTS

IV.1 The knockdown of HSF-1

HSF-1 knockdown reduces HSF-1 transcriptional activity and Hsp70 protein levels

HSF-1 was specifically knocked down in H1339 small cell lung carcinoma (SCLC) cells and EPLC-272H non-small lung carcinoma (NSCLC) cells by transfection with shRNA (HSF-1 k.d.). As a control, cells were transfected with an empty plasmid (ctrl). After puromycin selection the HSF-1 k.d. cells showed a drastic reduction of HSF-1 and activated phosphorylated HSF-1 (pHSF-1) as well as Hsp70 protein levels compared to empty vector control cells (Fig. 2A). In H1339 cells, Hsp27 was weakly expressed under normal conditions but strongly induced after treatment with 100 nM NVP-AUY922 for 24 h. The HSF-1 k.d. completely inhibited the NVP-AUY922-induced Hsp27 expression in H1339 cells. In contrast, in EPLC-272H cells the high basal Hsp27 expression could hardly be increased by a treatment with NVP-AUY922 or decreased by HSF-1 knockdown (Fig. 2A).
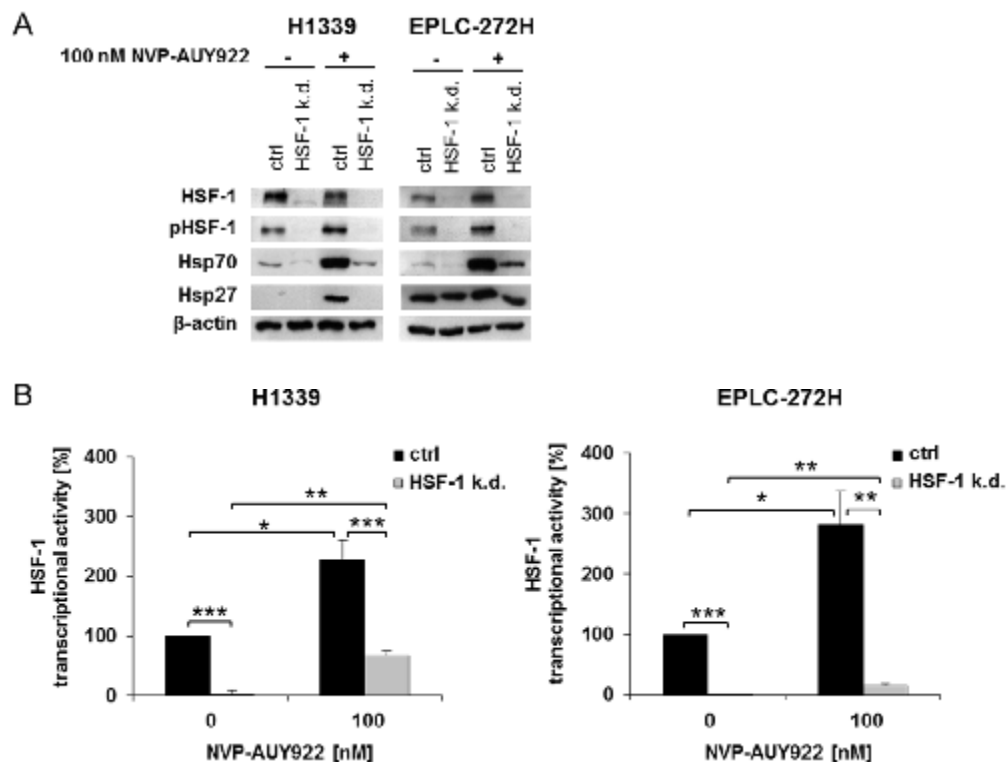

Fig. 2 A loss of HSF-1 reduces the HSP expression and HSF-1 activity

A. Representative immunoblot showing the expression of HSF-1, HSF-1 phospho S326 (pHSF-1), Hsp70, Hsp27 and β-actin in H1339 and EPLC-272H cells transfected with control (ctrl) or HSF-1 (HSF-1 k.d.) shRNA. Cells were treated with 100 nM NVP-AUY922 for 24 h. **B.** Transcriptional activity assay of ctrl and HSF-1 k.d. cells transfected with a HSF-1 responsive firefly luciferase construct. Cells were treated with 100 nM NVP-AUY922 for 24 h. Significance *p ≤ 0.05; **p ≤ 0.01; ***p ≤ 0.001.

The reduction in active pHSF-1 was associated with a loss in HSF-1 transcriptional activity in both cell lines (Fig. 2B). Treatment with the Hsp90 inhibitor NVP-AUY922 for 24 h resulted in an activation of HSF-1 in both, control and HSF-1 knockdown cells. However, the NVP-AUY922-mediated induction of HSF-1 activity was significantly lower in HSF-1 k.d. cells compared to control cells. (Fig. 2B).

In line with this finding and the Hsp70 expression levels detected by immunoblot (Fig. 2A), the intracellular Hsp70 levels in HSF-1 k.d. cells and their induction by Hsp90 inhibitor NVP-AUY922 were found to be significantly reduced compared to control cells (Fig. 3A). Hsp70 is also present on the plasma membrane (mHsp70) of many different tumor types [54-56] where it mediates protection against ionizing irradiation [1, 57] and plays a role in NK cell-mediated anti-cancer immune response, *in vitro* and *in vivo* [64-66]. Despite a drastic reduction in the cytosol of H1339 and EPLC-272H cells, the knockdown of HSF-1 did not lead to significant changes in the amount of Hsp70 positive cells or differences in the cell surface density (mean fluorescence intensity (MFI)) of Hsp70 compared to control cells (Fig. 3B, C) [1]. This is in line with previous data from our group demonstrating in an autologous tumor cell system that the density of the Hsp70 membrane expression is independent of intracellular Hsp70 levels [65]. Even after NVP-AUY922 treatment, neither the percentage of Hsp70 positive control cells nor the MFI of Hsp70 was altered.
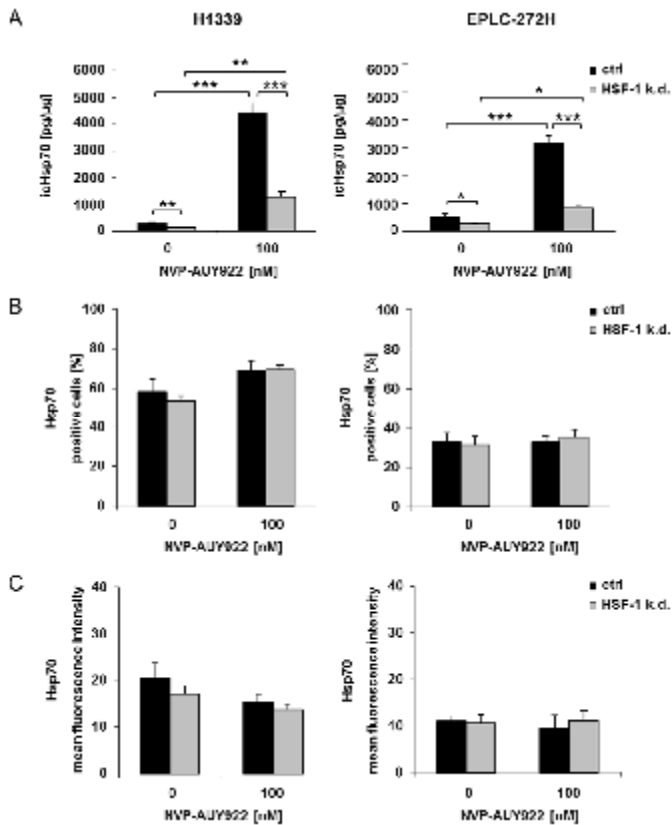

Fig. 3 Intracellular and membrane expression of Hsp70 after HSF-1 knockdown

A. ELISA of intracellular Hsp70 protein amount of H1339 and EPLC-272H ctrl and HSF-1 k.d. cells treated with 100 nM NVP-AUY922 for 24 h. Significance *p ≤ 0.05; **p ≤ 0.01; ***p ≤ 0.001.

B. Percentage of Hsp70 positive cells and **C.** mean fluorescence intensity of ctrl and HSF-1 k.d. cells treated with 100 nM NVP-AUY922 for 24 h.

HSF-1 knockdown reduces MICB and impairs the NK cell-mediated cytotoxicity against H1339 lung cancer cells

As HSF-1 also has been described to regulate the transcription of the NK cell ligands MICA and MICB [76, 77], I investigated whether a knockdown of HSF-1 alters the intracellular (ic) and/or cell surface expression of the NK cell ligands MICA and MICB on H1339 and EPLC-272H lung tumor cells and hence, affects NK cell-mediated cytotoxicity.

Intracellular and membrane expression of MICA/B was measured by ELISA and FACS, respectively. As shown in Figure 4A, the HSF-1 knockdown did not reduce intracellular levels of MICA in H1339 cells. Corresponding to that, there was no significant change in the cell surface expression of MICA (Fig. 4B, C). EPLC-272H cells were not tested for MICA expression as it is known that these cells do not express MICA on their cell surface [78].
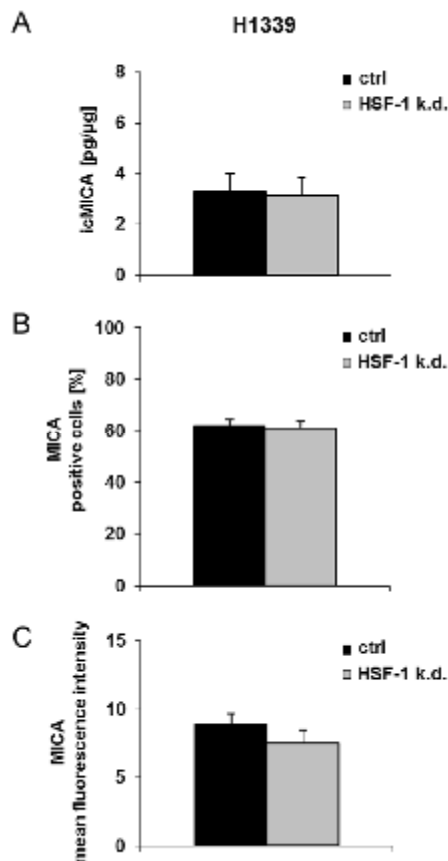

The intracellular MICB levels were significantly downregulated by HSF-1 knockdown in H1339 cells (Fig. 5A). In line with this, the MICB membrane expression of H1339 HSF-1 k.d. cells was also significantly reduced compared to control cells (Fig. 5B, C), whereas the intracellular and membrane MICB expression of EPLC-272H cells was not affected by an HSF-1 knockdown.

H1339 control and HSF-1 k.d. cells were used as target cells for IL-2-activated NK cells. A successful stimulation of purified NK cells was shown by an up-regulated cell surface density of the NK cell markers CD94, CD56 and NKG2D (Fig. 6A) [79]. The cytotoxicity of stimulated NK cells against HSF-1 knockdown cells was strongly reduced compared to control cells as demonstrated by europium (Fig. 6B) and degranulation assay (Fig. 6C).

Fig. 4 Intracellular and membrane expression of MICA after HSF-1 knockdown
A. ELISA of intracellular MICA protein amount of H1339 ctrl and HSF-1 k.d. cells. **B.** Percentage of MICA positive cells and **C.** mean fluorescence intensity of ctrl and HSF-1 k.d. cells.
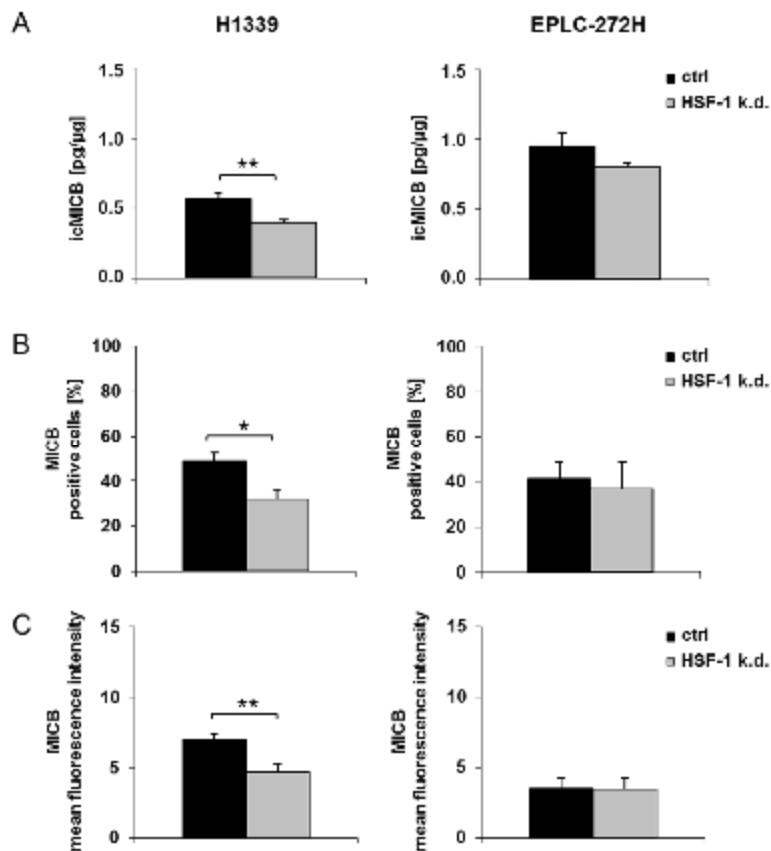
Fig. 5 Intracellular and membrane expression of MICB after HSF-1 knockdown
A. ELISA of intracellular MICB protein amount of H1339 and EPLC-272H ctrl and HSF-1 k.d. cells. Significance **p ≤ 0.01.
B. Percentage of MICB positive cells and **C.** mean fluorescence intensity of ctrl and HSF-1 k.d. cells. Significance *p ≤ 0.05; **p ≤ 0.01.

The knockdown of HSF-1 sensitizes H1339 tumor cells towards Hsp90 inhibition

Since the loss of HSF-1 has been shown to increase sensitivity to Hsp90 inhibition in certain cell types [80], I tested the sensitizing effects of an HSF-1 k.d. on H1339 and EPLC-272H lung cancer cells. Targeting HSF-1 and additional inhibition of Hsp90 for 24 h or 48 h resulted in concentration-dependent reduced proliferation rates in H1339 cells. In contrast, HSF-1 knockdown did not sensitize EPLC-272H cells to Hsp90 inhibition (Fig. 7A, B).

In line with this, the NVP-AUY922-induced cell death was significantly increased in H1339 HSF-1 k.d. cells, but not in EPLC-272H HSF-1 k.d. cells, compared to their respective controls (Fig. 8A). Next, I analyzed the induction of apoptosis after treatment with NVP-AUY922, as determined by Annexin V and Caspase-3 staining. As expected, the treatment with NVP-AUY922 induces significant higher apoptosis in H1339 HSF-1 knockdown cells compared to control cells whereas no significant changes could be detected in EPLC-272H knockdown cells compared to controls (Fig. 8B, C).
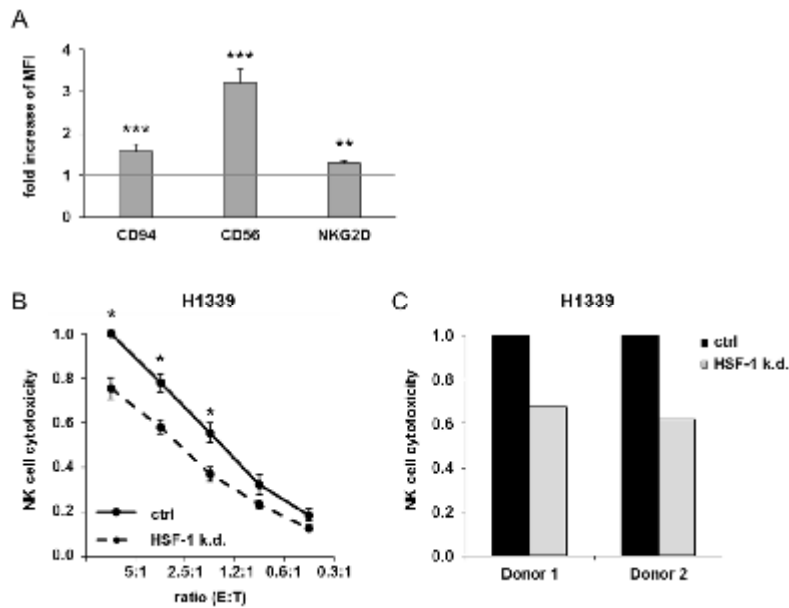
Fig. 6 Loss of HSF-1 impairs NK cell-mediated cytotoxicity

A. The expression of CD94, CD56 and NKG2D on NK cells was determined by FACS analysis. The fold increase in mean fluorescence intensity (MFI) of cell surface markers on stimulated compared to unstimulated NK cells is shown. Significance $**p \leq 0.01$; $***p \leq 0.001$.

B. NK cells were stimulated for 4 days with 100 U/ml IL-2. The cytotoxicity of IL-2-stimulated NK cells was measured after a 4-h co-incubation with H1339 tumor cells transfected with control (ctrl) or HSF-1 (HSF-1 k.d.) shRNA by europium assay. The cytotoxicity of stimulated NK cells against control tumor cells at an E:T (effector to target) ratio of 5:1 was set to one. Significant differences between control and HSF-1 knockdown cells are indicated ($*p \leq 0.05$). **C.** NK cells from two different healthy donors were stimulated for 4 days with 100 U/ml IL-2. The cytotoxicity of IL-2-stimulated NK cells was measured after a 4-h co-incubation with H1339 tumor cells transfected with control (ctrl) or HSF-1 (HSF-1 k.d.) shRNA by the CD107a degranulation assay. The relative cytotoxicity of NK cells incubated with HSF-1 k.d. cells compared to NK cells incubated with control tumor cells is shown for each NK cell donor.
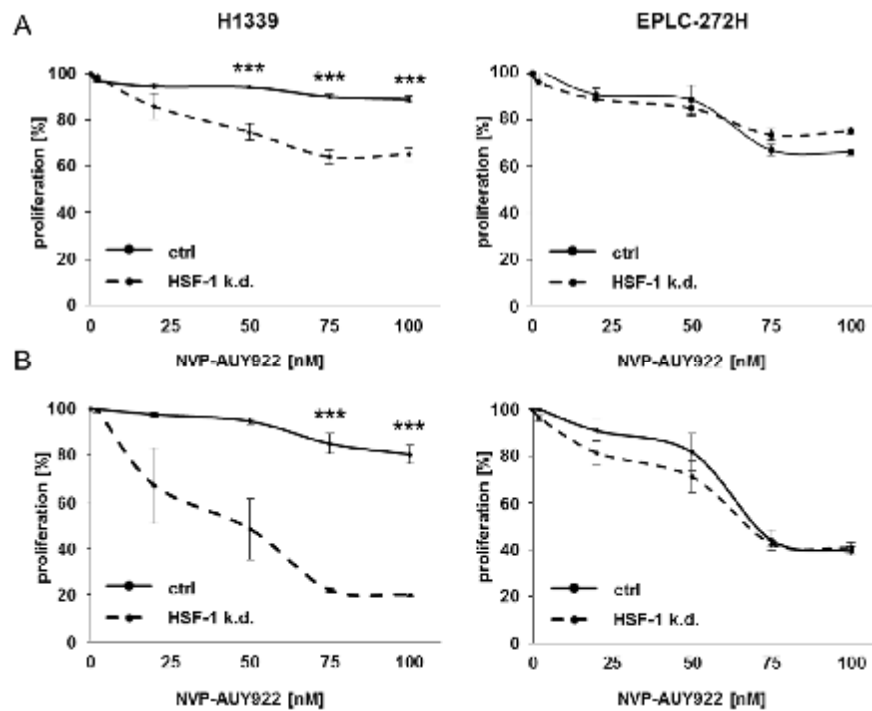

Fig. 7 H1339 HSF-1 knockdown cells are more sensitive to Hsp90 inhibition
A. Proliferation assay of H1339 and EPLC-272H ctrl and HSF-1 k.d. cells treated with 0, 20, 50, 75 and 100 nM NVP-AUY922 for 24 h and **B.** 48 h. Significance $***p \leq 0.001$.
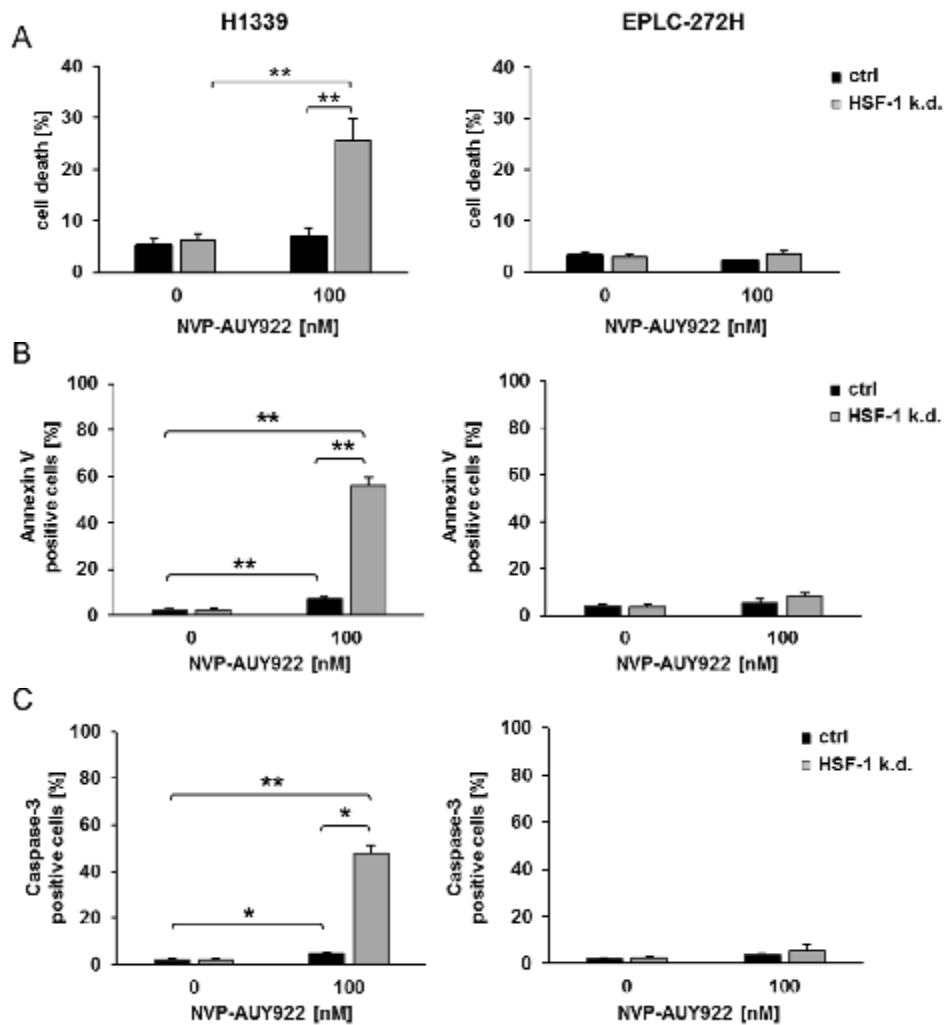
Fig. 8 Hsp90 inhibition-induced apoptosis is increases in H1339 cells after HSF-1 knockdown

A. Measurement of cell death by PI staining, **B.** apoptosis induction by Annexin V and **C.** Caspase-3 staining of H1339 and EPLC-272H ctrl and HSF-1 k.d. cells treated with 100 nM NVP-AUY922 for 24 h. Significance *p ≤ 0.05; **p ≤ 0.01.

A combined HSF-1 knockdown and Hsp90 inhibition results in radiosensitization of H1339 cells

A lack of HSF-1 alone does neither radiosensitize H1339 cells nor EPLC-272H cells as determined by clonogenic cell survival and D_{50} values (dose to reduce survival fraction to 50 %) (Fig. 9A, Tab. 1A). Even though intracellular Hsp70 is strongly reduced, membrane Hsp70 (mHsp70) levels are not affected by a HSF-1 knockdown (Fig. 3). These results indicate that not only cytosolic but also mHsp70 might have an impact on radiosensitivity [1].

Next, I studied the combined effects of a HSF-1 knockdown and Hsp90 inhibition on the radiosensitivity of H1339 and EPLC-272H cells. Low concentrations of NVP-AUY922 (1 and 2 nM)

had no effect on control cells, but significantly increased the radiosensitivity of H1339 HSF-1 knockdown cells (Fig. 9B, Tab. 1B). A higher NVP-AUY922 concentration of 5 nM also increased the radiosensitivity of H1339 control cells but the radiosensitizing effect was much more pronounced in HSF-1 k.d. cells. Surprisingly, radiosensitivity of EPLC-272H HSF-1 k.d. cells did not differ from control cells after Hsp90 inhibition.
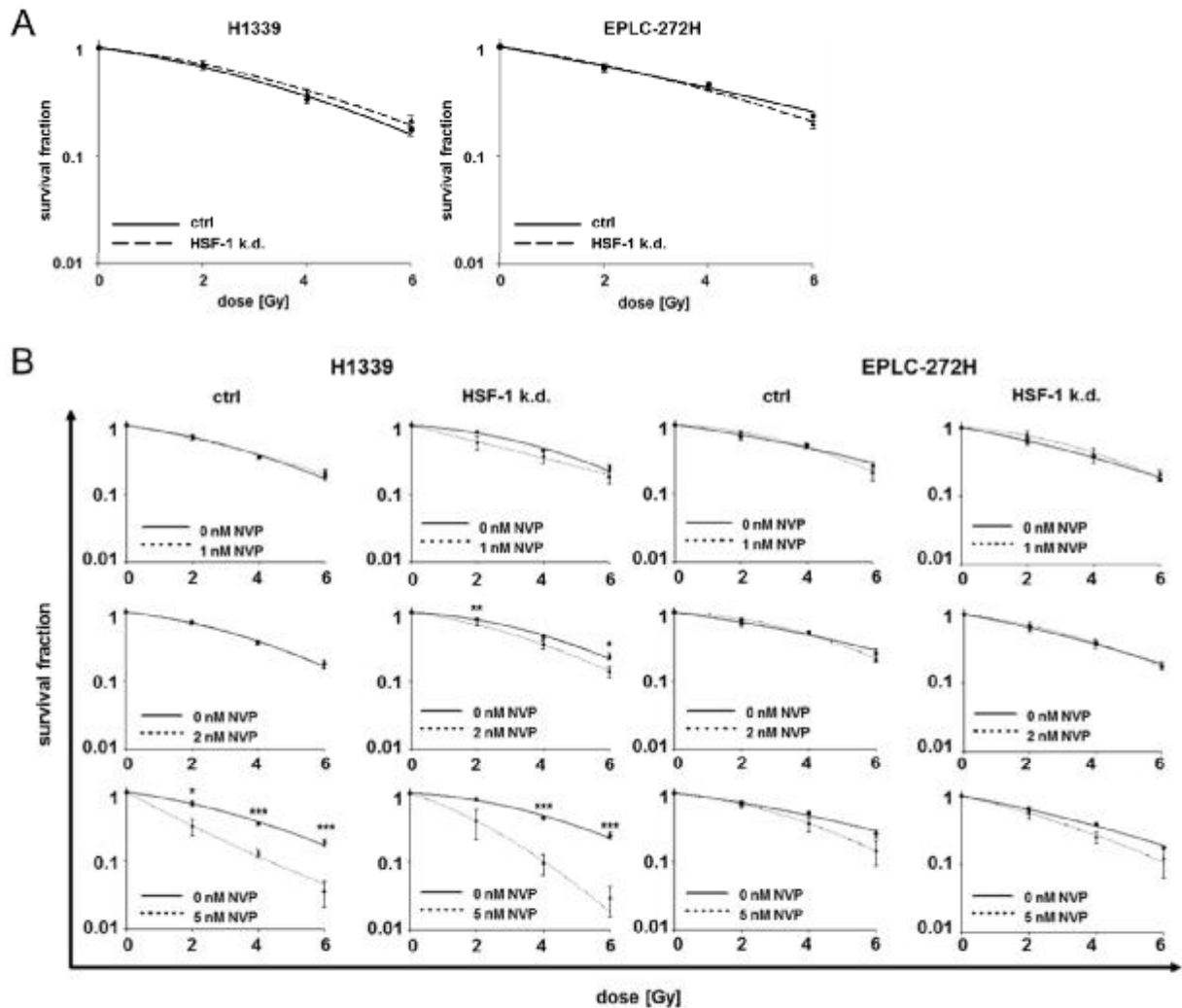
Fig. 9 Radiosensitivity after HSF-1 knockdown alone and in combination with Hsp90 inhibition

A. Colony forming assay of H1339 and EPLC-272H ctrl and HSF-1 k.d. cells after irradiation with 0, 2, 4 and 6 Gy. **B.** Colony forming assay of ctrl and HSF-1 k.d. cells. Cells were treated with 0, 1, 2 and 5 nM NVP-AUY922 for 24 h and then irradiated with 0, 2, 4 and 6 Gy. Significance *$p \leq 0.05$; **$p \leq 0.01$; ***$p \leq 0.001$.

Tab. 1 Summary of radiobiological parameters

A.

	D_{50} dosis [Gy]		SER (50%)	
	ctrl	HSF-1 k.d.	ctrl	HSF-1 k.d.
H1339	2.01	2.21	1	0.91
EPLC-272H	1.87	2.00	1	0.93

B.

NVP-AUY922 [nM]	SER (50%) H1339		SER (50%) EPLC-272H	
	ctrl	HSF-1 k.d.	ctrl	HSF-1 k.d.
0	1	1	1	1
1	1.09	**1.92**	0.61	0.63
2	0.94	**1.53**	0.60	0.85
5	**1.89**	**2.38**	0.94	1.12

Tab. 1 Summary of radiobiological parameters
A. Loss of HSF-1 has no influence on radiosensitivity of H1339 and EPLC-272H cells. D_{50}, dose to reduce survival fraction to 50 %. Sensitizing enhancement ratio (SER) $=D_{50}$(irradiation ctrl)/D_{50}(irradiation HSF-1 k.d.).
B. Radiosensitizing effect of Hsp90 inhibition is much more pronounced in H1339 HSF-1 k.d. cells compared to control cells. SER (D_{50}(irradiation)/D_{50}(irradiation + drug)) greater than 1.20 is indicative for radiosensitization (indicated in bold).
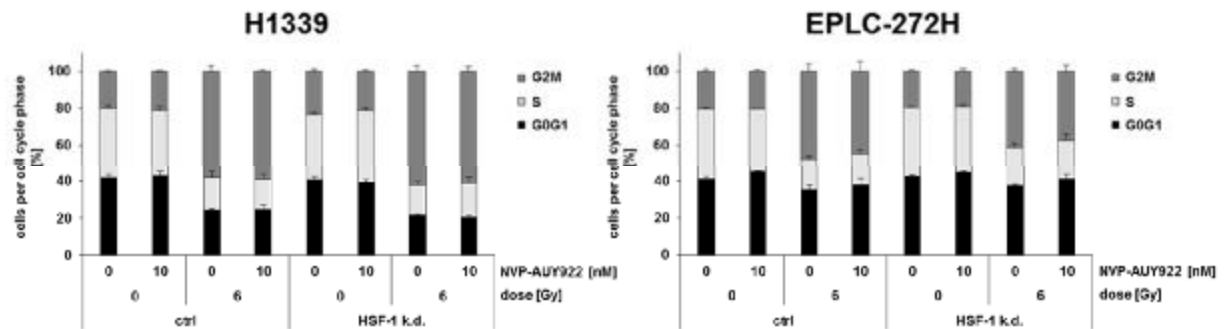

Fig. 10 HSF-1 k.d. cells show no difference in cell cycle distribution after combined Hsp90 inhibition and irradiation
H1339 and EPLC-272H ctrl and HSF-1 k.d. cells were treated with 10 nM NVP-AUY922 for 24 h and irradiated with 6 Gy. Cells were stained with PI to analyze cell cycle distribution 24 h after irradiation.
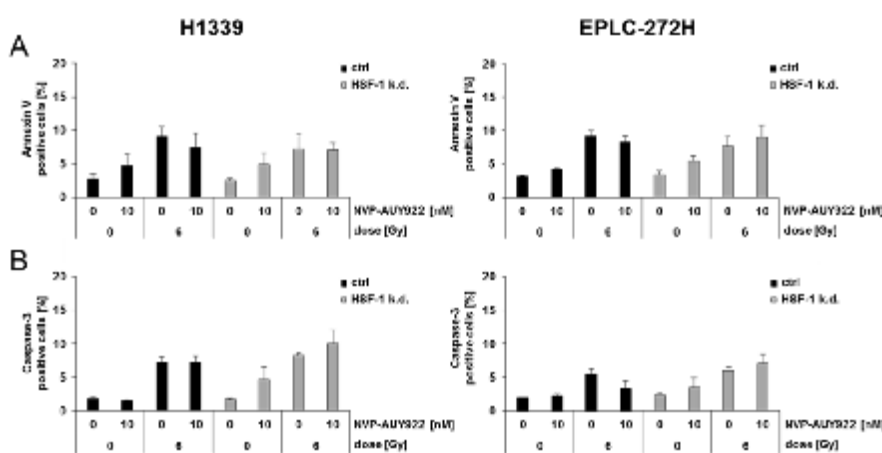

Fig. 11 HSF-1 knockdown and control cells show no difference in apoptosis induction after combined Hsp90 inhibition and irradiation
A. Measurement of apoptosis induction 24 h after irradiation by Annexin V and **B.** Caspase-3 staining of H1339 and EPLC-272H ctrl and HSF-1 k.d. cells treated with 10 nM NVP-AUY922 for 24 h following irradiation with 6 Gy.

Hsp90 inhibition and irradiation induce increased DNA damage in H1339 HSF-1 k.d. tumor cells

To identify the mechanisms underlying the radiosensitizing effect of Hsp90 inhibition in H1339 HSF-1 knockdown tumor cells, I analyzed their cell cycle phase distribution by flow cytometry. Although no radiosensitizing effects in EPLC-272H HSF-1 k.d. cells could be detected, I also examined cell cycle phase distribution in these cells to figure out whether any changes can be detected.

As seen in Figure 10, the loss of HSF-1 or Hsp90 inhibition alone had no effect on the cell cycle of both, H1339 and EPLC-272H cells. Even in HSF-1 k.d. cells an Hsp90 inhibition did not cause any changes in the cell cycle. Both, control und HSF-1 knockdown cells showed an increase in the G2/M phase 24 h after irradiation which was not further affected by a treatment with NVP-AUY922.

Next, I examined apoptosis induction in control and HSF-1 knockdown cells after Hsp90 inhibition and irradiation. As shown for both cell lines in Figure 11A and B, irradiation increased the apoptosis induction in control and HSF-1 k.d. cells to the same extent, as determined by Annexin V and Caspase-3 staining. Even in combination with Hsp90 inhibition there was no significant difference in radiation-induced apoptosis induction between control and HSF-1 k.d. cells.

To elucidate the mechanisms that are responsible for the NVP-AUY922-mediated radiosensitization in HSF-1 knockdown cells, I examined the DNA damage in H1339 ctrl and HSF-1 k.d. cells. The results of the alkaline comet assay (representative pictures are shown in Figure 12A) clearly demonstrate significantly more DNA damage 24 h after the combined treatment with the Hsp90 inhibitor NVP-AUY922 and irradiation in HSF-1 k.d. cells compared to control cells (Fig. 12A, B).

In H1339 control as well as in HSF-1 k.d. cells the DNA damage in the irradiated and NVP-AUY922 treated cells is significantly higher compared to that of the respective non-irradiated, drug-treated control cells (Fig. 12B).
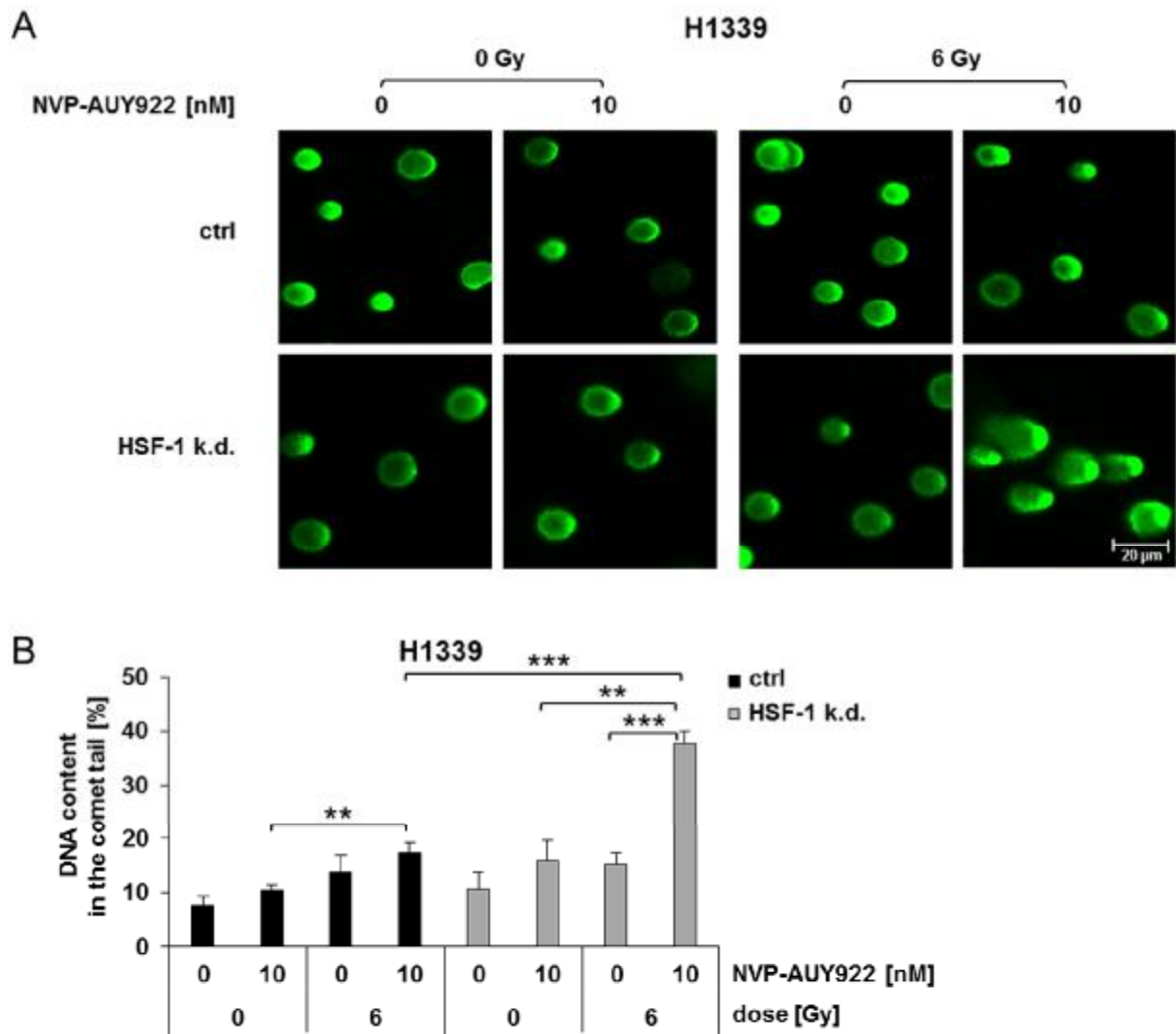
A

B

Fig. 12 HSF-1 knockdown leads to more DNA damage after combined Hsp90 inhibition and irradiation

A. Comet assay 24 h after irradiation. Representative pictures of H1339 ctrl and HSF-1 k.d. cells treated with 10 nM NVP-AUY922 for 24 h and irradiated with 6 Gy.

B. Quantification of the comet assay. Significance ***$p \leq 0.001$.

Hsp90 inhibition delays the repair of radiation-induced DNA DSBs in H1339 HSF-1 k.d. cells

The alkaline comet assay is indicative for single and double strand DNA breaks. To determine the exact amount of DNA double strand breaks (DSBs), the mean fluorescence intensity (MFI) of phosphorylated histone H2AX (γH2AX) and the number of 53BP1 foci were determined, as these markers are both DSB repair enzymes. The induction of DSB repair was measured 30 min and 24 h after irradiation of non-treated or NVP-AUY922 (10 nM) treated tumor cells by flow cytometry (γH2AX MFI) and immunofluorescence staining (53BP1 foci) assays.

29

30 min after irradiation with a dose of 6 Gy the expression of γH2AX in control and HSF-1 knockdown cells increased by a factor of 2–3, whereas exposure to Hsp90 inhibition alone or in combination with irradiation showed no effects on the initial DNA damage in both, H1339 control and HSF-1 k.d., cell lines (data not shown). 24 h after irradiation, no difference between irradiated control and HSF-1 knockdown cells could be detected. In line with the results of the comet assay, a combined drug-irradiation treatment led to a significant increase in the γH2AX expression specifically in HSF-1 k.d. cells (Fig. 13A). In contrast, a pretreatment with NVP-AUY922 (10 nM) did not alter γH2AX expression in control cells 24 h after irradiation.

These results were confirmed by an evaluation of 53BP1 foci 24 h after irradiation. Approximately 1 foci per nucleus was counted in non-irradiated cells, independent of the drug-pretreatment (Fig. 13B). Irradiation at 6 Gy increased the estimated range of 53BP1 foci to 20-30 per nucleus in control and HSF-1 k.d. cells. When treated with radiation plus NVP-AUY922 H1339 HSF-1 k.d. cells demonstrated a higher proportion of nuclei with estimated 30-40 53BP1 foci in contrast to control cells, where the estimated number of foci per nucleus ranged from 20-30. Representative pictures of the 53BP1 foci are shown in Figure 13B. Since these images are taken only from one microscopic cell layer, the estimated number of 53BP1 foci differs from that shown in Figure 13B. In order to obtain less 53BP1 foci and thus increase counting precision, the tumor cells were irradiated with lower irradiation doses (2 and 4 Gy). 24 h after irradiation with 2 and 4 Gy about 1.8 and 3 foci per nucleus, respectively, could be counted in control cells, irrespectively of a pretreatment with Hsp90 inhibitor. In contrast, combined drug-IR treatment induced more 53BP1 foci in HSF-1 k.d. cells compared to IR alone. At a dose of 2 Gy cells show about 1.8 foci per nucleus, similar to the results of the control cells. Around 2.1 foci per nucleus were detected in HSF-1 k.d. cells after a combined drug-irradiation treatment. The tendency of NVP-AUY922 to increase the number of 53BP1 foci in HSF-1 k.d cells after IR was confirmed at a dose of 4 Gy, where the difference of a combined treatment (~4.5 foci/nucleus) versus irradiation alone (~3 foci/nucleus) was significant (Fig. 13C).

These data suggest that a combined drug-IR treatment significantly augments the number of DSBs that persist 24 h after irradiation in HFS-1 k.d. cells in a dose-dependent manner. There was no difference in the initial DNA damage of control and HSF-1 k.d. cells after irradiation alone or in combination with Hsp90 inhibition. Hence, I hypothesized that the DNA DSB repair might be impaired in H1339 HSF-1 k.d. cells after combined drug-IR treatment.
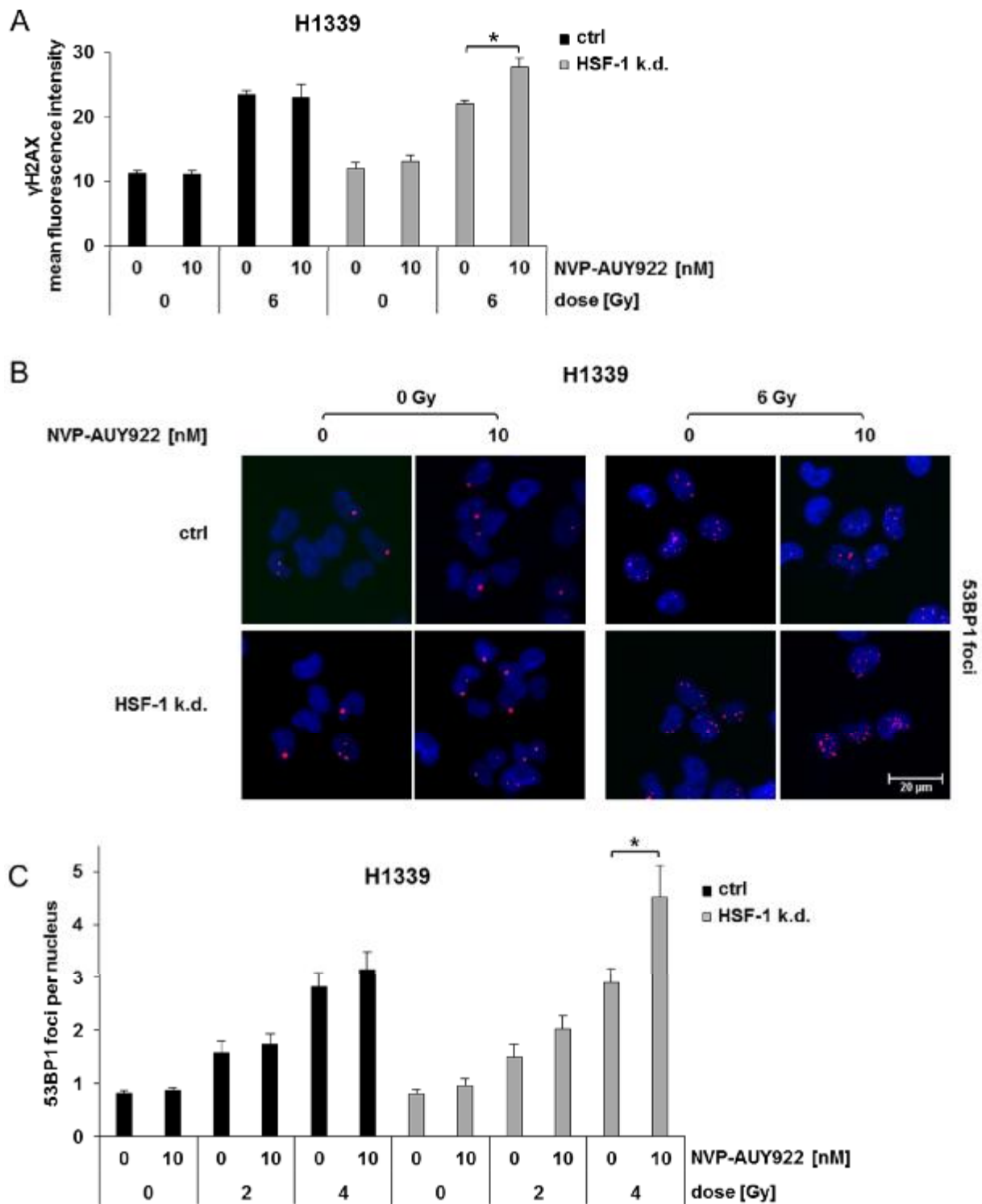
Fig. 13 HSF-1 knockdown increases DNA double strand breaks after combined Hsp90 inhibition and irradiation

A. Mean fluorescence intensity of γH2AX measured by flow cytometry 24 h after irradiation. H1339 ctrl and HSF-1 k.d. cells were treated with 10 nM NVP-AUY922 for 24 h following irradiation (0, 2, 4, 6 Gy). Significance *p ≤ 0.05. **B.** Representative pictures of 53BP1 foci in H1339 ctrl and HSF-1 k.d. cells 24 h after irradiation. Cells were treated with 10 nM NVP-AUY922 for 24 h following irradiation with 6 Gy. **C.** Quantification of 53BP1 foci. H1339 ctrl and HSF-1 k.d. cells were treated with 10 nM NVP-AUY922 for 24 h following irradiation with 2 or 4 Gy. Significance *p ≤ 0.05.

NVP-AUY922 and irradiation combined treatment impairs Rad51-mediated homologous recombination in H1339 HSF-1 k.d. cells

In eukaryotic cells, the two main pathways that are involved in DSB repair are homologous recombination (HR) and non-homologous end joining (NHEJ) [81-83]. It was previously shown, that Hsp90 inhibition reduces HR associated proteins such as BRCA2 and Rad51 [84] and that NVP-AUY922 delays Rad51 foci formation after irradiation [46]. To investigate whether and how NVP-AUY922 affects the homologous recombination in H1339 HSF-1 knockdown cells, I studied Rad51 foci formation 4 h after IR or combined drug-IR treatment (10 nM NVP-AUY922 and 4 Gy). In H1339 cells, Rad51 mainly resides to the nucleoli. Similar results are seen in U-2 OS (osteosarcoma), A-431 (epidermoid carcinoma) and U-251 MG (glioblastoma) cells [85]. Irradiation alone significantly induced the formation of Rad51 foci in control as well as in HSF-1 knockdown cells at similar levels (Fig. 14A). Pretreatment with NVP-AUY922 significantly reduced the number of Rad51 foci in both cell lines. This is in line with the results of Noguchi et al. [84] and Zaidi et al. [46]. Representative pictures of one microscopic cell layer are shown in Figure 14A. Interestingly, radiation-induced HR was significantly more impaired after Hsp90 inhibition in HSF-1 k.d. cells compared to control cells (Fig. 14B).

Based on my current data I cannot completely exclude the possibility of the involvement of NHEJ but my results reveal that an HSF-1 knockdown in combination with Hsp90 inhibition and irradiation has a larger effect on HR.

I could show that the knockdown of HSF-1 improves the therapeutical effects of a combined drug-irradiation treatment and thus, these findings can provide a new effective alternative for treatment of solid tumors. However, further studies are required to elucidate the exact mechanism.
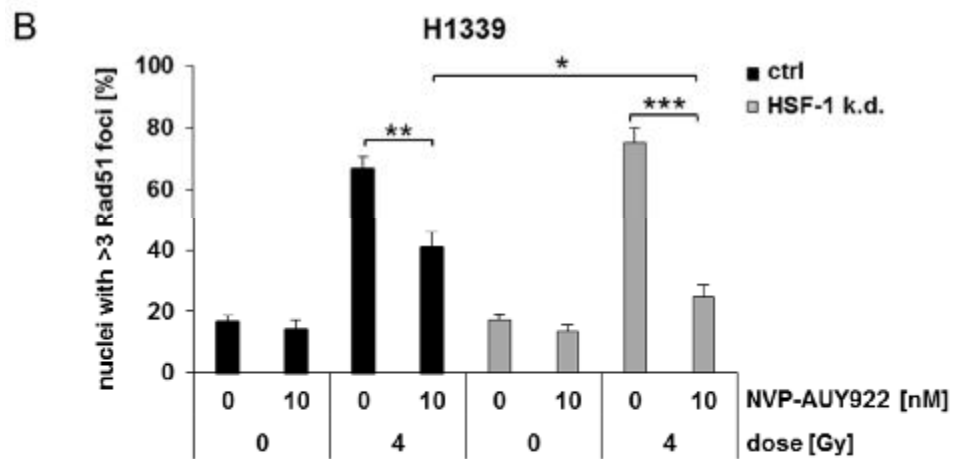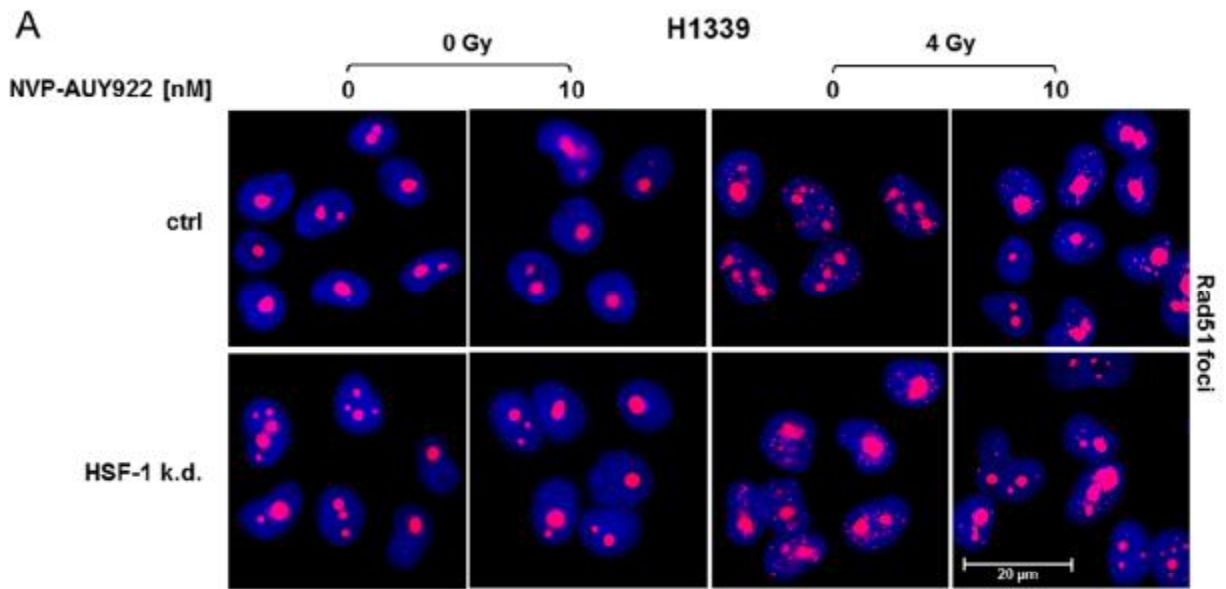
Fig. 14 Homologous recombination is more affected by combined treatment of Hsp90 inhibition and irradiation in HSF-1 knockdown cells compared to control cells

A. Representative pictures of Rad51 foci in H1339 ctrl and HSF-1 k.d. cells 4 h after irradiation. Cells were treated with 10 nM NVP-AUY922 for 24 h following irradiation with 4Gy.

B. Quantification of Rad51 foci 4 h after irradiation. H1339 ctrl and HSF-1 k.d. cells were treated with 10 nM NVP-AUY922 for 24 h following irradiation with 4 Gy. Significance *p ≤ 0.05; **p ≤ 0.01; ***p ≤ 0.001.

33

IV.2 The knockdown of Hsp27

Hsp27 knockdown does neither sensitize tumor cells to Hsp90 inhibition nor increase radiosensitivity after NVP-AUY922 treatment

Hsp27 levels are considered to be regulated by HSF-1 in a similar manner like Hsp70 levels. As seen in Figure 2A, in H1339 cells, Hsp27 was weakly expressed under normal conditions but strongly induced after treatment with NVP-AUY922. The HSF-1 knockdown completely inhibited the NVP-AUY922-induced Hsp27 expression in H1339 cells. In contrast, in EPLC-272H cells the high basal Hsp27 expression could hardly be increased by a treatment with NVP-AUY922. Furthermore, an HSF-1 knockdown could not decrease the high Hsp27 levels, as shown by immunoblot (Fig. 2A).

According to that, in H1339 cells, but not in EPLC-272H cells, a HSF-1 knockdown affected the sensitivity to Hsp90 inhibition (Fig. 7, 8) and radiosensitivity after combined drug-IR treatment (Fig. 9B). I assumed that the resistance of EPLC-272H control and HSF-1 knockdown cells to Hsp90 inhibition might be due to the high basal Hsp27 expression. Therefore, I analyzed the effects of an Hsp27 knockdown on the sensitivity to Hsp90 inhibition and radioresistance in the human lung cancer cell lines H1339 and EPLC-272H.
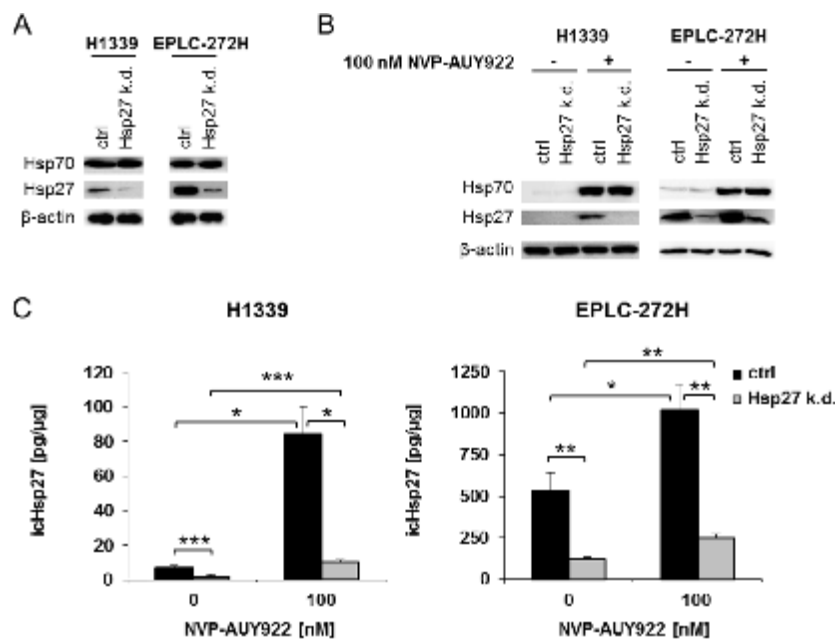
Fig. 15 Knockdown of Hsp27
A. Representative immunoblot showing the expression of Hsp70, Hsp27 and β-actin in H1339 and EPLC-272H cells transfected with control (ctrl) or Hsp27 (Hsp27 k.d.) shRNA and **B.** after treatment with 100 nM NVP-AUY922 for 24 h. **C.** ELISA of intracellular Hsp27 protein amount of H1339 and EPLC-272H ctrl and HSF-1 k.d. cells treated with 100 nM NVP-AUY922 for 24 h. Significance *p ≤ 0.05; **p ≤ 0.01; ***p ≤ 0.001.

Hsp27 was specifically knocked down in H1339 and EPLC-272H lung carcinoma cells by transfection with shRNA (Hsp27 k.d.). As a control, cells were transfected with a plasmid that contains a non-effective 29-mer scrambled shRNA cassette (ctrl). After puromycin selection the

H1339 and EPLC-272H Hsp27 k.d. cells showed a drastic reduction of Hsp27 protein levels compared to control cells (Fig. 15A, C). The Hsp27 knockdown did not affect the levels of Hsp70 in both cell lines. It is worth mentioning that the basal Hsp27 levels in EPLC-272H ctrl cells were much higher compared to that in H1339 ctrl cells. Treatment with the Hsp90 inhibitor NVP-AUY922 for 24 h resulted in an increase of Hsp27 in both cell lines (ctrl and Hsp27 k.d.), although the increase was much more pronounced in H1339 ctrl cells (~ 12-fold) compared to EPLC-272H ctrl cells (~ 2-fold). However, the Hsp27 protein levels which are induced by Hsp90 inhibition in Hsp27 k.d. cells were significantly lower compared to that in control cells (Fig. 15B, C).

Belkacemi et al. [86] showed that an Hsp27 knockdown in combination with Hsp90 inhibition results in a decrease in cell viability and proliferation in glioblastoma multiforme cells. Hence, I tested the sensitizing effects of an Hsp27 k.d. in lung cancer cells. The knockdown of Hsp27 did not sensitize H1339 and EPLC-272H lung cancer cells to Hsp90 inhibition (Fig. 16).
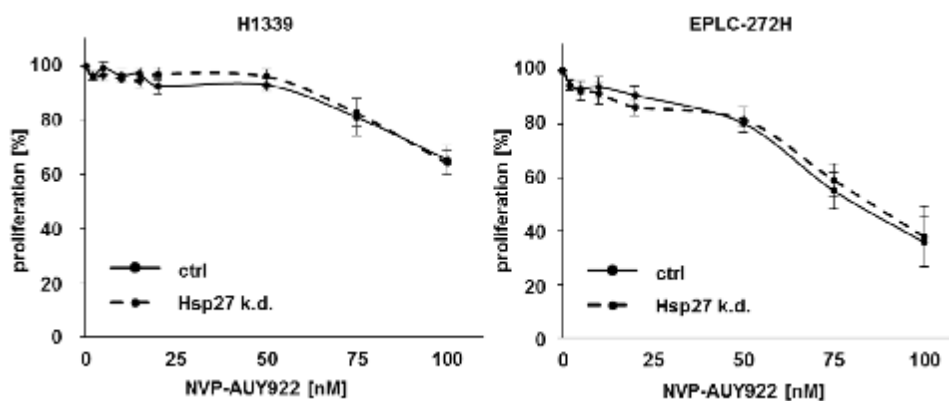
Fig. 16 Sensitivity to Hsp90 inhibition is not increased by the knockdown of Hsp27
Proliferation assay of H1339 and EPLC-272H ctrl and HSF-1 k.d. cells treated with 0, 2, 5, 10, 20, 50, 75 and 100 nM NVP-AUY922 for 24 h.

A lack of Hsp27 alone does neither radiosensitize H1339 cells nor EPLC-272H cells as determined by clonogenic cell survival (Fig. 17A). Furthermore, I studied the combined effects of an Hsp27 knockdown and Hsp90 inhibition on the radiosensitivity of H1339 and EPLC-272H cells. Surprisingly, radiosensitivity of H1339 and EPLC-272H Hsp27 k.d. cells did not differ from control cells after Hsp90 inhibition even with a higher (5 nM) concentration of NVP-AUY922 (Fig. 17B).
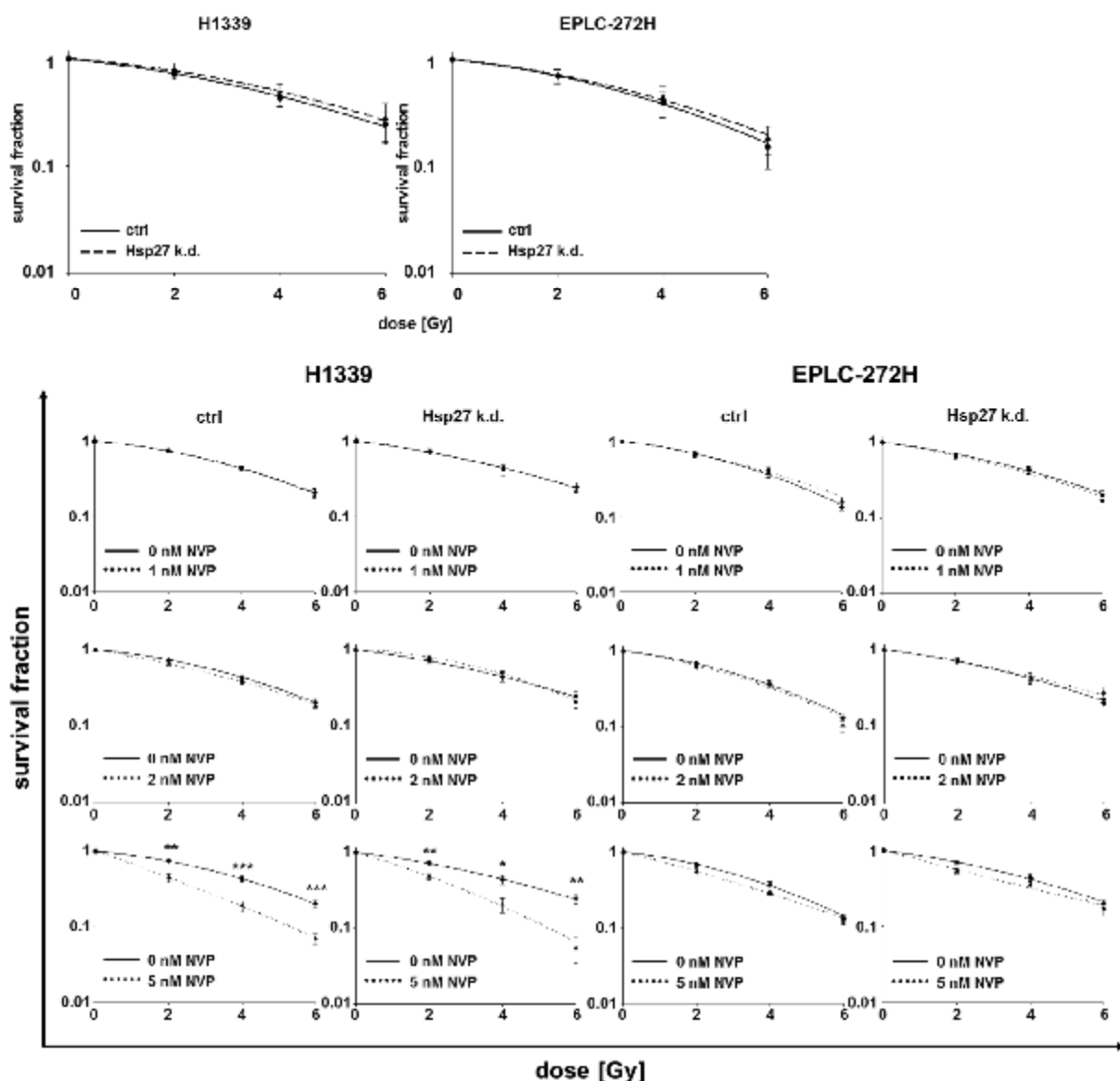
Fig. 17 Radiosensitivity after Hsp27 knockdown alone and in combination with Hsp90 inhibition

A. Colony forming assay of H1339 and EPLC-272H ctrl and Hsp27 k.d. cells after irradiation with 0, 2, 4 and 6 Gy. **B.** Colony forming assay of ctrl and Hsp27 k.d. cells. Cells were treated with 0, 1, 2 and 5 nM NVP-AUY922 for 24 h and then irradiated with 0, 2, 4 and 6 Gy. Significance *p ≤ 0.05; **p ≤ 0.01; ***p ≤ 0.001.

The double knockdown of HSF-1 and Hsp27 in EPLC-272H cells does neither affect sensitivity to Hsp90 inhibition nor radioresistance after NVP-AUY922 treatment

EPLC-272H cells that lack either HSF-1 or Hsp27 did not show any effects in sensitivity to Hsp90 inhibition or radiosensitivity after Hsp90 inhibition.

Whereas EPLC-272H HSF-1 k.d. cells have high basal levels of Hsp27 but reduced Hsp70 expression, Hsp27 k.d. cells have reduced Hsp27 levels but normal basal Hsp70 protein amounts.

36

Hence, I hypothesized that the reduction of HSF-1, and therefore Hsp70, in combination with the knockdown of Hsp27 might lead to an increase in sensitivity to NVP-AUY922 and radiosensitivity after Hsp90 inhibition.

Thus, Hsp27 was specifically knocked down in EPLC-272H HSF-1 k.d. cells (HSF-1/Hsp27 k.d.). After selection by single cell cloning the HSF-1/Hsp27 k.d. cells showed a strong reduction of HSF-1 as well as activated phosphorylated HSF-1 (pHSF-1), Hsp70 and Hsp27 protein levels compared to control cells (Fig. 18).
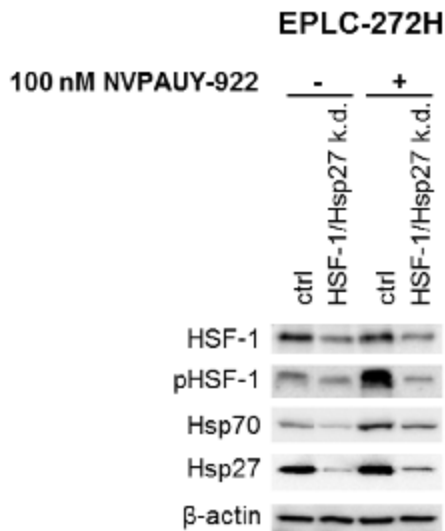
Fig. 18 Double knockdown of HSF-1 and Hsp27 in EPLC-272H cells

Representative immunoblot showing the expression of HSF-1, HSF-1 phospho S326 (pHSF-1), Hsp70, Hsp27 and β-actin in ctrl and HSF-1/Hsp27 double knockdown EPLC-272H cells. Cells were treated with 100 nM NVP-AUY922 for 24 h.
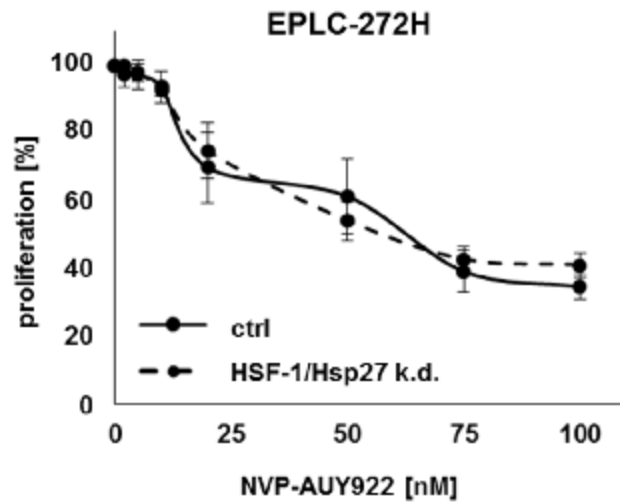
Fig. 19 Sensitivity to Hsp90 inhibition is not increased by the double knockdown of HSF-1 and Hsp27 in EPLC-272H cells

Proliferation assay of EPLC-272H ctrl and HSF-1/Hsp27 k.d. cells treated with 0, 2, 5, 10, 20, 50, 75 and 100 nM NVP-AUY922 for 24 h.

Treatment with the Hsp90 inhibitor NVP-AUY922 for 24 h increased pHSF-1 as well as Hsp70 protein levels in control cells. In contrast, after NVP-AUY922 treatment for 24 h HSF-1/Hsp27 double knockdown cells showed no induction of pHSF-1. Furthermore, Hsp70 as well as Hsp27 protein levels were hardly induced upon Hsp90 inhibition (Fig.18).

Unexpectedly, EPLC-272H HSF-1/Hsp27 k.d. cells showed no increase in sensitivity to Hsp90 inhibition (Fig. 19) and the radiosensitivity did not differ from control cells (Fig. 20A), even after pretreatment with different concentrations of NVP-AUY922 (Fig.20B).
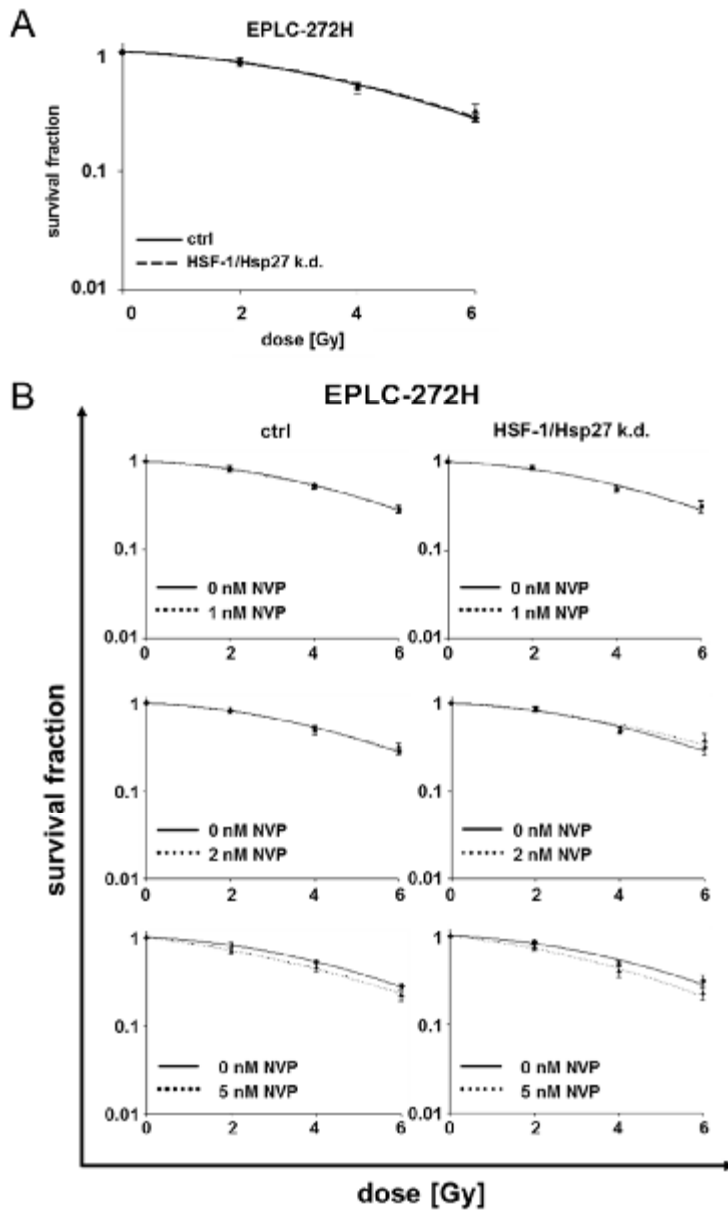
Fig. 20 Radiosensitivity after HSF-1 and Hsp27 double knockdown alone and in combination with Hsp90 inhibition
A. Colony forming assay of EPLC-272H ctrl and HSF-1/Hsp27 k.d. cells after irradiation with 0, 2, 4 and 6 Gy. **B.** Colony forming assay of ctrl and HSF-1/Hsp27 k.d. cells. Cells were treated with 0, 1, 2 and 5 nM NVP-AUY922 for 24 h and then irradiated with 0, 2, 4 and 6 Gy.

The knockdown of Hsp27 leads to a reduced G2/M phase 24 h after irradiation

Even though, a knockdown of Hsp27 did not radiosensitize H1339 and EPLC-272h cells, I analyzed the cell cycle phase distribution 24 h after irradiation with a dose of 6 Gy. The knockdown of Hsp27 per se has no effects on the cell cycle phase distribution. However, the irradiation-induced G2/M arrest of Hsp27 knockdown cells was significantly decreased in both H1339 and EPLC-272H cells, whereas the percentage of cells in G0G1 phase was increased compared to irradiated control cells (Fig. 21).
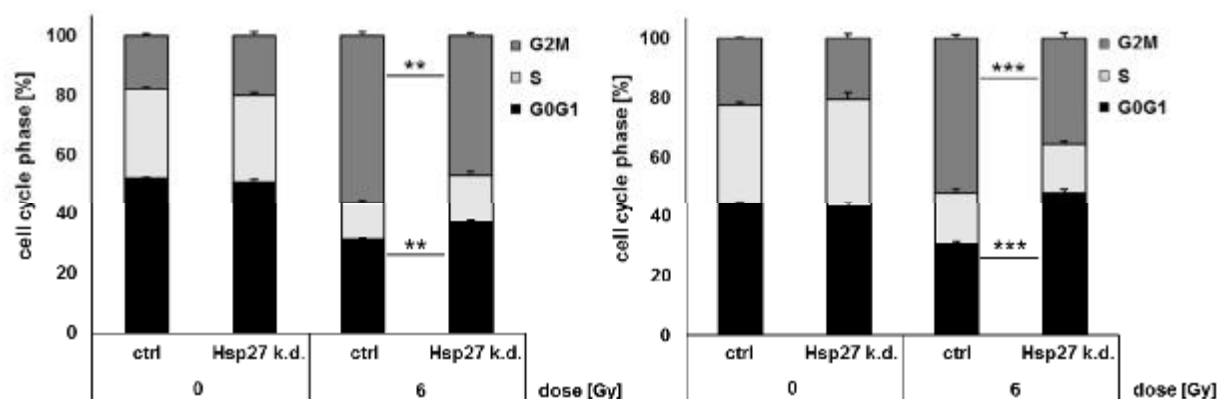
Fig. 21 G2/M arrest in Hsp27 knockdown cells is impaired 24 h after irradiation

H1339 and EPLC-272H ctrl and Hsp27 k.d. cells were treated irradiated with 6 Gy. Cells were stained with PI to analyze cell cycle distribution 24 h after irradiation. Significance **p ≤ 0.01; ***p ≤ 0.001.

Cell cycle phase distribution also plays a role in mediating radiosensitivity. Cells are most radiosensitive in the G2/M phase, less sensitive in the G0G1 phase, and most radioresistant during the S phase. Hence, 24 h after the first irradiation with a dose of 6 Gy, cells were irradiated a second time with doses of 2, 4 or 6 Gy. As seen in Figure 22, H1339 and EPLC-272 Hsp27 k.d. cells tend to be less radiosensitive after the second irradiation compared to control cells, with this effect being significant when EPLC-272H cells were irradiated twice with 6 Gy.
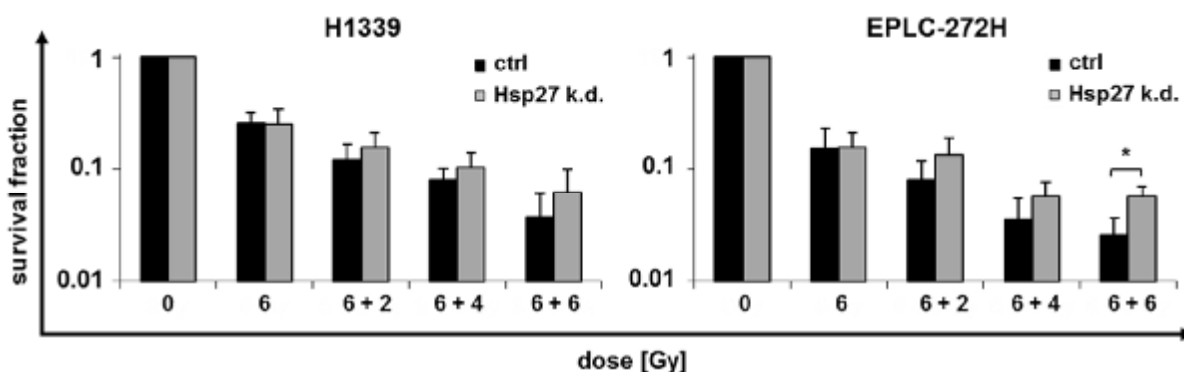
Fig. 22 Hsp27 knockdown cells appear to be less radiosensitive after repeated irradiation than control cells

Colony forming assay of H1339 and EPLC-272H ctrl and Hsp27 k.d. cells. Cells were irradiated with a dose of 6 Gy and 24 h later they were given a second dose of 2, 4 or 6 Gy. Significance *p ≤ 0.05.

The cell cycle analysis indicates that there might be a defect in the G2/M checkpoint, in which DNA double strand break (DSB) repair takes place, as the cells that lack Hsp27 pass earlier from G2 to M phase after irradiation and hence, return sooner to normal cell cycle phase distribution compared to control cells. To identify the molecular mechanisms behind these observations, I analyzed proteins that are involved in cell cycle regulation and DNA damage signaling.

As shown in Figure 23, the knockdown of Hsp27 impairs phosphorylation of ATM (Ataxia-Telangiectasia mutated) after irradiation in both H1339 and EPLC-272H cell lines. ATM is a master regulator of DNA damage signaling.

It is known that the p38 MAPK (mitogen-activated protein kinase) pathway is activated in response to DSBs and therefore leads to the G2/M arrest [87, 88]. One of the main downstream targets of p38 MAPK is the mitogen-activated protein kinase (MAPK)-activated protein kinase 2 (MAPKAPK-2 or MK2) [89], that is also activated after DNA damage [90, 91]. The activation of MK2 is required for the induction of a G2/M cell cycle arrest [90, 92]. My studies showed that the radiation-induced phosphorylation of MK2 is mostly affected by Hsp27 knockdown in both lung cancer cell lines. Interestingly, Hsp27 is a substrate of MK2. Figure 23 shows that Hsp27 phosphorylation at Ser82 is slightly increased in control cells 24 h after irradiation. As expected, this phosphorylation was abrogated in Hsp27 knockdown cells.

In addition, the phosphorylation of Cdc2 (cell division cycle protein 2) at Tyr15 after irradiation is reduced in Hsp27 knockdown cells (Fig. 23). The dephosphorylation at Tyr15 is an essential step in activating the CyclinB1/Cdc2 complex which drives the transition from G2 to M phase [93-96]. Presently these studies are continued to further investigate the role of Hsp27 in radiation-induced DNA damage and cell cycle signaling pathways.
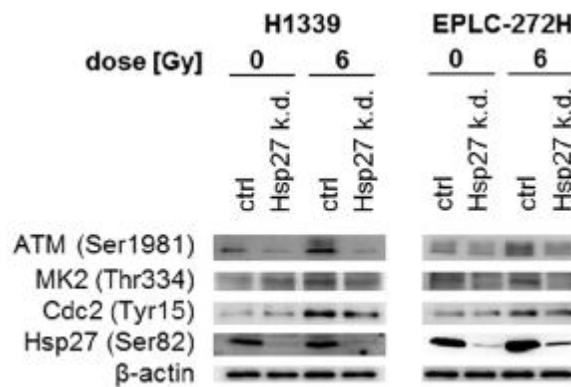

Fig. 23 Hsp27 knockdown affects proteins in DNA damage and cell cycle signaling pathways

Representative immunoblot showing the expression of the phosphorylated forms of ATM (Ser1981), MK2 (Thr334), Cdcd2 (Tyr15) and Hsp27 (Ser82) 24h after irradiation with a dose of 6 Gy. β-actin was used as loading control.

V. DISCUSSION

The heat shock proteins Hsp90, Hsp70 and Hsp27 as well as the transcription factor heat shock factor 1 (HSF-1) are frequently over-expressed in many tumor cell types [16-18], including lung carcinoma.

Elevated HSP levels contribute to a malignant tumor phenotype and mediate resistance to chemo- and radiotherapy [19, 20]. The inhibition of Hsp90 is considered as a promising concept to enhance radiosensitivity [21-25]. It was shown that the Hsp90 inhibitor NVP-AUY922 either alone or in combination with radiation affects cell cycle, apoptosis and DNA repair mechanisms [43-45] and thus might increase radiosensitivity of tumor cells [25, 46]. However, the inhibition of Hsp90 induces the release of HSF-1 from the Hsp90 complex and as a result activates HSF-1 which in turn stimulates the transcription of Hsp70 and Hsp27 [13-15, 47-52]. Since Hsp70 and Hsp27 act as anti-apoptotic molecules that promote tumor cell survival, herein I aimed to study the combined effects of an HSF-1 knockdown (k.d.) and Hsp90 inhibition on the radiosensitivity of lung cancer cell lines.

I observed that the combined treatment with HSF-1 shRNA and Hsp90 inhibitor leads to a reduction of Hsp90 inhibitor-induced Hsp27 and Hsp70 expression and significantly diminishes proliferation of H1339 cells. My results are consistent with published data [80] and show also for the small cell lung carcinoma cell line H1339 that a loss of HSF-1 leads to an increase in sensitivity to Hsp90 inhibition, also shown by the increase in apoptosis marker in HSF-1 k.d. cells.

My previous data have already shown that the reduction of HSF-1 alone does not radiosensitize H1339 and EPLC-272H cells [1]. This is inconsistent with a publication from Li and Martinez in which downregulation of HSF-1 alone was shown to sensitize cancer cells to radiotherapy [97]. The discrepancy to their results might be either explained by different tumor cell lines which were used or by the fact that membrane expression of Hsp70 has not been taken into account. It has been shown that mHsp70-positive tumor cells are better protected against ionizing irradiation compared to their mHsp70-negative counterparts [1, 57]. A better understanding of the Hsp70 associated pathways which contribute to the development of radiation resistance might enable novel strategies to increase the radiation sensitivity of tumor cells.

It was previously shown that the heat shock response inhibitor NZ28 alone significantly increased the radiation response in human lung and breast tumor cells. When combined with the Hsp90 inhibitor NVP-AUY922 the concentration of NZ28 could be significantly reduced to achieve the same radiosensitization [3]. These results demonstrate that a dual targeting of the heat shock response and Hsp90 with NZ28 and NVP-AUY922 potentiates the radiation response of tumor cells that are otherwise resistant to ionizing radiation. Further experiments revealed that NZ28

simultaneously inhibits several transcription factors and is therefore not specific to HSF-1 [2]. Therefore, in my thesis I combined a specific HSF-1 knockdown, Hsp90 inhibition and irradiation to study the impact of HSF-1 on radiosensitivity.

The survival curves show that a HSF-1 knockdown in combination with Hsp90 inhibition radiosensitizes H1339 cells. Compared to control cells, lower concentrations of NVP-AUY922 were needed to obtain a radiosensitizing effect in H1339 HSF-1 k.d. cells. In contrast, EPLC-272H HSF-1 k.d. cells showed no differences in susceptibility to a combined drug-IR treatment compared to control cells.

Findings of Stingl et al. [44] point to the fact that NVP-AUY922 affects apoptosis and thus induces a radiosensitizing effect in HT 1080 (fibrosarcoma) and GaMG (glioblastoma) cells. In line with these findings, Niewidok et al. [43] and Gandhi et al. [98] could show that the depletion of pro-apoptotic proteins results in radiosensitization in NVP-AUY922 treated lung and prostate carcinoma cells, *in vitro*. In contrast to these studies, NVP-AUY922 combined with radiation had no effect on cell cycle distribution or apoptosis induction in both H1339 and EPLC-272H cells, even if the expression of HSF-1 was reduced. These different results might be due to the differences in the applied concentration of this Hsp90 inhibitor, which was much lower in my study. Nevertheless, this low concentration of NVP-AUY922 led to a significant increase in DNA damage in H1339 HSF-1 k.d. cells, 24 h after irradiation. In line with these findings, I also found that the loss of HSF-1 and inhibition of Hsp90 led to an increase of the DNA double strand break markers γH2AX and 53BP1 in H1339 cells, 24 h after irradiation. As double strand breaks are the most lethal form of DNA damage, the radiosensitizing effect in this experimental setup might be due to DSBs. Zaidi et al. [46] could show that NVP-AUY922 impaired homologous recombination after irradiation. My results for H1339 ctrl cells are in line with these findings. Furthermore, HSF-1 knockdown in H1339 cells in combination with Hsp90 inhibition strongly enhances the impairment of Rad51-mediated homologous recombination.

These results show for the first time in H1339 lung cancer cells that a combined and selective targeting of Hsp90 and HSF-1 can improve radiotherapy effectiveness by impairing homologous recombination. Hence, these data might offer a new possibility to treat lung cancer by dual targeting of HSF-1 and Hsp90 thereby reducing the concentration of Hsp90 inhibitor and thus, alleviating negative side effects. In future, this might be a promising approach to improve the efficacy of chemoradiotherapy.

An important open question refers to the fact how to target HSF-1 in patient's tumors. One auspicious approach is to use therapeutic siRNA to knockdown HSF-1. Despite great progress in developing siRNA therapy, there are still a number of problems that have to be addressed [99]. Another way is to address the heat shock response/HSF-1 with the help of small drug-like

inhibitors. KRIBB11 is so far the only inhibitor that directly binds to HSF-1 [100, 101]. All other currently available inhibitors display a wide variety of inhibitory activities, and their particular mode of action is not restricted to HSF-1 (reviewed in [102, 103]). Therefore, more basic research is necessary to identify molecules that selectively target HSF-1 and thus improve siRNA therapy.

Another point that has to be considered is that HSF-1 plays a role in a multitude of physiological processes, also under non-stressed conditions [104]. HSF-1 not only up-regulates the transcription of heat shock proteins but also increases the transcription of MICA and MICB (major histocompatibility class I chain-related proteins A and B) genes [68] by binding to their heat shock elements (HSE) in the promoter regions [69].

Hsp70 and MICA/B on tumor cells are important recognition structures for activated natural killer (NK) cells which are key components of the innate immune system as they have an essential function in the first line anticancer immune response.

Whereas HSF-1 knockdown did not affect membrane expression of Hsp70 and MICA, membrane expression of MICB was found to be significantly reduced in H1339 cells. According to these results, Venkataraman et al. [77] have shown that MICA is less inducible by HSF-1 than MICB due to a weaker binding capacity of HSF-1 to the HSE. HSF-1 knockdown in H1339 cells led to a reduction in the NK cell-mediated cytotoxicity most likely mediated by the downregulation of MICB in the membrane.

In summary, my data show that the knockdown of HSF-1 alone does not increase radiosensitivity, but even reduces NK cell-mediated lysis of tumor cells. Radiotherapy has been found to enhance NK cell cytotoxicity and thereby can contribute to the anti-tumor immune response [105-107]. Further studies are needed to figure out which effect might dominate in the *in vivo* situation.

However, my data point into the direction that the combination of HSF-1 knockdown and Hsp90 inhibition might provide a promising approach to improve the outcome of radiotherapy.

Despite these interesting results which are obtained for H1339 cells, an HSF-1 knockdown did neither increase sensitivity to Hsp90 inhibition nor affected radiosensitivity in EPLC-272H cells when combined with NVP-AUY922.

EPLC-272H cells have very high basal Hsp27 levels which could not be decreased by HSF-1 knockdown. As it has been shown that Hsp27 protein levels are associated with radioresistance in tumor cells [108-111], Hsp27 was downregulated in H1339 and EPLC-272H cells.

The single knockdown of Hsp27 as well as the double knockdown of HSF-1 and Hsp27 in EPLC-272H cells did not radiosensitize these lung tumor cell lines, even when combined with Hsp90 inhibition.

Unexpectedly, 24 h after irradiation both H1339 and EPLC-272H Hsp27 knockdown cells exhibit a reduced G2/M arrest compared to control cells. As G2/M is the most radiosensitive phase in cell cycle, cells were irradiated a second time. Indeed, Hsp27 knockdown cells were less radiosensitive after the second irradiation. Therefore, I asked the question how Hsp27 influences the G2/M checkpoint, as the data indicate a deregulation in the cell cycle arrest.

It was previously shown in head-and-neck squamous cell carcinoma cells that the phosphorylation of ATM (Ataxia-Telangiectasia mutated), a master regulator of DNA damage signaling, is impaired after irradiation by Hsp27 knockdown [52]. This finding is consistent with my data. Vice versa, it was shown in human fibroblasts that the radiation-induced phosphorylation of Hsp27 was abrogated by an inhibition of ATM. This finding needs to be examined in H1339 and EPLC-272H ctrl/ Hsp27 k.d. cells.

Further studies of cell cycle proteins revealed that the phosphorylation of MK2, a target protein of p38 MAPK [112, 113], is also inhibited after irradiation in Hsp27 knockdown cells. Under normal conditions Cdc2 is activated via dephosphorylation on tyrosine 15 (Tyr15) and thus drives G2 to M transition [114]. After irradiation Hsp27 knockdown cells display less Tyr15-phosphorylated Cdc2, indicating that Cdc2 is (more) active and thus, Hsp27 k.d. cells enter mitosis earlier after irradiation compared to control cells that remain in the G2 arrest. Therefore, G1 phase is also increased in Hsp27 knockdown cells after irradiation. Venkatakrishnan et al. showed that Hsp27 regulates p53 transcriptional activity leading to p21 upregulation and G2/M phase cell cycle arrest [115]. H1339 and EPLC-272H are both p53 mutants [116, 117]. Reinhardt et al. stated that p53-deficient cells rely on ATM- and ATR-mediated checkpoint signaling through the p38 MAPK/MK2 pathway for survival after DNA damage [91], therefore, I assume that Hsp27 is likely to interfere with this pathway.

On the basis of my previous data and data from the literature, I assume an involvement of Hsp27 in the DNA damage/cell cycle signaling pathway (Fig. 24) as follows:

In control cells, DNA damage, especially DSBs, activates ATM and the p38 MAPK pathway [87, 88, 118, 119]. Whether the activation of the p38 MAPK-MK2 axis after irradiation is ATM-dependent needs to be elucidated. Radiation induces the phosphorylation and activation of MK2 which phosphorylates Hsp27 [120] and inactivates Cdc25 [92]. It is also necessary to examine whether Chk2 (checkpoint kinase 2), activated mainly by ATM, is involved in the inactivation of Cdc25 [121]. Under non-stress conditions, Cdc25 dephosphorylates and thereby activates Cdc2 what leads to the activation of the CyclinB/Cdc2 complex driving progression of the cell cycle [96]. After DNA damage, Cdc25 is inactivated by its MK2-dependent phosphorylation, and therefore Cdc2 maintains the Tyr15 phosphorylation and the CyclinB/Cdcd2 complex remains inactive. Hence, cells undergo a G2 arrest, which is important for the DNA is repair. The phosphorylation

of Hsp27 by MK2 might also influence ATM phosphorylation, which could be part of a feedback loop as the phosphorylation status of Hsp27 is also a general stress sensor [122].

In contrast, in Hsp27 knockdown cells, DNA damage does not induce the phosphorylation of ATM and MK2. Therefore, Cdc25 is active and dephosphorylates Cdc2 at Tyr15, thereby activating the CyclinB/Cdc2 complex which initiates mitosis. I hypothesize that Hsp27 knockdown cells undergo mitosis, even though the DNA repair is incomplete, because the signal to arrest in G2 phase is missing due to an Hsp27 knockdown-mediated deregulation of the cell cycle. A scheme summarizing the role of Hsp27 in DNA damage and cell cycle is shown in Figure 24.
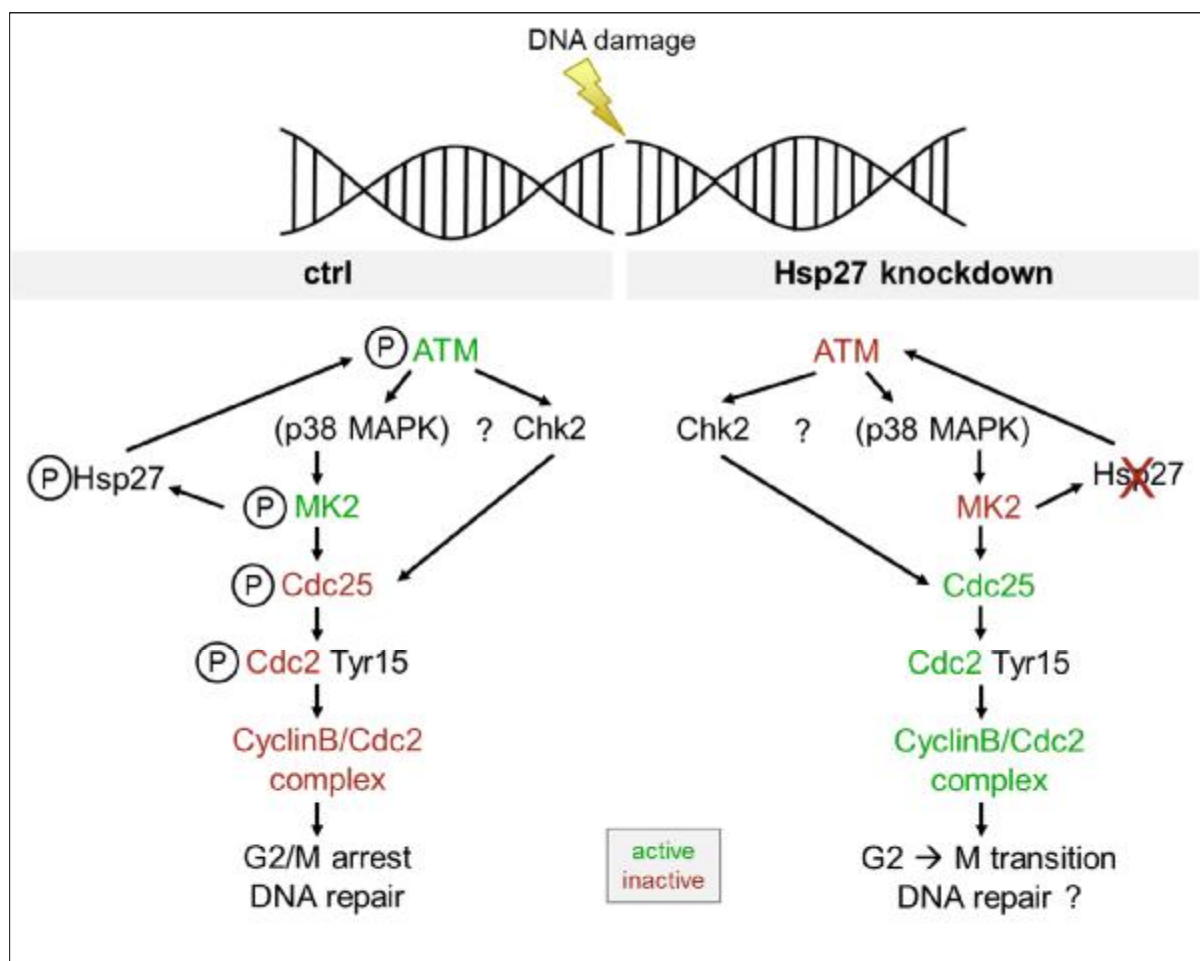

Fig. 24 Scheme of Hsp27 involvement in DNA damage / cell cycle signaling pathways

VI. LITERATURE

1. Murakami, N., et al., *Role of membrane Hsp70 in radiation sensitivity of tumor cells.* Radiat Oncol, 2015. **10**: p. 149.
2. Schilling, D., et al., *NZ28-induced inhibition of HSF1, SP1 and NF-kappaB triggers the loss of the natural killer cell-activating ligands MICA/B on human tumor cells.* Cancer Immunol Immunother, 2015. **64**(5): p. 599-608.
3. Schilling, D., et al., *Sensitizing tumor cells to radiation by targeting the heat shock response.* Cancer Lett, 2015. **360**(2): p. 294-301.
4. Torre, L.A., et al., *Global cancer statistics, 2012.* CA Cancer J Clin, 2015. **65**(2): p. 87-108.
5. Wood, S.L., et al., *Molecular histology of lung cancer: from targets to treatments.* Cancer Treat Rev, 2015. **41**(4): p. 361-75.
6. Herbst, R.S., J.V. Heymach, and S.M. Lippman, *Lung cancer.* N Engl J Med, 2008. **359**(13): p. 1367-80.
7. Park, M.R., et al., *Progression-free survival: an important prognostic marker for long-term survival of small cell lung cancer.* Tuberc Respir Dis (Seoul), 2014. **76**(5): p. 218-25.
8. Novello, S., et al., *Early response to chemotherapy in patients with non-small-cell lung cancer assessed by [18F]-fluoro-deoxy-D-glucose positron emission tomography and computed tomography.* Clin Lung Cancer, 2013. **14**(3): p. 230-7.
9. Sakurai, H. and Y. Enoki, *Novel aspects of heat shock factors: DNA recognition, chromatin modulation and gene expression.* Febs j, 2010. **277**(20): p. 4140-9.
10. Dai, C., et al., *Heat shock factor 1 is a powerful multifaceted modifier of carcinogenesis.* Cell, 2007. **130**(6): p. 1005-18.
11. Jin, X., et al., *Targeted deletion of Hsf1, 2, and 4 genes in mice.* Methods Mol Biol, 2011. **787**: p. 1-20.
12. Zhao, Y.H., et al., *Upregulation of lactate dehydrogenase A by ErbB2 through heat shock factor 1 promotes breast cancer cell glycolysis and growth.* Oncogene, 2009. **28**(42): p. 3689-701.
13. Sorger, P.K. and H.R. Pelham, *Yeast heat shock factor is an essential DNA-binding protein that exhibits temperature-dependent phosphorylation.* Cell, 1988. **54**(6): p. 855-64.
14. McMillan, D.R., et al., *Targeted disruption of heat shock transcription factor 1 abolishes thermotolerance and protection against heat-inducible apoptosis.* J Biol Chem, 1998. **273**(13): p. 7523-8.
15. Xie, Y., et al., *Heat shock factor 1 contains two functional domains that mediate transcriptional repression of the c-fos and c-fms genes.* J Biol Chem, 2003. **278**(7): p. 4687-98.
16. Moulick, K., et al., *Affinity-based proteomics reveal cancer-specific networks coordinated by Hsp90.* Nat Chem Biol, 2011. **7**(11): p. 818-26.
17. Soo, E.T., et al., *Heat shock proteins as novel therapeutic targets in cancer.* In Vivo, 2008. **22**(3): p. 311-5.
18. Bonay, M., et al., *Expression of heat shock proteins in human lung and lung cancers.* Am J Respir Cell Mol Biol, 1994. **10**(4): p. 453-61.
19. Ciocca, D.R. and S.K. Calderwood, *Heat shock proteins in cancer: diagnostic, prognostic, predictive, and treatment implications.* Cell Stress Chaperones, 2005. **10**(2): p. 86-103.
20. Garrido, C., et al., *Heat shock proteins 27 and 70: anti-apoptotic proteins with tumorigenic properties.* Cell Cycle, 2006. **5**(22): p. 2592-601.
21. Pearl, L.H. and C. Prodromou, *Structure and mechanism of the Hsp90 molecular chaperone machinery.* Annu Rev Biochem, 2006. **75**: p. 271-94.
22. Whitesell, L. and S.L. Lindquist, *HSP90 and the chaperoning of cancer.* Nat Rev Cancer, 2005. **5**(10): p. 761-72.

23. Kabakov, A.E., V.A. Kudryavtsev, and V.L. Gabai, *Hsp90 inhibitors as promising agents for radiotherapy.* J Mol Med (Berl), 2010. **88**(3): p. 241-7.

24. Kaplan, K.B. and R. Li, *A prescription for 'stress'--the role of Hsp90 in genome stability and cellular adaptation.* Trends Cell Biol, 2012. **22**(11): p. 576-83.

25. Schilling, D., et al., *Radiosensitization of normoxic and hypoxic h1339 lung tumor cells by heat shock protein 90 inhibition is independent of hypoxia inducible factor-1alpha.* PLoS One, 2012. **7**(2): p. e31110.

26. Kabakov, A.E., Y.M. Makarova, and Y.V. Malyutina, *Radiosensitization of human vascular endothelial cells through Hsp90 inhibition with 17-N-allilamino-17-demethoxygeldanamycin.* Int J Radiat Oncol Biol Phys, 2008. **71**(3): p. 858-65.

27. Bisht, K.S., et al., *Geldanamycin and 17-allylamino-17-demethoxygeldanamycin potentiate the in vitro and in vivo radiation response of cervical tumor cells via the heat shock protein 90-mediated intracellular signaling and cytotoxicity.* Cancer Res, 2003. **63**(24): p. 8984-95.

28. Enmon, R., et al., *Combination treatment with 17-N-allylamino-17-demethoxy geldanamycin and acute irradiation produces supra-additive growth suppression in human prostate carcinoma spheroids.* Cancer Res, 2003. **63**(23): p. 8393-9.

29. Machida, H., et al., *Geldanamycin, an inhibitor of Hsp90, sensitizes human tumour cells to radiation.* Int J Radiat Biol, 2003. **79**(12): p. 973-80.

30. Russell, J.S., et al., *Enhanced cell killing induced by the combination of radiation and the heat shock protein 90 inhibitor 17-allylamino-17- demethoxygeldanamycin: a multitarget approach to radiosensitization.* Clin Cancer Res, 2003. **9**(10 Pt 1): p. 3749-55.

31. Bull, E.E., et al., *Enhanced tumor cell radiosensitivity and abrogation of G2 and S phase arrest by the Hsp90 inhibitor 17-(dimethylaminoethylamino)-17-demethoxygeldanamycin.* Clin Cancer Res, 2004. **10**(23): p. 8077-84.

32. Harashima, K., et al., *Heat shock protein 90 (Hsp90) chaperone complex inhibitor, radicicol, potentiated radiation-induced cell killing in a hormone-sensitive prostate cancer cell line through degradation of the androgen receptor.* Int J Radiat Biol, 2005. **81**(1): p. 63-76.

33. Dote, H., et al., *Inhibition of hsp90 compromises the DNA damage response to radiation.* Cancer Res, 2006. **66**(18): p. 9211-20.

34. Eccles, S.A., et al., *NVP-AUY922: a novel heat shock protein 90 inhibitor active against xenograft tumor growth, angiogenesis, and metastasis.* Cancer Res, 2008. **68**(8): p. 2850-60.

35. Chinnaiyan, P., G.W. Allen, and P.M. Harari, *Radiation and new molecular agents, part II: targeting HDAC, HSP90, IGF-1R, PI3K, and Ras.* Semin Radiat Oncol, 2006. **16**(1): p. 59-64.

36. Matsumoto, Y., H. Machida, and N. Kubota, *Preferential sensitization of tumor cells to radiation by heat shock protein 90 inhibitor geldanamycin.* J Radiat Res, 2005. **46**(2): p. 215-21.

37. Machida, H., et al., *Heat shock protein 90 inhibitor 17-allylamino-17-demethoxygeldanamycin potentiates the radiation response of tumor cells grown as monolayer cultures and spheroids by inducing apoptosis.* Cancer Sci, 2005. **96**(12): p. 911-7.

38. Dote, H., et al., *ErbB3 expression predicts tumor cell radiosensitization induced by Hsp90 inhibition.* Cancer Res, 2005. **65**(15): p. 6967-75.

39. Kelland, L.R., et al., *DT-Diaphorase expression and tumor cell sensitivity to 17-allylamino, 17-demethoxygeldanamycin, an inhibitor of heat shock protein 90.* J Natl Cancer Inst, 1999. **91**(22): p. 1940-9.

40. Eiseman, J.L., et al., *Pharmacokinetics and pharmacodynamics of 17-demethoxy 17-[[(2-dimethylamino)ethyl]amino]geldanamycin (17DMAG, NSC 707545) in C.B-17 SCID mice*

bearing MDA-MB-231 human breast cancer xenografts. Cancer Chemother Pharmacol, 2005. **55**(1): p. 21-32.

41. Brough, P.A., et al., *4,5-diarylisoxazole Hsp90 chaperone inhibitors: potential therapeutic agents for the treatment of cancer.* J Med Chem, 2008. **51**(2): p. 196-218.

42. Jensen, M.R., et al., *NVP-AUY922: a small molecule HSP90 inhibitor with potent antitumor activity in preclinical breast cancer models.* Breast Cancer Res, 2008. **10**(2): p. R33.

43. Niewidok, N., et al., *Hsp90 Inhibitors NVP-AUY922 and NVP-BEP800 May Exert a Significant Radiosensitization on Tumor Cells along with a Cell Type-Specific Cytotoxicity.* Transl Oncol, 2012. **5**(5): p. 356-69.

44. Stingl, L., et al., *Novel HSP90 inhibitors, NVP-AUY922 and NVP-BEP800, radiosensitise tumour cells through cell-cycle impairment, increased DNA damage and repair protraction.* Br J Cancer, 2010. **102**(11): p. 1578-91.

45. Hashida, S., et al., *Hsp90 inhibitor NVP-AUY922 enhances the radiation sensitivity of lung cancer cell lines with acquired resistance to EGFR-tyrosine kinase inhibitors.* Oncol Rep, 2015. **33**(3): p. 1499-504.

46. Zaidi, S., et al., *The HSP90 inhibitor NVP-AUY922 radiosensitizes by abrogation of homologous recombination resulting in mitotic entry with unresolved DNA damage.* PLoS One, 2012. **7**(4): p. e35436.

47. Powers, M.V. and P. Workman, *Targeting of multiple signalling pathways by heat shock protein 90 molecular chaperone inhibitors.* Endocr Relat Cancer, 2006. **13 Suppl 1**: p. S125-35.

48. Zou, J., et al., *Repression of heat shock transcription factor HSF1 activation by HSP90 (HSP90 complex) that forms a stress-sensitive complex with HSF1.* Cell, 1998. **94**(4): p. 471-80.

49. Mendillo, M.L., et al., *HSF1 Drives a Transcriptional Program Distinct from Heat Shock to Support Highly Malignant Human Cancers.* Cell, 2012. **150**(3): p. 549-562.

50. Trepel, J., et al., *Targeting the dynamic HSP90 complex in cancer.* Nat Rev Cancer, 2010. **10**(8): p. 537-49.

51. Guttmann, D.M. and C. Koumenis, *The heat shock proteins as targets for radiosensitization and chemosensitization in cancer.* Cancer Biol Ther, 2011. **12**(12): p. 1023-31.

52. Guttmann, D.M., et al., *Inhibition of Hsp27 radiosensitizes head-and-neck cancer by modulating deoxyribonucleic acid repair.* Int J Radiat Oncol Biol Phys, 2013. **87**(1): p. 168-75.

53. Shamovsky, I. and E. Nudler, *New insights into the mechanism of heat shock response activation.* Cell Mol Life Sci, 2008. **65**(6): p. 855-61.

54. Multhoff, G., et al., *A stress-inducible 72-kDa heat-shock protein (HSP72) is expressed on the surface of human tumor cells, but not on normal cells.* Int J Cancer, 1995. **61**(2): p. 272-9.

55. Ferrarini, M., et al., *Unusual expression and localization of heat-shock proteins in human tumor cells.* Int J Cancer, 1992. **51**(4): p. 613-9.

56. Hantschel, M., et al., *Hsp70 plasma membrane expression on primary tumor biopsy material and bone marrow of leukemic patients.* Cell Stress Chaperones, 2000. **5**(5): p. 438-42.

57. Gehrmann, M., et al., *Dual function of membrane-bound heat shock protein 70 (Hsp70), Bag-4, and Hsp40: protection against radiation-induced effects and target structure for natural killer cells.* Cell Death Differ, 2005. **12**(1): p. 38-51.

58. Ma, Y., et al., *How to improve the immunogenicity of chemotherapy and radiotherapy.* Cancer Metastasis Rev, 2011. **30**(1): p. 71-82.

59. Fionda, C., et al., *Heat shock protein-90 inhibitors increase MHC class I-related chain A and B ligand expression on multiple myeloma cells and their ability to trigger NK cell degranulation.* J Immunol, 2009. **183**(7): p. 4385-94.

60.   Boll, B., et al., *Heat shock protein 90 inhibitor BIIB021 (CNF2024) depletes NF-kappaB and sensitizes Hodgkin's lymphoma cells for natural killer cell-mediated cytotoxicity.* Clin Cancer Res, 2009. **15**(16): p. 5108-16.

61.   Zhang, C., et al., *Sodium butyrate upregulates expression of NKG2D ligand MICA/B in HeLa and HepG2 cell lines and increases their susceptibility to NK lysis.* Cancer Immunol Immunother, 2009. **58**(8): p. 1275-85.

62.   Armeanu, S., et al., *Natural killer cell-mediated lysis of hepatoma cells via specific induction of NKG2D ligands by the histone deacetylase inhibitor sodium valproate.* Cancer Res, 2005. **65**(14): p. 6321-9.

63.   Fernandez-Messina, L., H.T. Reyburn, and M. Vales-Gomez, *Human NKG2D-ligands: cell biology strategies to ensure immune recognition.* Front Immunol, 2012. **3**: p. 299.

64.   Multhoff, G., et al., *Heat shock protein 70 (Hsp70) stimulates proliferation and cytolytic activity of natural killer cells.* Exp Hematol, 1999. **27**(11): p. 1627-36.

65.   Multhoff, G., et al., *Heat shock protein 72 on tumor cells: a recognition structure for natural killer cells.* J Immunol, 1997. **158**(9): p. 4341-50.

66.   Elsner, L., et al., *The heat shock protein HSP70 promotes mouse NK cell activity against tumors that express inducible NKG2D ligands.* J Immunol, 2007. **179**(8): p. 5523-33.

67.   Stangl, S., et al., *Control of metastasized pancreatic carcinomas in SCID/beige mice with human IL-2/TKD-activated NK cells.* J Immunol, 2006. **176**(10): p. 6270-6.

68.   Gonzalez, S., et al., *NKG2D ligands: key targets of the immune response.* Trends Immunol, 2008. **29**(8): p. 397-403.

69.   Groh, V., et al., *Cell stress-regulated human major histocompatibility complex class I gene expressed in gastrointestinal epithelium.* Proc Natl Acad Sci U S A, 1996. **93**(22): p. 12445-50.

70.   Wiskirchen, J., et al., *Long-term effects of repetitive exposure to a static magnetic field (1.5 T) on proliferation of human fetal lung fibroblasts.* Magn Reson Med, 1999. **41**(3): p. 464-8.

71.   Zaarur, N., et al., *Targeting heat shock response to sensitize cancer cells to proteasome and Hsp90 inhibitors.* Cancer Res, 2006. **66**(3): p. 1783-91.

72.   Schilling, D., et al., *Induction of plasminogen activator inhibitor type-1 (PAI-1) by hypoxia and irradiation in human head and neck carcinoma cell lines.* BMC Cancer, 2007. **7**: p. 143.

73.   Bryceson, Y.T., et al., *Cytolytic granule polarization and degranulation controlled by different receptors in resting NK cells.* J Exp Med, 2005. **202**(7): p. 1001-12.

74.   Singh, N.P., et al., *A simple technique for quantitation of low levels of DNA damage in individual cells.* Exp Cell Res, 1988. **175**(1): p. 184-91.

75.   Sipinen, V., et al., *In vitro evaluation of baseline and induced DNA damage in human sperm exposed to benzo[a]pyrene or its metabolite benzo[a]pyrene-7,8-diol-9,10-epoxide, using the comet assay.* Mutagenesis, 2010. **25**(4): p. 417-25.

76.   Groh, V., et al., *Recognition of stress-induced MHC molecules by intestinal epithelial gammadelta T cells.* Science, 1998. **279**(5357): p. 1737-40.

77.   Venkataraman, G.M., et al., *Promoter region architecture and transcriptional regulation of the genes for the MHC class I-related chain A and B ligands of NKG2D.* J Immunol, 2007. **178**(2): p. 961-9.

78.   Isernhagen, A., et al., *The MICA-129Met/Val dimorphism affects plasma membrane expression and shedding of the NKG2D ligand MICA.* Immunogenetics, 2016. **68**(2): p. 109-23.

79.   Multhoff, G., et al., *A 14-mer Hsp70 peptide stimulates natural killer (NK) cell activity.* Cell Stress Chaperones, 2001. **6**(4): p. 337-44.

80.   Chen, Y., et al., *Targeting HSF1 sensitizes cancer cells to HSP90 inhibition.* Oncotarget, 2013. **4**(6): p. 816-29.

81. Ciccia, A. and S.J. Elledge, *The DNA damage response: making it safe to play with knives.* Mol Cell, 2010. **40**(2): p. 179-204.
82. Hiom, K., *Coping with DNA double strand breaks.* DNA Repair (Amst), 2010. **9**(12): p. 1256-63.
83. Pardo, B., B. Gomez-Gonzalez, and A. Aguilera, *DNA repair in mammalian cells: DNA double-strand break repair: how to fix a broken relationship.* Cell Mol Life Sci, 2009. **66**(6): p. 1039-56.
84. Noguchi, M., et al., *Inhibition of homologous recombination repair in irradiated tumor cells pretreated with Hsp90 inhibitor 17-allylamino-17-demethoxygeldanamycin.* Biochem Biophys Res Commun, 2006. **351**(3): p. 658-63.
85. Uhlen, M., et al., *Proteomics. Tissue-based map of the human proteome.* Science, 2015. **347**(6220): p. 1260419.
86. Belkacemi, L. and M.O. Hebb, *HSP27 knockdown produces synergistic induction of apoptosis by HSP90 and kinase inhibitors in glioblastoma multiforme.* Anticancer Res, 2014. **34**(9): p. 4915-27.
87. Bulavin, D.V., S.A. Amundson, and A.J. Fornace, *p38 and Chk1 kinases: different conductors for the G(2)/M checkpoint symphony.* Curr Opin Genet Dev, 2002. **12**(1): p. 92-7.
88. Mikhailov, A., M. Shinohara, and C.L. Rieder, *Topoisomerase II and histone deacetylase inhibitors delay the G2/M transition by triggering the p38 MAPK checkpoint pathway.* J Cell Biol, 2004. **166**(4): p. 517-26.
89. Kotlyarov, A., et al., *MAPKAP kinase 2 is essential for LPS-induced TNF-alpha biosynthesis.* Nat Cell Biol, 1999. **1**(2): p. 94-7.
90. Manke, I.A., et al., *MAPKAP kinase-2 is a cell cycle checkpoint kinase that regulates the G2/M transition and S phase progression in response to UV irradiation.* Mol Cell, 2005. **17**(1): p. 37-48.
91. Reinhardt, H.C., et al., *p53-deficient cells rely on ATM- and ATR-mediated checkpoint signaling through the p38MAPK/MK2 pathway for survival after DNA damage.* Cancer Cell, 2007. **11**(2): p. 175-89.
92. Lemaire, M., et al., *CDC25B phosphorylation by p38 and MK-2.* Cell Cycle, 2006. **5**(15): p. 1649-53.
93. Morgan, D.O., *Principles of CDK regulation.* Nature, 1995. **374**(6518): p. 131-4.
94. Morgan, D.O., *Cyclin-dependent kinases: engines, clocks, and microprocessors.* Annu Rev Cell Dev Biol, 1997. **13**: p. 261-91.
95. Morgan, D.O., *Regulation of the APC and the exit from mitosis.* Nat Cell Biol, 1999. **1**(2): p. E47-53.
96. Bulavin, D.V., et al., *Initiation of a G2/M checkpoint after ultraviolet radiation requires p38 kinase.* Nature, 2001. **411**(6833): p. 102-7.
97. Li, Q. and J.D. Martinez, *Loss of HSF1 results in defective radiation-induced G(2) arrest and DNA repair.* Radiat Res, 2011. **176**(1): p. 17-24.
98. Gandhi, N., et al., *Novel Hsp90 inhibitor NVP-AUY922 radiosensitizes prostate cancer cells.* Cancer Biol Ther, 2013. **14**(4): p. 347-56.
99. Heimberger, T., et al., *The heat shock transcription factor 1 as a potential new therapeutic target in multiple myeloma.* Br J Haematol, 2013. **160**(4): p. 465-76.
100. Yoon, Y.J., et al., *KRIBB11 inhibits HSP70 synthesis through inhibition of heat shock factor 1 function by impairing the recruitment of positive transcription elongation factor b to the hsp70 promoter.* J Biol Chem, 2011. **286**(3): p. 1737-47.
101. Lecomte, S., et al., *Roles of heat shock factor 1 and 2 in response to proteasome inhibition: consequence on p53 stability.* Oncogene, 2010. **29**(29): p. 4216-24.
102. Whitesell, L. and S. Lindquist, *Inhibiting the transcription factor HSF1 as an anticancer strategy.* Expert Opin Ther Targets, 2009. **13**(4): p. 469-78.

103. McConnell, J.R., L.K. Buckton, and S.R. McAlpine, *Regulating the master regulator: Controlling heat shock factor 1 as a chemotherapy approach.* Bioorg Med Chem Lett, 2015. **25**(17): p. 3409-14.

104. Vihervaara, A. and L. Sistonen, *HSF1 at a glance.* J Cell Sci, 2014. **127**(Pt 2): p. 261-6.

105. Pinel, M.I., E.B. Esteves, and V.M. Rumjanek, *Natural killer cell activity in Hodgkin's disease patients undergoing radiation therapy or chemotherapy and radiation therapy.* Clin Lab Haematol, 1998. **20**(5): p. 303-6.

106. Miller, G.M., M.L. Andres, and D.S. Gridley, *NK cell depletion results in accelerated tumor growth and attenuates the antitumor effect of total body irradiation.* Int J Oncol, 2003. **23**(6): p. 1585-92.

107. Gridley, D.S., et al., *Comparison of proton and electron radiation effects on biological responses in liver, spleen and blood.* Int J Radiat Biol, 2011. **87**(12): p. 1173-81.

108. Aloy, M.T., et al., *Protective role of Hsp27 protein against gamma radiation-induced apoptosis and radiosensitization effects of Hsp27 gene silencing in different human tumor cells.* Int J Radiat Oncol Biol Phys, 2008. **70**(2): p. 543-53.

109. Weichselbaum, R.R., et al., *Radiation-resistant and repair-proficient human tumor cells may be associated with radiotherapy failure in head- and neck-cancer patients.* Proc Natl Acad Sci U S A, 1986. **83**(8): p. 2684-8.

110. Kassem, H., et al., *A potential role of heat shock proteins and nicotinamide N-methyl transferase in predicting response to radiation in bladder cancer.* Int J Cancer, 2002. **101**(5): p. 454-60.

111. Gibbons, N.B., et al., *Heat-shock proteins inhibit induction of prostate cancer cell apoptosis.* Prostate, 2000. **45**(1): p. 58-65.

112. Engel, K., et al., *Constitutive activation of mitogen-activated protein kinase-activated protein kinase 2 by mutation of phosphorylation sites and an A-helix motif.* J Biol Chem, 1995. **270**(45): p. 27213-21.

113. Ben-Levy, R., et al., *Identification of novel phosphorylation sites required for activation of MAPKAP kinase-2.* EMBO J, 1995. **14**(23): p. 5920-30.

114. Shaltiel, I.A., et al., *The same, only different - DNA damage checkpoints and their reversal throughout the cell cycle.* J Cell Sci, 2015. **128**(4): p. 607-20.

115. Venkatakrishnan, C.D., et al., *HSP27 regulates p53 transcriptional activity in doxorubicin-treated fibroblasts and cardiac H9c2 cells: p21 upregulation and G2/M phase cell cycle arrest.* Am J Physiol Heart Circ Physiol, 2008. **294**(4): p. H1736-44.

116. Winter, S.F., et al., *Development of antibodies against p53 in lung cancer patients appears to be dependent on the type of p53 mutation.* Cancer Res, 1992. **52**(15): p. 4168-74.

117. Wang, M., et al., *EGF receptor inhibition radiosensitizes NSCLC cells by inducing senescence in cells sustaining DNA double-strand breaks.* Cancer Res, 2011. **71**(19): p. 6261-9.

118. Zhou, B.B. and S.J. Elledge, *The DNA damage response: putting checkpoints in perspective.* Nature, 2000. **408**(6811): p. 433-9.

119. Kastan, M.B. and J. Bartek, *Cell-cycle checkpoints and cancer.* Nature, 2004. **432**(7015): p. 316-23.

120. Gurgis, F.M., W. Ziaziaris, and L. Munoz, *Mitogen-activated protein kinase-activated protein kinase 2 in neuroinflammation, heat shock protein 27 phosphorylation, and cell cycle: role and targeting.* Mol Pharmacol, 2014. **85**(2): p. 345-56.

121. Reinhardt, H.C. and M.B. Yaffe, *Kinases that control the cell cycle in response to DNA damage: Chk1, Chk2, and MK2.* Curr Opin Cell Biol, 2009. **21**(2): p. 245-55.

122. Landry, J., et al., *Human HSP27 is phosphorylated at serines 78 and 82 by heat shock and mitogen-activated kinases that recognize the same amino acid motif as S6 kinase II.* J Biol Chem, 1992. **267**(2): p. 794-803.

VII. SUMMARIES OF THE INCLUDED PUBLICATIONS

A) Role of membrane Hsp70 in radiation sensitivity of tumor cells

Naoya Murakami*, Annett Kühnel*, Thomas E. Schmid*, Katarina Ilicic, Stefan Stangl, Isabella S. Braun, Mathias Gehrmann, Michael Molls, Jun Itami and Gabriele Multhoff

*authors contributed equally to this work

Background: The major stress-inducible heat shock protein 70 (Hsp70) is frequently overexpressed in the cytosol and integrated in the plasma membrane of tumor cells. Following stress such as non-lethal irradiation Hsp70 synthesis is upregulated. Intracellular located Hsp70 is known to exert cytoprotective properties, however, less is known about membrane (m)Hsp70. Herein, the role of mHsp70 in the sensitivity towards irradiation in tumor sublines that differ in their cytosolic and/or mHsp70 levels was investigated.

Principal findings: CX+/CX− tumor cells were used that exhibited similar cytosolic but differed significantly in their mHsp70 levels, 4 T1 ctrl/4 T1 Hsp70 knockdown (k.d.) cells which showed significant differences in their cytosolic and mHsp70 levels and H1339 and EPLC-272H ctrl/ HSF-1 k.d. lung carcinoma cells that had similar mHsp70 but significantly different cytosolic Hsp70 levels.

The DNA double strand break (DSB) marker γH2AX was significantly upregulated in irradiated CX− and 4 T1 Hsp70 k.d. with low basal mHsp70 levels, but not in their mHsp70 high expressing counterparts, irrespectively of their cytosolic Hsp70 content. After irradiation γH2AX, Caspase 3/7 and Annexin V were upregulated in the lung carcinoma cells H1339 and EPLC-272H, but no significant differences were observed between ctrl and HSF-1 k.d. sublines that exhibit identical mHsp70 but strongly differ in their cytosolic Hsp70 levels.

According to that, clonogenic cell survival was significantly lower in CX− and 4 T1 Hsp70 k.d. cells with low mHsp70 expression, than in CX+ and 4 T1 ctrl cells, whereas no difference in clonogenic cell survival was observed in ctrl and HSF-1 k.d. sublines of H1339 and EPLC-272H with identical mHsp70 but different cytosolic Hsp70 levels.

Conclusion: In summary, these results point at an important role of mHsp70 on radiation resistance.

Own contributions to the publication

- Establishing of H1339 and EPLC-272H control and HSF-1 knockdown cell lines
- Conception and performance of all experiments in which ctrl/HSF-1 k.d. cells were used, including data analysis, processing and statistical analysis
- Performing of clonogenic cell survival assays with CX-/CX+ and 4T1 ctrl/Hsp70 k.d. cell lines, including data analysis, processing and statistical analysis
- Major contributions in writing the manuscript

B) NZ28-induced inhibition of HSF1, SP1 and NF-κB triggers the loss of the natural killer cell-activating ligands MICA/B on human tumor cells

Daniela Schilling*, Annett Kühnel*, Fabian Tetzlaff, Sarah Konrad, Gabriele Multhoff
*authors contributed equally to this work

Background: The activity of natural killer (NK) cells is regulated by activating and inhibiting receptors, whereby the C-type lectin natural killer group 2D (NKG2D) receptor serves as the major activating receptor on NK cells which recognizes major histocompatibility class I chain-related proteins A and B (MICA/B). The MICA/B expression has been described to be regulated by the transcription factor heat shock factor 1 (HSF-1). Inhibition of heat shock protein 90 (Hsp90) is known to induce the heat shock response via activation of HSF-1 which is associated with tumor development, metastasis and therapy resistance and with an increased susceptibility to NK cell-mediated lysis.

Principal findings: The effects of Hsp90 inhibitor NVP-AUY922, HSF-1 inhibitor NZ28 and HSF-1 knockdown on the sensitivity of lung (H1339) and breast (MDA-MB-231, T47D) cancer cells to NK cell-mediated cytotoxicity and the expression of the NKG2D ligands MICA/B were tested.
Although NVP-AUY922 activates HSF-1, neither the MICA/B surface density on tumor cells nor their susceptibility to NK cell-mediated lysis was affected.
A single knockdown of HSF-1 decreased the surface expression of MICB but not that of MICA, and thereby, the NK cell-mediated lysis was only partially blocked. In contrast, NZ28 completely blocked the MICA/B membrane expression on tumor cells and thereby strongly inhibited the NK cell-mediated cytotoxicity. This effect might be explained by a simultaneous inhibition of the transcription factors HSF-1, SP1 and NF-κB by NZ28.

Conclusion: These findings suggest that the immune-activatory and -inhibitory effects of new anticancer therapeutics should be investigated.

Own contributions to the publication

- Establishing of H1339 control and HSF-1 knockdown cell lines
- NK cell isolation by magnetic separation and characterization
- Conception and performance of all experiments in which ctrl/HSF-1 k.d. cells were used, including data analysis, processing and statistical analysis
- Major contributions in writing the manuscript

C) Sensitizing tumor cells to radiation by targeting the heat shock response

Daniela Schilling, Annett Kühnel, Sarah Konrad, Fabian Tetzlaff, Christine Bayer, Julia Yaglom, Gabriele Multhoff

Background: Elevated levels of heat shock proteins (HSPs) contribute to tumor cell survival and mediate protection against radiation-induced cell death. Hsp90 inhibitors are promising radiosensitizers but also activate heat shock factor 1 (HSF-1) and thereby induce the synthesis of cytoprotective Hsp70. In this study, the heat shock response inhibitor NZ28 either alone or in combination with the Hsp90 inhibitor NVPAUY922 was investigated for radiosensitizing effects, alterations in cell cycle distribution and effects on migratory/invasive capacity of radioresistant tumor cells.

Principal findings: NZ28 reduced the constitutive and NVPAUY922-induced Hsp70 expression by inhibition of the HSF-1 activity and inhibited migration and invasion in human lung and breast tumor cells. Treatment of tumor cells with NZ28 significantly increased their radiation response. One possible mechanism might be a decrease of the radioresistant S-phase. When combined with the Hsp90 inhibitor NVP-AUY922 the concentration of NZ28 could be significantly reduced (1/10th–1/20th) to achieve the same radiosensitization.

Conclusion: These results demonstrate that a dual targeting of Hsp70 and Hsp90 with NZ28 and NVP-AUY922 potentiates the radiation response of tumor cells that are otherwise resistant to ionizing radiation.

Own contributions to the publication

- Performing of clonogenic cell survival assays with H1339, including data analysis, processing and statistical analysis
- Establishing and performing the HSE luciferase assay with H1339 and EPLC-272H cells, including data analysis, processing and statistical analysis
- Contributions in writing the manuscript

VIII. APPENDIX

Eidesstattliche Erklärung

Ich, Annett Kühnel, erkläre an Eides statt, dass ich die der Fakultät Wissenschaftszentrum Weihenstephan für Ernährung, Landnutzung und Umwelt (WZW) der Technischen Universität München zur Promotionsprüfung vorgelegte Arbeit mit dem Titel:

"The effect of heat shock factor 1 (HSF-1) and heat shock proteins Hsp70 and Hsp27 on radiosensitivity and immunogenicity"

am Lehrstuhl für Experimentelle Radioonkologie und Strahlentherapie am Klinikum rechts der Isar der TU München unter der Anleitung und Betreuung durch Prof. Dr. Gabriele Multhoff ohne sonstige Hilfe erstellt und bei der Auffassung nur die gemäß § 6 Abs. 6 und 7 Satz 2 angegebenen Hilfsmittel benutzt habe.

Ich habe keine Organisation eingeschaltet, die gegen Entgelt Betreuerinnen und Betreuer für die Anfertigung von Dissertation sucht, oder die mir obliegenden Pflichten hinsichtlich der Prüfungsleistungen für mich ganz oder teilweise erledigt.

Ich habe die Dissertation in dieser oder ähnlicher Form in keinem anderen Prüfungsverfahren als Prüfungsleistung vorgelegt.

Ich habe den angestrebten Doktorgrad noch nicht erworben und bin nicht in einem früheren Promotionsverfahren für den angestrebten Doktorgrad endgültig gescheitert.

Die öffentlich zugängliche Promotionsordnung der TUM ist mir bekannt, insbesondere habe ich die Bedeutung von § 28 (Nichtigkeit der Promotion) und § 29 (Entzug des Doktorgrades) zur Kenntnis genommen. Ich bin mir der Konsequenzen einer falschen Eidesstattlichen Erklärung bewusst.

München, den 10. Mai 2016   _____

                                                                          Annett Kühnel

Danksagung

Curriculum vitae

Personal data

Name:	Annett Kühnel
Date of birth:	3rd July 1987
Place of birth:	Köthen (Anhalt)

Personal and professional development

04/2013 - 06/2016	Doctorate (Dr. rer. nat.) Department of Radiation Oncology Klinikum rechts der Isar, Technical University Munich
08/2015 - 01/2016	Biologist at VRagments; biological consulting during the prototype development of a serious game for health in Virtual Reality
2012 - 2013	Travels in Europe, America and Asia
2010 - 2012	Master of Science, Molecular Medicine Institute of Molecular Virology, University Ulm Subject of the master thesis: "The effect of semen on mucosal epithelial integrity and HIV transmission" Supervised by Prof. Kirchhoff and Prof. Münch
2007 - 2010	Bachelor of Science, Biology Institute of Genetics, Martin-Luther-University Halle-Wittenberg Subject of the bachelor thesis: "Functional analysis of the telomere-associated isoform Mod(mdg4)-64.2 in *Drosophila melanogaster*"
2000 - 2007	Abitur, Ludwigsgymnasium Köthen Advanced courses in biology, mathematics, psychology

Awards and scholarships

2015	Laura Bassi prize of the TU Munich
2014	Poster prize radiation biology, annual meeting ÖGRO/BAYRO, Innsbruck
2007 - 2012	Scholarship holder of the Hans-Böckler foundation
2007	Karl-von-Frisch-Abitur award (biology), VBIO Saxony-Anhalt

Engagement

2011 - 2012	Supervisor of a children's group in Ulm at Nature and Biodiversity Conservation Union Germany (NABU)
2008 - 2010	Active member in the council of student representatives of biology Martin-Luther-University Halle-Wittenberg (financial issues, evaluation of the degree program, event organization)
2007	Member of the organizational team „Abiball"
2005 - 2007	Private tutoring in mathematics and biology

Trainings / workshops

2016	Business administration basics
2015	"E-Camp! Develop market opportunities based on research results" UnternehmerTUM - center for innovation and business creation at the TU Munich
2015	Successful cooperation in teams
2015	Team leadership
2014	"Getting started with a [junior] research group: Setting the compass" $science^{plus®}$ workshop, Golin science management
2014	Labor law
2014	Research project management
2012	Time management and self-organization
2011	Intercultural competence
2010	Rhetoric

Reprint permissions

A) Radiation Oncology

B) Cancer Immunology, Immunotherapy

C) Cancer Letters

You are free to:
- Share — copy and redistribute the material in any medium or format

The licensor cannot revoke these freedoms as long as you follow the license terms. (http://creativecommons.org/licenses/by-nc-nd/4.0/)

User license*	Read, print and download	Redistribute or re-publish the final article (e.g. display in a repository)	Text and data mine	Translate the article	Reuse portions or extracts from the article in other works	Sell or re-use for commercial purposes
CC BY-NC-ND 4.0	Yes	Yes	Yes	Yes For private use only and not for distribution	Yes	No

Included publications

RADIATION ONCOLOGY

RESEARCH

Open Access

CrossMark

Role of membrane Hsp70 in radiation sensitivity of tumor cells

Naoya Murakami[1,2†], Annett Kühnel[1†], Thomas E. Schmid[1†], Katarina Ilicic[1], Stefan Stangl[1], Isabella S. Braun[1], Mathias Gehrmann[1], Michael Molls[1], Jun Itami[2] and Gabriele Multhoff[1,3*]

Abstract

Background: The major stress-inducible heat shock protein 70 (Hsp70) is frequently overexpressed in the cytosol and integrated in the plasma membrane of tumor cells via lipid anchorage. Following stress such as non-lethal irradiation Hsp70 synthesis is up-regulated. Intracellular located Hsp70 is known to exert cytoprotective properties, however, less is known about membrane (m)Hsp70. Herein, we investigate the role of mHsp70 in the sensitivity towards irradiation in tumor sublines that differ in their cytosolic and/or mHsp70 levels.

Methods: The isogenic human colon carcinoma sublines CX^+ with stable high and CX^- with stable low expression of mHsp70 were generated by fluorescence activated cell sorting, the mouse mammary carcinoma sublines 4 T1 (4 T1 ctrl) and Hsp70 knock-down (4 T1 Hsp70 KD) were produced using the CRISPR/Cas9 system, and the Hsp70 down-regulation in human lung carcinoma sublines H1339 ctrl/H1339 HSF-1 KD and EPLC-272H ctrl/EPLC-272H HSF-1 KD was achieved by small interfering (si)RNA against Heat shock factor 1 (HSF-1). Cytosolic and mHsp70 was quantified by Western blot analysis/ELISA and flow cytometry; double strand breaks (DSBs) and apoptosis were measured by flow cytometry using antibodies against γH2AX and real-time PCR (RT-PCR) using primers and antibodies directed against apoptosis related genes; and radiation sensitivity was determined using clonogenic cell surviving assays.

Results: CX^+/CX^- tumor cells exhibited similar cytosolic but differed significantly in their mHsp70 levels, 4 T1 ctrl/ 4 T1 Hsp70 KD cells showed significant differences in their cytosolic and mHsp70 levels and H1339 ctrl/H1339 HSF-1 KD and EPLC-272H ctrl/EPLC-272H HSF-1 KD lung carcinoma cell sublines had similar mHsp70 but significantly different cytosolic Hsp70 levels. γH2AX was significantly up-regulated in irradiated CX^- and 4 T1 Hsp70 KD with low basal mHsp70 levels, but not in their mHsp70 high expressing counterparts, irrespectively of their cytosolic Hsp70 content. After irradiation γH2AX, Caspase 3/7 and Annexin V were up-regulated in the lung carcinoma sublines, but no significant differences were observed in H1339 ctrl/H1339 HSF-1 KD, and EPLC-272H ctrl/EPLC-272H HSF-1 KD that exhibit identical mHsp70 but different cytosolic Hsp70 levels. Clonogenic cell survival was significantly lower in CX^- and 4 T1 Hsp70 KD cells with low mHsp70 expression, than in CX+ and 4 T1 ctrl cells, whereas no difference in clonogenic cell survival was observed in H1339 ctrl/H1339 HSF-1 KD and EPLC-272H ctrl/ EPLC-272H HSF-1 KD sublines with identical mHsp70 but different cytosolic Hsp70 levels.

Conclusion: In summary, our results indicate that mHsp70 has an impact on radiation resistance.

Keywords: Heat shock protein 70, Membrane localization, Apoptosis, X-ray irradiation, Radiation resistance

* Correspondence: Gabriele.Multhoff@tum.de
†Equal contributors
[1]Department of Radiation Oncology, Klinikum rechts der Isar, Technische Universität München, Munich, Germany
[3]Clinical Cooperation Group - Innate Immunity in Tumor Biology, Institute of Biomedical Imaging (IBMI), Helmholtz Zentrum München, Munich, Germany
Full list of author information is available at the end of the article

BioMed Central

Murakami *et al. Radiation Oncology* (2015) 10:149

Page 2 of 13

Background

Apart from surgery and chemotherapy, radiotherapy is one of the three key treatment modalities to treat localized solid tumors. The major goal of therapeutic irradiation is to inflict deleterious damage selectively in tumor cells. While some cancer cells are directly killed by irradiation, others appear to activate mechanisms of resistance. Similar to other stress stimuli such as hyperthermia, hypoxia, reactive oxygen species (ROS), heavy metals, cytotoxic drugs, glucose deprivation also ionizing irradiation induces a complex stress reaction in the exposed tumor and normal tissues [1, 2]. Heat shock protein 70 (Hsp70), one of the major stress-inducible members of the 70 kDa stress protein family (HSP70) whose expression is mainly regulated by Heat Shock Factor 1 (HSF-1) consists of at least 8 homologous members, exerts tumorigenic functions by sustaining proliferative cell signaling, increasing invasive and metastatic activity and migration and by preventing apoptotic signaling [3, 4]. Hsp70 is frequently constitutively overexpressed in the cytosol and present on the plasma membrane of many different tumor types [5–7] to promote cancer cell survival, tumorigenicity and anti-apoptotic activities, such as interfering with the apoptosis signal regulating kinase 1 (ASK1) and the co-chaperone CHIP [5–11], blocking BAX translocation to the mitochondria [12] or by interfering with lysosomal membranes and thereby inhibiting their permeabilization [13]. Apart from its intracellulat localization, Hsp70 can be transported to and anchored on the plasma membrane of tumor, but not normal cells, via tumor-specific lipid vesicular transport which is not completely unravelled [14]. Membrane Hsp70-positive tumors have been shown to actively release Hsp70 in exosomes [14, 15] that can fuse with the plasma membrane. Since normal cells do not present Hsp70 on their cell surfaces, mHsp70 serves as a tumor-specific targeting structure for *in vivo* imaging [16, 17], and lipid-bound Hsp70 in the blood might provide a novel tumor biomarker in liquid biopsies [14, 15].

As mentioned before, cytosolic Hsp70 exerts cytoprotective properties by interfering with anti-apoptotic signaling pathways [18]. In mammalian cells, apoptosis can be caused by either intrinsic or extrinsic pathways [19] whereby apoptotic factors such as cytochrome *c* which are released by mitochondria with a disturbed membrane potential induce the intrinsic pathway [20, 21], and the binding of extracellular protein death ligands of the tumor necrosis factor (TNF) family to pro-apoptotic death receptors (DRs) on the cell surface can initiate the extrinsic apoptotic cascade [20].

Overexpression of Hsp70 can provide tumor cells with a selective survival advantage in part due to its ability to inhibit multiple pathways of cell death, including both intrinsic and extrinsic apoptosis [10, 22, 23]. Hsp70 can bind directly to the pro-apoptotic Bcl-2 family member BAX, which is part of the intrinsic apoptosis pathway and thus prevents its activation and translocation to the mitochondria [24, 25]. Hsp70 can also interact with death receptors DR4 and DR5 of the extrinsic apoptotic pathway and thus inhibits the assembly of the death-inducing signaling complexes [26]. Therefore, inhibition of cytosolic Hsp70 provides a promising concept in anti-cancer therapies. It also has been described that mHsp70-positive tumor cells are better protected against ionizing irradiation compared to their mHsp70-negative counterparts [27]. Herein, we want to study the impact of cytosolic versus mHsp70 in the radiosensitivity of four isogenic tumor cell systems.

Materials and methods

Cells and cell culture

Three human and one mouse carcinoma subline of different origin was used in the study. The size of mouse carcinoma cells significantly smaller than that of the human tumor cell lines. The human adeno colon carcinoma cell line CX-2 (Tumorzellbank, DKFZ Heidelberg, Germany) gave rise to the sublines CX$^+$ with a stable high and CX$^-$ with a low mHsp70 expression after fluorescence activated cell sorting [27, 28]. The HSF-1 knock-down (HSF-1 KD) and ctrl human lung cancer cell lines H1339 (small cell lung carcinoma, SCLC) and EPLC-272H (non-small cell lung carcinoma, NSCLC; kindly provided by Prof. Rudolf Huber, Dpt. of Pneumonology, University Munich, Germany) as well as the CX$^+$/CX$^-$ sublines were cultured in Roswell Park Memorial Institute (RPMI)1640 medium (GIBCO, Eggenstein, Germany) supplemented with 10 % *v/v* heat-inactivated fetal calf serum (FCS) (PAA, Pasching, Austria), 1 % *v/v* antibiotics (100 IU/ml penicillin, 100 μg/ml streptomycin, GIBCO), 2 mM L-glutamine (GIBCO) and 1 mM sodium pyruvate (GIBCO). All adherent growing tumor cells were trypsinized for less than 3 min with trypsin-ethylene diamine-tetra-acetic acid (EDTA) (GIBCO), and single cell suspensions were seeded at constant cell densities of 1.5×10^6 cells in 15 ml fresh medium in T-75 ventilated culture flasks (Greiner, Nuertingen, Germany).

For knock-down of Hsp70 in the lung carcinoma cells H1339 and EPLC-272H HSF1 RNAi-Ready pSIREN-RetroQ vectors with a puromycin resistance (BD Biosciences) was used. Target sequence for HSF-1 small interfering RNA was 5′-TATGGACTCCAACCTGGA-TAA-3′ [29]. Retroviruses were produced by transfection of Phoenix cells with pSIREN-RetroQ/HSF1 shRNA (shHSF1) or pSIREN-RetroQ (control) (kindly provided by Profs. J. Yaglom and M. Sherman, Boston University School of Medicine, USA) using Ca-phosphate. Tumor cells were infected with virus containing supernatants in the presence of 10 μg/ml polybrene. Selection was performed with 2 μg/ml puromycin.

Murakami *et al. Radiation Oncology* (2015) 10:149

Page 3 of 13

The mouse mammary carcinoma derived 4 T1 cell line (ATCC®CRL-2539™, American Type Culture Collection, Manassas, USA) was used to knock-down Hsp70 by the CRISPR/Cas9 system [17, 30]. The RNA-guided Cas9 nuclease [31], derived from *Streptococcus pyogenes* was used to induce specific DSBs in regions of the chromosome that are coding for Hsp70 (HSPA1A/B). After DSBs were introduced to specific loci, damaged DNA was repaired by non-homologous end joining (NHEJ) [32] which resulted in shift of the sequence and a knock-down (KD) of the targeted gene was achieved [33]. By using this procedure the subline 4 T1 Hsp70 KD was generated which showed a significant but not complete reduction in cytosolic and mHsp70. As a control, 4 T1 cells were transfected with a control vector 4 T1 (ctrl). To obtain a complete Hsp70 knock-out a second and third treatment cycle using the CRISPR/Cas9 system was necessary [17]. The 4 T1 sublines were cultured in Roswell Park Memorial Institute 1640 medium (GIBCO, Eggenstein, Germany) supplemented with 10 % v/v heat-inactivated fetal calf serum (FCS) (GIBCO), 1 % v/v antibiotics (penicillin-streptomycin, GIBCO), 2 mM L-glutamine (GIBCO), non-essential amino acids, and β-mercaptoethanol. All adherent tumor cells were trypsinized for 5 min with trypsin-ethylene diamine-tetra acetic acid (EDTA) (GIBCO), and single cell suspensions were seeded at constant cell densities of 1.0×10^6 cells in 20 ml fresh medium in T-75 ventilated culture flasks (Greiner, Nuertingen, Germany). Following exposure to stress the 4 T1 Hsp70 KD cell line showed a moderate up-regulation of Hsp70 in the cytosol which was less pronounced than that of 4 T1 ctrl cells (data not shown).

All tumor cell sublines were routinely checked and determined as negative for mycoplasma contamination.

SDS-PAGE, western blot analysis, ELISA
Cytosolic proteins were obtained as described previously [1]. Briefly, 2×10^6 cells were lysed in 10 mM Tris-buffered saline (TBST buffer, pH 7.5) containing 1 % Nonidet P-40 (NP-40; Sigma Aldrich, St. Louis, MO, USA) on ice for 45 min. Non-soluble material was pelleted by centrifugation at 10,000 g and discarded. Protein concentration was determined with the bicinchoninic acid method (BCA Protein Assay Kit; Pierce, Thermo Fisher Scientific Inc., Rockford, IL, USA). Equal protein amounts (20 μg) were subjected to the 10 % sodium dodecyl sulfate-polyacrylamide gel (SDS-PAGE) following a standard protocol [34]. 10 ng and 25 ng of recombinant Hsp70 protein [35] were loaded as positive control and for protein quantification. After SDS-PAGE, the proteins were transferred to nitrocellulose membranes (Millipore Corp., Bedford, MA, USA) and/or PVDF membranes following a standard protocol [36]. Non-specific binding of the membranes was blocked with 5 % skim milk

in PBS supplemented with 1 % Tween-20. Blots were incubated with the Hsp70 primary antibody (cmHsp70.1, IgG1; multimmune, Munich, Germany) and a β-actin antibody (A5316, Sigma-Aldrich) at 4 °C for 14 h. After two washing steps, membranes were incubated with a secondary antibody (goat anti-mouse IgG peroxidase-conjugated; Promega, Madison, WI, USA) at room temperature for 1 h. All antibodies were diluted in 1 % skim milk in PBS supplemented with 1 % Tween-20. Immune complexes were detected using the ECL detection system (Amersham Biosciences, Buckinghamshire, UK). Blots were imaged digitally (ChemiDoc Touch Imaging System, Biorad Laboratories, Hercules, CA, USA) and quantified using Image Lab Software (Biorad Laboratories) with automatic settings. The absolute amount of Hsp70 was determined by the ratio of the ß-actin-normalized integrated volumes of bands, related to Hsp70 positive controls with known amounts which were used as internal standards.

Hsp70 concentrations were verified by ELISA (R&D systems) in cell lysates following the manufacturer's recommendations. Hsp70 concentrations were calculated relative to the total protein content of each sample.

Irradiation of tumor cells
CX sublines were irradiated with a single dose of 0 Gy (sham) to 20 Gy, using the Gulmay RS225A irradiation machine (Gulmay Medical Ltd., Camberley, UK) at a dose rate of 0.90 Gy/min (15 mA, 200 keV). A dose of 20 Gy was chosen for γH2AX and Caspase 3/7 and Annexin V assays because concentrations below did not result in statistically significant results but showed the same trend. 4 T1, H1339 and EPLC-272H cell sublines were irradiated with a single dose of 0 Gy (sham) to 6 Gy with same irradiation equipment as used for the CX sublines.

Flow cytometry of mHsp70
Single cell suspensions of untreated and treated CX, 4 T1, H1339 and EPLC-272H sublines were collected at different time-points after irradiation. A sample of 0.4×10^6 cells was washed once with 10 % FCS in phosphate-buffered saline (PBS) and incubated with fluorescein isothiocyanate (FITC)-conjugated mouse monoclonal antibody specific for mHsp70 (cmHsp70.1, IgG1; multimmune GmbH, Munich, Germany) or a FITC-labeled isotype-matched IgG-negative control antibody (code 345815; BD Biosciences, NJ, USA) on ice in the dark for 30 min. Only propidium iodide-negative, viable cells were gated and the mean fluorescence intensity (mfi) of antibody-bound cells was analyzed by a FACSCalibur flow cytometer (Becton Dikinson, Heidelberg, Germany). The mfi is a relative value of the total intensity of the signal derived from cmHsp70.1-FITC

Murakami *et al. Radiation Oncology* (2015) 10:149

Page 4 of 13

antibody stained, viable cells (50,000) subtracted by the intensity of the signal intensity which is derived by viable cells stained with an isotype-matched IgG1-FITC control antibody. Fluorescence data were plotted by using CellQuest software (Becton Dickinson, Heidelberg, Germany).

Flow cytometry of γH2AX

DSBs were assessed by using γH2AX (phosphorylated Histone H2AX) antibody. The single cell suspensions of either sham irradiated and/or irradiated CX, 4 T1, H1339 and EPLC-272H sublines were collected 1 h after irradiation using trypsin and by mechanical disruption. Single cell suspensions containing 0.6×10^6 cells were washed in 0.5 ml PBS and fixed with 70 % ethanol/acetic acid (3:1). Fixed cells were kept at –20 °C for up to two weeks before analysis. After removal of the fixative, cell pellets were re-suspended with 1 ml of 0.15 % Triton X-100 solution and incubated on ice with anti-phospho-Histone H2AX, Alexa Fluor 488 conjugate (Novus Biologicals). The mfi of cells that did bind the antibody was analyzed by flow cytometry.

Quantitative analysis of gene expression

48 h after irradiation total RNA was extracted from cell pellet containing 1.0×10^6 cells of CX or 4 T1 cells with MasterPureTM RNA Purification Kit (Epicentre, Madison, USA). The concentration of RNA was measured by a Nanodrop™ spectrophotometer at 260 nm. RNA was reversely transcribed into cDNA using High Capacity cDNA Reverse Transcription Kits (Life Technologies GmbH, Darmstadt, Germany). The resulting cDNA was subjected to quantitative RT-PCR using primers directed towards Caspase 3, Caspase 7, Caspase 8, Caspase 9, BAD and BAX. Actin B (ActB) was used as a house keeping gene. The reaction mix was prepared according to the standard protocol of the kit. RT-PCR was carried out with a LightCycler® 480 (Roche Diagnostics, Mannheim, Germany) with a standard thermal profile. Transcriptional changes were calculated with delta Ct method and normalized with the house keeping gene. Mean values were obtained from triplicate samples.

Expression of active Caspase 7, phosphorylated (p)BAD and BAX

Cell lysates (50 μg/ml) were subjected to SDS-PAGE (12.5 %) and after transfer, membranes [36] were incubated with a primary rabbit-anti-active Caspase 7, rabbit-anti-phospho-BAD (1:1000; Ser[136]), and rabbit-anti-BAX (1:1000; Cell Signaling Technology, Beverly, MA, USA) antibody. Following washing, the nitrocellulose (NC) membranes were incubated with a horseradish peroxidase (HRP) conjugated secondary anti-

rabbit IgG and detected using the ECL system, as described above.

Flow cytometry of active Caspase 3/7 and Annexin V

Apoptosis was assessed in all tumor sublines using CellEvent® Caspase 3/7 Green Detection Reagent (Life Technologies, Darmstadt, Germany). Single cell suspensions of sham irradiated and irradiated tumor cells were collected 24 and 48 h after irradiation using trypsin and mechanical disruption. The single cell suspension containing 0.4×10^6 were washed in 1 ml PBS and incubated with CellEvent® Caspase 3/7 Green Detection Reagent and SYTOX AADvanced® dead cell stain solution. The percentage of antibody-bound cells among viable cells was determined on a flow cytometer.

Apoptosis was determined in CX^+/CX^- and 4 T1 ctrl/ 4 T1 Hsp70 KD tumor sublines also by Annexin V-FITC staining. After washing with Annexin V binding buffer cells were incubated with Annexin V-FITC (Roche Diagnostics, Mannheim, Germany) for 15 min at room temperature. After another washing step in PBS/10 % *v/v* FCS and 2.5 mM $CaCl_2$, propidium iodide (PI) was added for 1 min. Then cells were analyzed on a FACSCalibur flow cytometer (BD).

Clonogenic cell survival assay

Single cell suspensions were seeded onto 12-well plates. CX tumor sublines were irradiated with 0, 2, 4, 6, and 10 Gy and 4 T1, H1339, and EPLC-272H tumor sublines were irradiated with 0, 2, 4, and 6 Gy at the Gulmay RS225A irradiation machine (Gulamy Medical Ltd., Cambereley, UK). A dose of 20 Gy resulted in too few colonies and thus could not be analyzed (data not shown). Cells were fixed in ice cold methanol after reaching colonies containing more than 50 cells and stained with 0.1 % crystal violet. All colonies with more than 50 cells were counted automatically using a Bioreader® (Bio-Sys GmbH, Karben, Germany). To create a radiation survival curve, the survival fraction at each radiation dose was normalized to that control which was sham-irradiated with 0 Gy.

Statistical analysis

Mean value was calculated and presented with standard deviation. The Student *t*-test was used to evaluate the relevance between variables. A *p*-value of ≤0.05 was considered as statistically significant.

Results

Comparison of cytosolic and mHsp70 levels in isogenic tumor sublines

We investigated cytosolic and mHsp70 levels in isogenic human colon carcinoma sublines CX^+/CX^-, mouse mammary carcinoma cell lines 4 T1 ctrl/4 T1 Hsp70 knock-

Murakami *et al. Radiation Oncology* (2015) 10:149

Page 5 of 13

down (4 T1 Hsp70 KD), human lung carcinoma cell sublines H1339 ctrl/H1339 HSF-1 KD and EPLC-272H ctrl/EPLC-272H HSF-1 KD. Figure 1 shows representative Western blots of tumor cell lysates of all cell lines under non-stressed conditions using cmHsp70.1 antibody for the detection of Hsp70. A defined amount of recombinant Hsp70 protein (10 ng and 25 ng) was loaded onto the gel for quantification and β-actin was used as a loading control and for normalization. Although CX^+ (36.4 ± 4.8 ng) and CX^- (32.9 ± 5.0 ng) tumor sublines revealed similar cytosolic Hsp70 levels (Fig. 1a and c), the tumor sublines differed significantly in their mHsp70 expression under non-stressed conditions (sham; Fig. 2a). Following irradiation at 20 Gy the mHsp70 expression was significantly up-regulated on CX^- but not CX^+ tumor cells (20 Gy; Fig. 2a). A lower irradiation dose of 10 Gy showed a similar trend with respect to the mHsp70 expression on CX^- cells but did not reach statistical significance (data not shown).
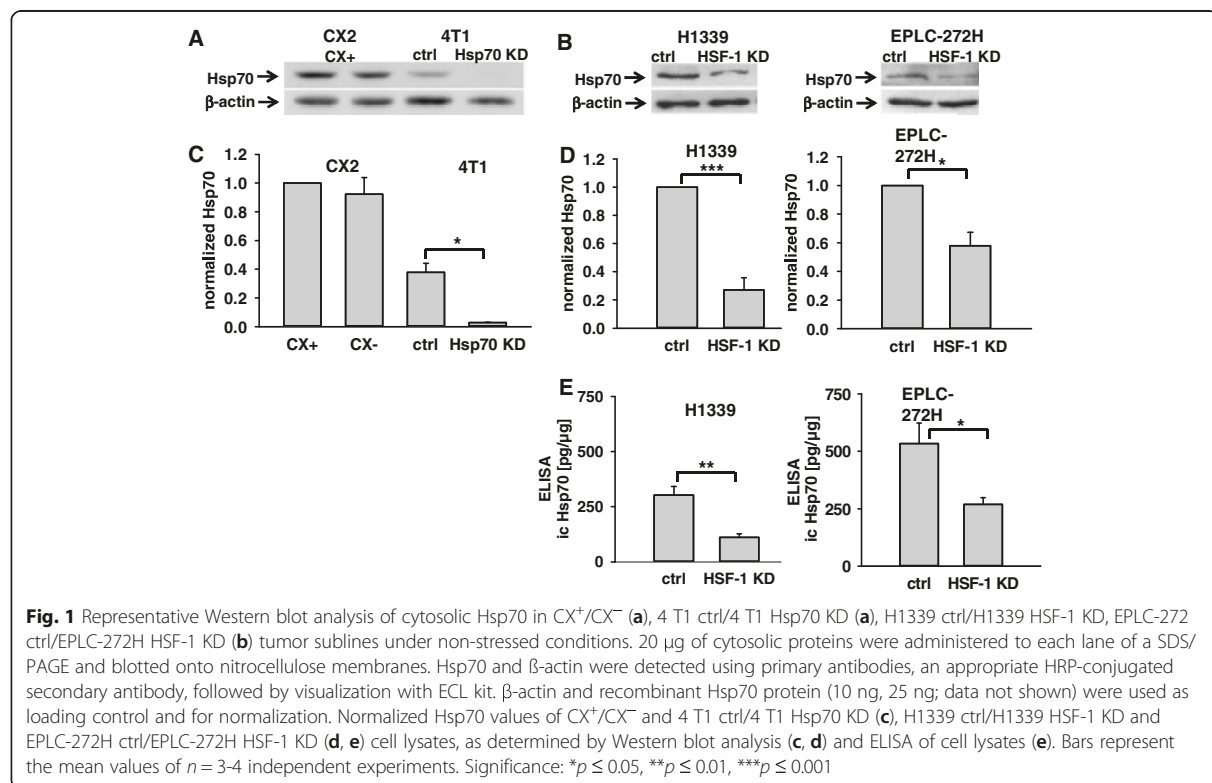
No differences in the cytosolic Hsp70 levels were detected in 4 T1 cells that had been transfected with a control vector (ctrl) versus 4 T1 wild type (WT) cells (data not shown). A CRISPR/Cas9 Hsp70 knock-down (4 T1 Hsp70 KD) revealed significantly lower cytosolic Hsp70 levels than in 4 T1 ctrl (Fig. 1a and b) and 4 T1 WT cells (data not shown), and mHsp70 levels were significantly higher in 4 T1 ctrl versus 4 T1 Hsp70 KD cells under non-stressed conditions (sham; Fig. 2b).

Following irradiation at 6 Gy the mHsp70 expression was significantly up-regulated in 4 T1 Hsp70 KD cells but not in 4 T1 ctrl cells (6 Gy; Fig. 2b). A lower irradiation dose of 4 Gy showed a similar trend but the values did not reach statistical significance (data not shown). 4 T1 mouse mammary carcinoma cells showed lower Hsp70 levels in the cytosol than human CX^+/CX^- cells (Fig. 1a). Although the density of Hsp70 molecules on the cell surface is similar in mouse and human tumor cells, the mfi appears to be higher in 4 T1 cells due to their smaller size.

A siRNA knock-down of HSF-1 in H1339 and EPLC-272H lung carcinoma cells resulted in a significant down-regulation of Hsp70 in the cytosol of these tumor sublines, as determined by Western blot analysis (Fig. 1d) and ELISA (Fig. 1e). However, the reduced cytosolic Hsp70 levels induced by HSF-1 knock-down did not affect the mHsp70 levels, under non-stressed conditions (Fig. 2c and d) and following irradiation at 6 Gy (Fig. 2d).

Comparison of radiation-induced DNA double strand breaks (DSBs) in tumor sublines with different cytosolic and mHsp70 levels

A quantification of the γH2AX foci as a measure for DSBs was determined by flow cytometry one hour after irradiation of CX^+/CX^- cells (Fig. 3a) with 0 Gy (sham)
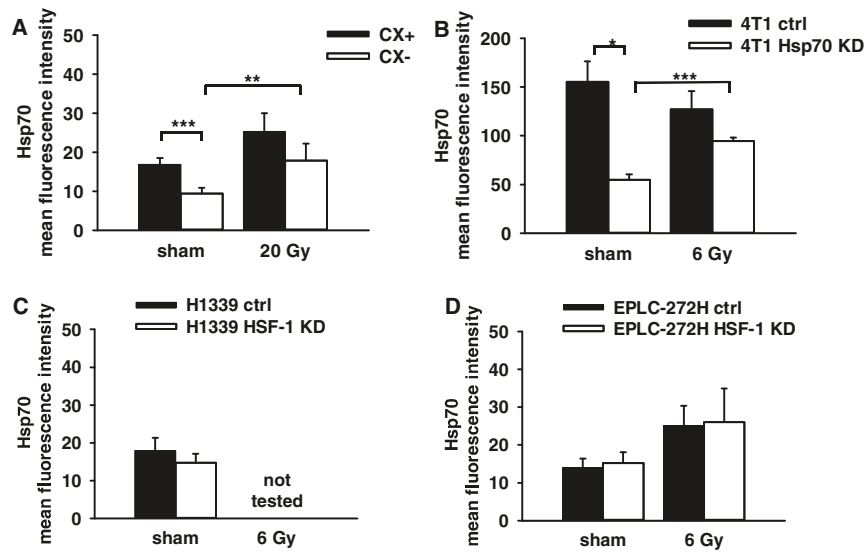

Fig. 1 Representative Western blot analysis of cytosolic Hsp70 in CX^+/CX^- (**a**), 4 T1 ctrl/4 T1 Hsp70 KD (**a**), H1339 ctrl/H1339 HSF-1 KD, EPLC-272 ctrl/EPLC-272H HSF-1 KD (**b**) tumor sublines under non-stressed conditions. 20 μg of cytosolic proteins were administered to each lane of a SDS/PAGE and blotted onto nitrocellulose membranes. Hsp70 and ß-actin were detected using primary antibodies, an appropriate HRP-conjugated secondary antibody, followed by visualization with ECL kit. β-actin and recombinant Hsp70 protein (10 ng, 25 ng; data not shown) were used as loading control and for normalization. Normalized Hsp70 values of CX^+/CX^- and 4 T1 ctrl/4 T1 Hsp70 KD (**c**), H1339 ctrl/H1339 HSF-1 KD and EPLC-272H ctrl/EPLC-272H HSF-1 KD (**d, e**) cell lysates, as determined by Western blot analysis (**c, d**) and ELISA of cell lysates (**e**). Bars represent the mean values of n = 3-4 independent experiments. Significance: *p ≤ 0.05, **p ≤ 0.01, ***p ≤ 0.001

Murakami *et al. Radiation Oncology* (2015) 10:149

Page 6 of 13

Fig. 2 Mean fluorescence intensity (mfi) of mHsp70 in CX$^+$/CX$^-$ cells 48 h after sham (0 Gy) and 20 Gy irradiation (**a**, n = 3-4), 4 T1 ctrl/4 T1 Hsp70 KD cells after sham (0 Gy) and 6 Gy irradiation (**b**, n = 3-4), H1339 ctrl/H1339 HSF-1 (**c**, n = 4) after sham (0 Gy) and EPLC-272H ctrl/EPLC-272H HSF-1 KD (**d**, n = 6) after sham (0 Gy) and 6 Gy irradiation. Bars represent the mean values and the corresponding standard error of the mean (SEM) of n = 3-6 independent experiments. Significance: *$p \leq$ 0.05, **$p \leq$ 0.01, ***$p \leq$ 0.001
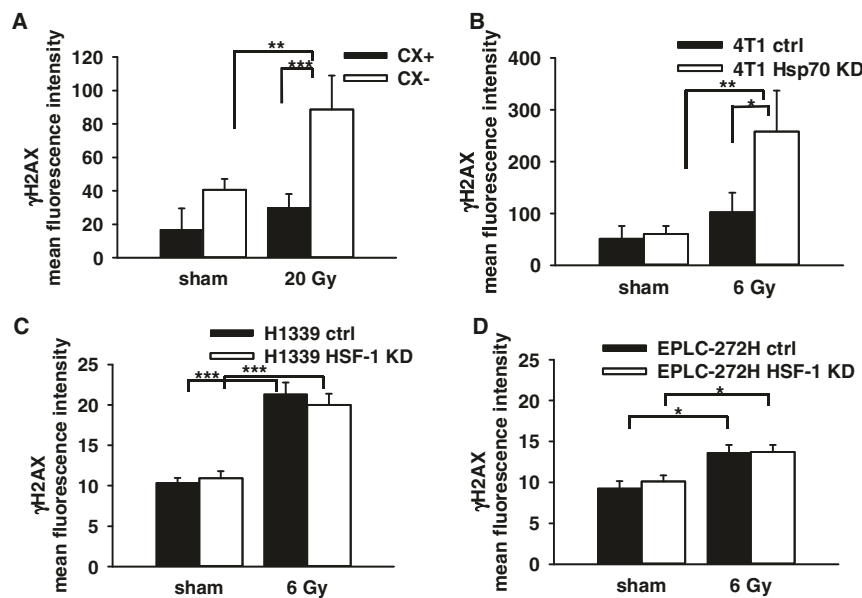
Fig. 3 Mean fluorescence intensity (mfi) of γH2AX foci in CX$^+$/CX$^-$ cells 1 h after sham (0 Gy) and 20 Gy irradiation (**a**), and 4 T1 ctrl/4 T1 Hsp70 KD cells (**b**), H1339 ctrl/H1339 HSF-1 cells (**c**), EPLC-272H ctrl/EPLC-272H HSF-1 KD cells (**d**) 1 h after sham (0 Gy) and 6 Gy irradiation, respectively (**b**, **c**, **d**). Bars represent the mean values and the corresponding standard error of the mean (SEM) of n = 3 independent experiments. Significance: *$p \leq$ 0.05, **$p \leq$ 0.01, ***$p \leq$ 0.001

Murakami *et al. Radiation Oncology* (2015) 10:149

Page 7 of 13

and 20 Gy, 4 T1 ctrl/4 T1 Hsp70 KD cells (Fig. 3b) with 0 Gy (sham) and 6 Gy, H1339 ctrl/H1339 HSF-1 KD (Fig. 3c) and EPLC-272H ctrl/EPLC-272H HSF-1 KD cells (Fig. 3d) with 0 Gy (sham) and 6 Gy. After irradiation a significant increase in γH2AX was observed in CX^- (40.58 ± 6.45 vs. 88.52 ± 14.19, $p \leq 0.01$) and 4 T1 Hsp70 KD cells (60.64 ± 15.20 vs. 257.81 ± 32.04, $p \leq 0.01$), whilst no statistically significant increase was observed in non-irradiated versus irradiated CX^+ and 4 T1 ctrl (or WT cells, data not shown) with initially high mHsp70 expression. The γH2AX mfi values of irradiated CX^+/CX^- (20 Gy; $p \leq 0.001$) and 4 T1 ctrl/4 T1 Hsp70 KD (6 Gy; $p \leq 0.05$) sublines also differed significantly. γH2AX did not differ significantly in the sublines H1339 ctrl/H1339 HSF-1 KD and EPLC-272H/EPLC-272H HSF-1 KD that show an identical mHsp70 expression (Fig. 3c and d). However, significant differences in γH2AX foci were observed in sham (0 Gy) and irradiated (6 Gy) lung cancer sublines were compared (Fig. 3c and d).

Comparison of radiation-induced apoptosis in tumor sublines with different cytosolic and mHsp70 levels

For measuring radiation-induced apoptosis the percentage of active Caspase 3/7 positive cells was determined 48 h after sham (0 Gy) and 20 Gy irradiation of CX^+/CX^- tumor cells by flow cytometry (Fig. 4a). After radiation exposure, the number of apoptotic cells increased in both, CX^+ (3.11 % ± 0.06 % vs. 6.70 % ± 0.97 %, $p \leq 0.01$) and CX^- (4.16 % ± 0.16 % vs. 16.67 % ± 0.81 %, $p \leq 0.001$) cells, but, the percentage of apoptotic cells after irradiation (20 Gy) was significantly higher in CX^- than in CX^+ cells ($p \leq 0.001$). Fig. 4b shows similar results for the 4 T1 cell system 48 h after irradiation with 6 Gy. Apoptosis was significantly more pronounced in irradiated (6 Gy) compared to sham irradiated 4 T1 ctrl cells (0.60 % ± 0.06 % vs. 4.55 % ± 0.54 %, $p \leq 0.01$) and 4 T1 Hsp70 KD cells (0.16 % ± 0.06 % vs. 7.72 % ± 0.21 %, $p \leq 0.001$). Compared to irradiated 4 T1 ctrl cells, the percentage of apoptotic cells in 4 T1 Hsp70 KD cells with partial Hsp70 knock-down ($p \leq 0.001$) was
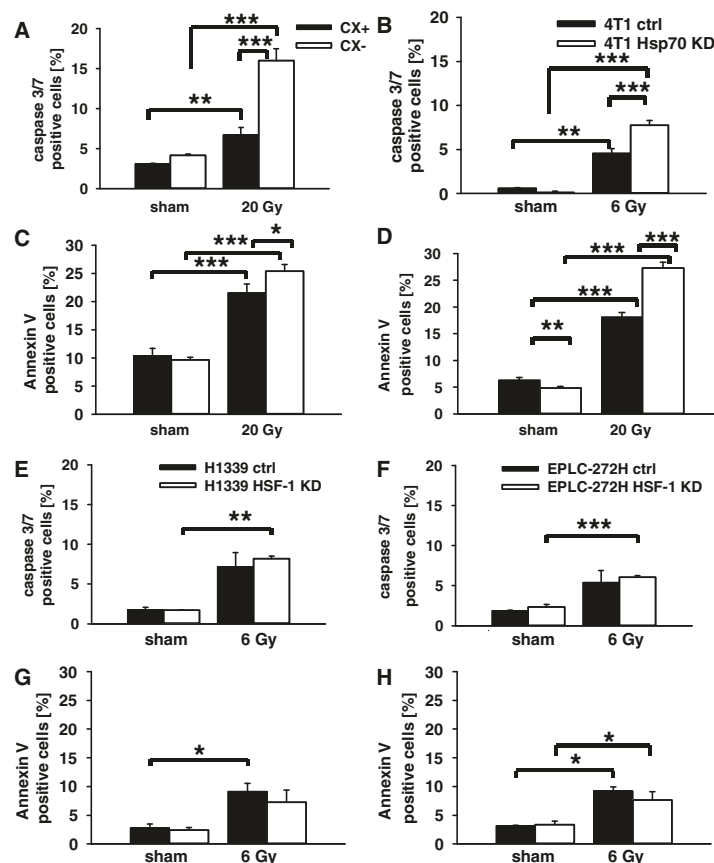

Fig. 4 Percentage of apoptotic cells as assessed by active Caspase 3/7 (**a**, **b**, **e**, **f**) and Annexin V (**c**, **d**, **g**, **h**) staining in CX^+/CX^- cells (**a**, **c**) 48 h after sham (0 Gy) and 20 Gy irradiation and 4 T1 ctrl/4 T1 Hsp70 KD cells (**b**, **d**), H1339 ctrl/H1339 HSF-1 cells (**e**, **g**), EPLC-272H ctrl/EPLC-272H HSF-1 KD cells (**f**, **h**) 48 h after sham (0 Gy) and 6 Gy irradiation, respectively. Bars represent the mean values and the corresponding standard error of the mean (SEM) of n = 3-4 experiments. Significance: *$p \leq 0.05$, **$p \leq 0.01$, ***$p \leq 0.001$

Murakami *et al. Radiation Oncology* (2015) 10:149

Page 8 of 13

again significantly higher (Fig. 4b). Apoptosis as measured with the Annexin V assay in CX⁺/CX⁻ (Fig. 4c) and 4 T1 ctrl/4 T1 Hsp70 KD (Fig. 4d) tumor cells after sham (0 Gy) and 20 Gy irradiation and H1339 ctrl/H1339 HSF-1 KD and EPLC-272H ctrl/EPLC-272H HSF-1 KD cells confirmed the results of the Caspase3/7 assay. A radiation dose of 4 Gy for 4 T1 ctrl/4 T1 Hsp70 KD cells and 10 Gy for CX⁺/CX⁻ cells showed a similar trend, however, the data did not reach statistical significance (data not shown).

In contrast, lung tumor sublines H1339 ctrl/H1339 HSF-1 KD and EPLC-272H ctrl/EPLC-272H HSF-1 KD with identical mHsp70 levels did not show significant differences in apoptosis, as determined by active Caspase 3/7 and Annexin V positivity under non-irradiated (sham) and irradiated (6 Gy) conditions (Fig. 4e and f), although an increased apoptosis was observed following irradiation at 6 Gy in both tumor cell systems.

For further evaluation of radiation-induced changes the relative gene expression levels of the 4 T1 tumor sublines were analyzed 1 h after radiation at 0 Gy and 6 Gy. After irradiation, a more than 2-fold up-regulation in the gene expression of Caspase 3, Caspase 7, and the Bcl-2 subfamily members BAD (BH3) and BAX (Bcl-2-like protein 4) was observed in the mHsp70 low expressing 4 T1 Hsp70 KD cell line but not in the 4 T1 ctrl cell line (Fig. 5a).

Significant differences in the gene expression ratios between 4 T1 ctrl and 4 T1 Hsp70 KD cells were observed for Caspase 7 (0.9-fold vs.3.3-fold, $p \leq 0.05$), BAX (1.1-fold vs. 2.5-fold, $p \leq 0.05$) and BAD (0.7-fold vs. 2.0-fold, $p \leq 0.05$). No differences in the gene expression analysis were observed in 4 T1 ctrl cells that had been transfected with a control vector versus 4 T1 WT cells (data not shown).

Due to their higher radiation-resistance no significant changes in apoptosis regulated gene expression was observed in CX⁺ and CX⁻ cells after irradiation with 20 Gy (data not shown). However, also in these tumor sublines, CX⁻ cells with the lower mHsp70 expression showed an increased expression in Caspase 3/7, BAD and BAX compared to CX⁺ cells.

With respect to the levels of apoptosis related proteins differences were observed in phosphorylated (p)BAD (Fig. 5b) and active Caspase 7 (Fig. 5c), as determined by Western blot analysis. The amount of anti-apoptotic pBAD decreased in 4 T1 Hsp70 KD cells 24 h after irradiation at 6 Gy, but not in 4 T1 ctrl cells, and active Caspase 7 was found to be up-regulated following irradiation in 4 T1 Hsp70 KD cells, but not in 4 T1 ctrl cells. No significant differences were observed in the amount of the cytosolic protein BAX after irradiation (data not shown). A
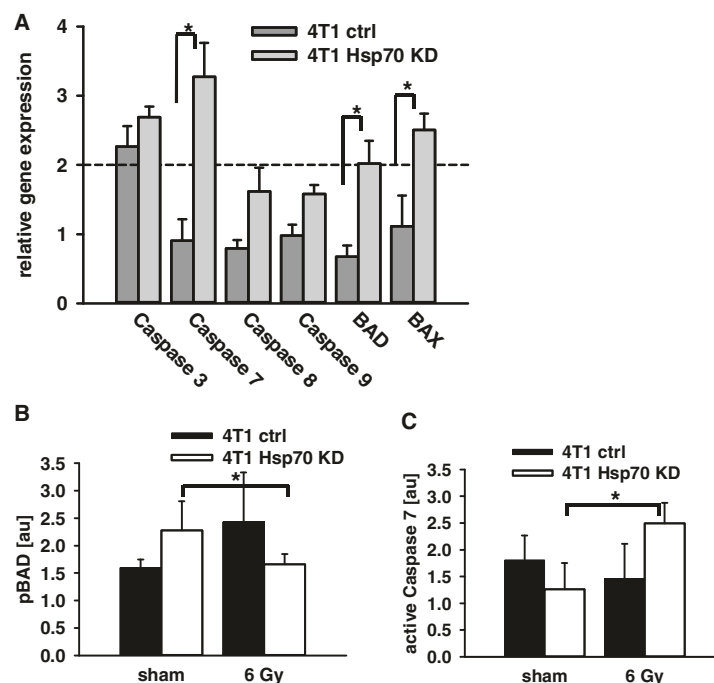

Fig. 5 Apoptosis related gene expression of Caspase 3, Caspase 7, Caspase 8, Caspase 9, BAD and BAX were analyzed using a quantitative RT-PCR in sham (0 Gy) and 6 Gy irradiated 4 T1 ctrl/4 T1 Hsp70 KD cells (**a**) 1 h after irradiation. Bars represent the mean values and the corresponding standard error of the mean (SEM). Significance: *$p \leq 0.05$. Protein expression of phosphorylated (p)BAD (**b**), active Caspase 7 (**c**) and BAX (data not shown) were determined 24 h after sham (0 Gy) and 6 Gy irradiation in 4 T1 ctrl/ 4 T1 Hsp70 KD (**b**). Significance: *$p = 0.05$

Murakami *et al. Radiation Oncology* (2015) 10:149

Page 9 of 13

similar trend which did not reach statistical significance was found in the CX$^+$/CX$^-$ tumor sublines.

Comparison of radiation-induced changes in the clonogenic cell survival in tumor sublines with different cytosolic and mHsp70 levels

Radiation sensitivity of CX (Fig. 6a), 4 T1 (Fig. 6b), H1339 (Fig. 6c) and EPLC-272H (Fig. 6d) tumor sublines was assessed in clonogenic cell survival assays. Data were fitted by the linear quadratic model (Y = (αD + βD^2) to describe the cell survival following irradiation. In line with the data obtained by the apoptosis assays (Fig. 4a), the CX$^+$ cell line, which shows a higher mHsp70 expression than the CX$^-$ cell line, was significantly more radiation-resistant at 2 Gy ($p \le 0.05$), 4 Gy ($p \le 0.01$), and 6 Gy ($p \le 0.05$), respectively. Despite differences in the mHsp70 expression density, CX$^+$ and CX$^-$ tumor sublines did not differ in their cytosolic Hsp70 levels (Fig. 1). The α/β ratio was 9.67 for CX$^+$ (D$_{50}$ = 2.09 Gy) and 35.9 for CX$^-$ (D$_{50}$ = 1.45 Gy).

Figure 6b shows the results of colony forming assays for 4 T1 ctrl and 4 T1 Hsp70 KD tumor cells. In line with the data of the apoptosis assay shown in Fig. 4b, 4 T1 Hsp70 KD cells which do express very little Hsp70 in the cytosol under non-stressed conditions and exhibited a lower expression density on the membrane were significantly more radiation-sensitive than 4 T1 ctrl at each individual radiation dose ($p \le 0.001$, $p \le 0.001$ and $p \le 0.001$ in 2, 4, and 6 Gy, respectively). The α/β ratio was 0.6 for 4 T1 ctrl (D$_{50}$ = 3.6 Gy) and 4.3 for 4 T1 Hsp70 KD (D$_{50}$ = 1.9 Gy). No significant difference in radiation sensitivity was observed when clonogenic cell survival was compared in 4 T1 ctrl cells that were transfected with a control vector and 4 T1 WT cells (data not shown).

H1339 and EPLC-272H lung carcinoma cells and their mHsp70 identical HSF-1 KD counterparts did not show any significant differences in clonogenic cell survival (Fig. 6c and d) despite significant differences in their cytosolic Hsp70 levels.

Discussion

Radiotherapy plays a central role in the therapy of solid tumors, either as a single treatment modality or in combination with surgery or systemic chemotherapy. However, therapeutic outcome is limited due to radiation-resistant tumor cell clones. Therefore, a better understanding of the biological mechanisms which are involved in radiation resistance of tumor cells might improve the outcome of clinical radiotherapy. Several biomarkers such as EpCAM [37], mutated *p53* [38] or Bcl-2 [39] have been investigated which were found to be associated to radiation sensitivity.

Hsp70 the major stress-inducible member of the HSP70 family [40] is rapidly up-regulated when cells experience stress, such as ionizing radiation, cytostatic compounds, heat and hypoxia, nutrient deficiency or any other stressful events [41–43]. It is important to note that high cytosolic levels of Hsp70 are frequently found in cancer cells even under physiological, non-stressed conditions [8, 22] and that an increased Hsp70 expression correlates with tumor progression, metastasis, resistance to cytostatic drugs and poor prognosis [8, 40, 41]. Hsp70 plays important roles in the protection
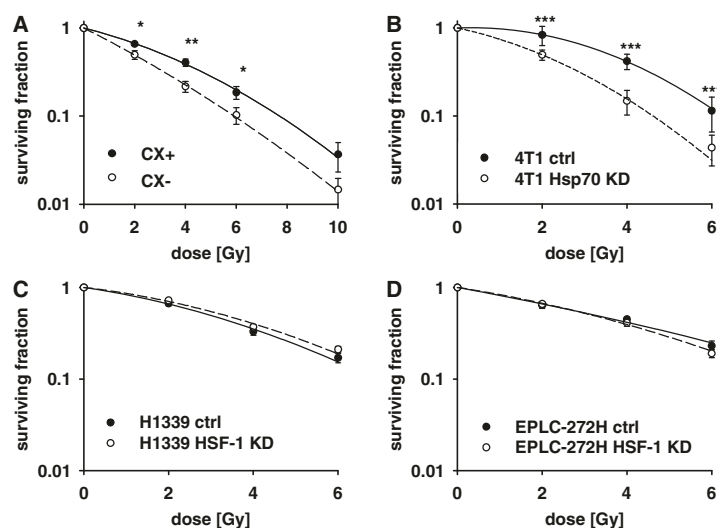

Fig. 6 Clonogenic cell survival data of CX$^+$/CX$^-$ cells (**a**), (*n* = 8) following irradiation at 4 Gy, 6 Gy and 10 Gy and 4 T1 ctrl/4 T1 Hsp70 KD cells (**b**), (*n* = 3), H1339 ctrl/H1339 HSF-1 cells (**c**), (*n* = 4), EPLC-272H ctrl/EPLC-272H HSF-1 KD cells (**d**), (*n* = 4) following irradiation at 2, 4 and 6 Gy, respectively. Significance: *$p \le 0.05$, **$p \le 0.01$, ***$p \le 0.001$

Murakami *et al. Radiation Oncology* (2015) 10:149

Page 10 of 13

against programmed cell death [10, 23] by interfering with apoptosis pathways downstream of the execution protease caspase-3-like [10], and as an inhibitor of apoptosis by the recruitment of pro-caspase 9 and binding to the apoptosome Apaf-1 [44, 45]. Together with its co-chaperone CHIP, Hsp70 can block TNFα-induced apoptosis through the formation of a complex consisting of Hsp70/CHIP and the apoptosis signal-regulating kinase 1 ASK1 [11, 46]. Furthermore, Hsp70 can inhibit the translocation of the pro-apoptotic molecule BAX to mitochondria [12]. A translocation and anchorage of Hsp70 into lysosomal membranes also has been found to promote tumor cell survival by stabilization of lysosomal membranes [22, 47]. In collaboration with the group of Jäättelä, we could show that tumor cells that do present Hsp70 on their plasma membrane also exhibit Hsp70 in their lysosomal membranes and thus are better protected towards apoptotic stimuli such as irradiation [22]. As shown previously, Hsp70 is transported to the plasma membrane via a non-classical ER/Golgi transport pathway, since inhibitors of this pathway such as Brefeldin A or Monensin did not block Hsp70 plasma membrane expression [5]. These findings are in line with earlier work of Hightower and Guidon [48] who have shown an ER-independent release of Hsp70 from viable cells with intact cell membrane. Similar to Hsp70 other molecules lacking a secretory signal such as IL1-α, IL-1β, HMGB1 are described to be exported and imported in a similar way [49]. The work of Jäättelää et al. [22] and our own data [17, 50] demonstrate a localization of Hsp70 in lysosomal membranes and endosomes. Therefore, we speculate that Hsp70 might be transported to the plasma membrane via fusion of Hsp70 carrying lipid vesicles with the plasma membrane. Potential lipid candidates which have been proven to interact with recombinant Hsp70 are phosphatidylserine PS and the lipid raft component globoyltriaosylceramide Gb3 [35, 51]. Furthermore, Hsp70 and peptides derived thereof have been found to be able to cross membranes of living tumor cells by the involvement of lipid rafts and endocytosis-dependent/independent mechanisms [16, 52, 53]. Therefore, it was assumed that after interaction of cytosolic Hsp70 with lipid vesicles containing PS or Gb3, Hsp70 can interact with these vesicles in the cytosol. After fusion of these vesicles with the plasma membrane, Hsp70 gets integrated into the plasma membrane.

Vice versa the fluorescently labelled antibody cmHsp70.1 which binds to mHsp70 on viable tumor cells translocates from the plasma membrane into early endosomes and lysosomes [17]. We hypothesize that this Hsp70-vesicle mediated translocation is reversible and also can occur from the cytosol to the membrane. Regarding these later findings herein, we asked the question as to whether plasma mHsp70 is

associated with resistance of tumor cells to apoptotic cell death and thus might negatively affect sensitivity of tumor cells towards radiation [5].

Screening of more than 1000 primary human tumor biopsies and the corresponding normal tissues revealed that human carcinomas, but none of the tested corresponding normal tissues, frequently present Hsp70 on their cell surface [5–7]. Functionally, mHsp70 serves as a tumor-specific target structure for cells of the innate immune system, especially Natural Killer (NK) cells that had been activated with Hsp70 peptide TKD plus low dose IL-2. Furthermore, Hsp70 stabilizes cell membranes under stress and acts cytoprotective against apoptosis inducing mechanisms [13, 22, 54].

Although cytosolic Hsp70 has been described to exert cytoprotective properties against irradiation [27] only little is known about the role of mHsp70 in the Hsp70-mediated radiation resistance. It has been shown that mHsp70-positive tumor cells are better protected against ionizing irradiation compared to their mHsp70-negative counterparts [27]. A better understanding of the Hsp70 associated pathways which contribute to the development of radiation resistance might stimulate novel strategies to increase the radiation sensitivity of tumor cells.

To address this research question three human and one mouse isogenic tumor cell system that differed not only in their cytosolic but also in their mHsp70 levels were analyzed comparatively. Although CX^+ tumor cells exhibited significantly higher mHsp70 expression levels than CX^- cells their cytosolic Hsp70 were similar [27, 28]. In contrast, the CRISPR/Cas9 Hsp70 knock-down mouse mammary carcinoma cell line 4 T1 did only express low levels of Hsp70 on the plasma membrane and in the cytosol, while 4 T1 ctrl and WT cells exhibited a strong membrane and cytosolic expression [17]. To further analyze the impact of mHsp70 in radiation resistance, Hsp70 was down-regulated in two lung carcinoma cells by a siRNA HSF-1 KD. In contrast to the CRISPR/Cas9 Hsp70 KD, an HSF-1 KD resulted in a significant decrease in cytosolic Hsp70 levels whilst mHsp70 expression remained unaffected.

Among other assays, of radiation-induced the measurement DSBs is an important endpoint for investigating radiation sensitivity because DSBs potentially lead to cell death if they are not repaired properly before start of the next cell division [55, 56]. The phosphorylation of H2A Histone family, member X (H2AX) on serine 139 which is then termed γH2AX provides a sensitive marker for DSBs. Since tumor sublines with low or missing mHsp70 expression in both isogenic cell systems (CX^-, 4 T1 Hsp70 KD) showed higher γH2AX fluorescence intensities than their high mHsp70 expressing counterparts, irrespectively of their cytosolic Hsp70 levels we speculate that mHsp70 might be involved in the protection of

Murakami *et al. Radiation Oncology* (2015) 10:149

Page 11 of 13

tumor cells against radiation-induced stress. In contrast, tumor sublines with identical mHsp70 expression but different cytosolic Hsp70 levels did not show differences in their γH2AX values.

Radiation-induced apoptosis was analyzed using activated Caspase 3/7 antibodies and Annexin V in flow cytometry in the non-irradiated and irradiated tumor sublines. In line with the results of the γH2AX assay, significantly more apoptotic cells were found in irradiated tumor cells with a low mHsp70 expression, whereas tumor sublines with identical mHsp70 levels did not differ in apoptosis, despite differences in their cytosolic Hsp70 levels.

Apoptosis can be induced either by an intrinsic or extrinsic pathway. Both pathways depend on the initiator Caspases 2, 8, 9 and 10 and the effector Caspases 3, 6 and 7. The intrinsic pathway of apoptosis gets activated in response to various noxious stimuli, such as radiation-induced DNA damage. The balance between pro- and anti-apoptotic Bcl-2 proteins controls the permeability of the outer mitochondrial membrane [57]. BAX and BAD are both pro-apoptotic members of the Bcl-2 family and mediate the release of cytochrome *c* from the mitochondria and thus induce the intrinsic apoptotic pathway [58].

In the current study, gene expression analysis was performed with representative initiator Caspases 8, 9 and effector Caspases 3 and 7 and the pro-apoptotic molecules BAD and BAX. Following irradiation, only Hsp70 KD cells lacking Hsp70 in the cytosol and on the plasma membrane showed a significant up-regulation of effector Caspases 3, 7 and BAD and BAX. These data point towards a dependency of the intrinsic apoptotic pathway on cytosolic and mHsp70 following radiation-induced DNA damage. Although not reaching statistical significance a similar trend could be seen in the isogenic CX+/CX− cell system. Previous findings of Gotoh and Stankiewicz [24, 25] showed that Hsp70 can block stress-induced apoptosis primarily by inhibiting the activation of BAX. In the absence of cytosolic Hsp70, BAX might be activated and thus could stimulate apoptosis. Despite differences in the BAX gene expression the cytosolic BAX protein levels did not differ significantly in the tested tumor sublines.

Traditionally, cellular radiation sensitivity is measured using the clonogenic cell survival assay as the gold standard. In line with the results of the DSB repair and apoptosis assays, the clonogenic cell survival was also significantly lower in tumor sublines with a low mHsp70 expression, irrespectively of their intracellular Hsp70 levels. These data also correspond well with the findings of Gehrmann et al. who showed that high mHsp70 expressing tumor cells are better protected against ionizing irradiation compared to their low mHsp70 expressing counterparts [27]. Moreover,

patients with membrane Hsp70-positive tumors have shown a significantly decreased overall survival compared to those with mHsp70-negative tumors [59].

Our current study demonstrates that a reduction of the amount of mHsp70 might improve the possibility to induce apoptosis through the intrinsic apoptotic pathway after X-ray irradiation. This finding is in line with previous reports showing that chemotherapy and radiotherapy predominantly initiate apoptosis through the intrinsic pathway [20]. By using an HSF-1 KD system which down-regulates cytosolic but not mHsp70 levels we could demonstrate that mHsp70 but not cytosolic Hsp70 levels have an impact on the radiation sensitivity of tumor cells. This is an important finding for the development of novel radiotherapy strategies for the treatment of radiation resistant tumor cells. Future studies assessing radiation-sensitization with inhibitors of the vesicular transport of Hsp70 to the plasma membrane of tumor cells could be taken into account. Furthermore, the mHsp70 status which could be determined in the serum of patients using a novel ELISA detecting liposomal Hsp70 which is actively released by mHsp70 positive viable tumor cells [60] might provide a useful tool to predict the radiation sensitivity of tumors over time. We have shown previously that the majority of Hsp70 found in the circulation of tumor patients is actively released in lipid vesicles. Patients with inflammatory diseases have significantly lower serum Hsp70 levels than tumor patients [61]. In these patients Hsp70 is released as a free protein which is predominantly derived from dying cells. Therefore, we speculate that significantly elevated Hsp70 serum levels which are detectable by the novel lipHsp70 ELISA [59] might have diagnostic/prognostic value.

Conclusion

The results of this study indicate that not only cytosolic but also mHsp70 has an impact on radiation sensitivity. Thus, mHsp70 expression is associated with defined variations in the regulation of survival pathways in response to radiation. The expression of mHsp70 on tumor cells should be considered as potential new biomarker to identify radiation-resistance of tumor cells.

Murakami *et al. Radiation Oncology* (2015) 10:149

Page 12 of 13

Author details
[1]Department of Radiation Oncology, Klinikum rechts der Isar, Technische Universität München, Munich, Germany. [2]Department of Radiation Oncology, National Cancer Center Hospital, Tokyo, Japan. [3]Clinical Cooperation Group - Innate Immunity in Tumor Biology, Institute of Biomedical Imaging (IBMI), Helmholtz Zentrum München, Munich, Germany.

References
1. Botzler C, Ellwart J, Günther W, Eissner G, Multhoff G. Synergistic effects of heat and ET-18-OCH3 on membrane expression of hsp70 and lysis of leukemic K562 cells. Exp Hematol. 1999;27(3):470–8. doi:10.1016/S0301-472X(98)00055-1.
2. Sharma S, Singh R, Kaur M, Kaur G. Late-onset dietary restriction compensates for age-related increase in oxidative stress and alterations of HSP70 and synapsin 1 protein levels in male Wistar rats. Biogerontology. 2010;11(2):197–209. doi:10.1007/s10522-009-9240-4.
3. Ciocca DR, Arrigo AP, Calderwood SK. Heat shock proteins and heat shock factor-1 in carcinogenesis and tumor development: an update. Arch Toxicol. 2013;87(1):19–48. doi:10.1007/s00204-012-0918-z.
4. Dakappagari N, Neely L, Tangri S, Lundgren K, Hipolito L, Estrellado A, et al. An investigation into the potential use of serum Hsp70 as a novel tumour biomarker for Hsp90 inhibitors. Biomarkers. 2010;15(1):31–8. doi:10.3109/13547500903261347.
5. Multhoff G, Botzler C, Wiesnet M, Müller E, Meier T, Wilmanns W, et al. A stress-inducible 72-kDa heat-shock protein (HSP72) is expressed on the surface of human tumor cells, but not on normal cells. Int J Cancer. 1995;61(2):272–9.
6. Ferrarini M, Heltai S, Zocchi MR, Rugarli C. Unusual expression and localization of heat-shock proteins in human tumor cells. Int J Cancer. 1992;51(4):613–9.
7. Hantschel M, Pfister K, Jordan A, Scholz R, Andreesen R, Schmitz G, et al. Hsp70 plasma membrane expression on primary tumor biopsy material and bone marrow of leukemic patients. Cell Stress Chaperones. 2000;5(5):438–42. PMC312874.
8. Aghdassi A, Phillips P, Dudeja V, Dhaulakhandi D, Sharif R, Dawra R, et al. Heat shock protein 70 increases tumorigenicity and inhibits apoptosis in pancreatic adenocarcinoma. Cancer Res. 2007;67(2):616–25.
9. Garrido C, Gurbuxani S, Ravagnan L, Kroemer G. Heat shock proteins: endogenous modulators of apoptotic cell death. Biochem Biophys Res Commun. 2001;286(3):433–42. doi:10.1006/bbrc.2001.5427.
10. Jäättelä M, Wissing D, Kokholm K, Kallunki T, Egeblad M. Hsp70 exerts its anti-apoptotic function downstream of caspase-3-like proteases. EMBO J. 1998;17(21):6124–34. doi:10.1093/emboj/17.21.6124.
11. Gao Y, Han C, Huang H, Xin Y, Xu Y, Luo L, et al. Heat shock protein 70 together with its co-chaperone CHIP inhibits TNF-alpha induced apoptosis by promoting proteasomal degradation of apoptosis signal-regulating kinase1. Apoptosis. 2010;15(7):822–33. doi:10.1007/s10495-010-0495-7.
12. Yang X, Wang J, Zhou Y, Wang Y, Wang S, Zhang W. Hsp70 promotes chemoresistance by blocking Bax mitochondrial translocation in ovarian cancer cells. Cancer Lett. 2012;321(2):137–43. doi:10.1016/j.canlet.2012.01.030.
13. Kirkegaard T, Roth AG, Petersen NH, Mahalka AK, Olsen OD, Moilanen I, et al. Hsp70 stabilizes lysosomes and reverts Niemann-Pick disease-associated lysosomal pathology. Nature. 2010;463(7280):549–53. doi:10.1038/nature08710.
14. Bayer C, Liebhardt ME, Schmid TE, Trajkovic-Arsic M, Hube K, Specht HM, et al. Validation of heat shock protein 70 as a tumor-specific biomarker for monitoring the outcome of radiation therapy in tumor mouse models. Int J Radiat Oncol Biol Phys. 2014;88(3):694–700. doi:10.1016/j.ijrobp.2013.11.008.
15. Gehrmann M, Specht HM, Bayer C, Brandstetter M, Chizzali B, Duma M, et al. Hsp70 - a biomarker for tumor detection and monitoring of outcome of radiation therapy in patients with squamous cell carcinoma of the head and neck. Radiat Oncol. 2014;9:131. doi:10.1186/1748-717X-9-131.
16. Stangl S, Varga J, Freysoldt B, Trajkovic-Arsic M, Siveke JT, Greten FR, et al. Selective in vivo imaging of syngeneic, spontaneous, and xenograft tumors

17. using a novel tumor cell-specific Hsp70 peptide-based probe. Cancer Res. 2014;74(23):6903–12. doi:10.1158/0008-5472.CAN-14-0413.
17. Gehrmann M, Stangl S, Foulds GA, Oellinger R, Breuninger S, Rad R, et al. Tumor imaging and targeting potential of an Hsp70-derived 14-mer peptide. PLoS One. 2014;9(8):e105344. doi:10.1371/journal.pone.0105344.
18. Rerole AL, Jego G, Garrido C. Hsp70: anti-apoptotic and tumorigenic protein. Methods Mol Biol (Clifton, NJ). 2011;787:205–30. doi:10.1007/978-1-61779-295-3_16.
19. Sayers TJ. Targeting the extrinsic apoptosis signaling pathway for cancer therapy. Cancer Immunol Immunother. 2011;60(8):1173–80. doi:10.1007/s00262-011-1008-4.
20. Igney FH, Krammer PH. Death and anti-death: tumour resistance to apoptosis. Nat Rev Cancer. 2002;2(4):277–88.
21. Kulikov AV, Shilov ES, Mufazalov IA, Gogvadze V, Nedospasov SA, Zhivotovsky B. Cytochrome c: the Achilles' heel in apoptosis. Cell Mol Life Sci. 2012;69(11):1787–97. doi:10.1007/s00018-011-0895-z.
22. Nylandsted J, Gyrd-Hansen M, Danielewicz A, Fehrenbacher N, Lademann U, Hoyer-Hansen M, et al. Heat shock protein 70 promotes cell survival by inhibiting lysosomal membrane permeabilization. J Exp Med. 2004;200(4):425–35.
23. Jäättelä M. Escaping cell death: survival proteins in cancer. Exp Cell Res. 1999;248(1):30–43.
24. Gotoh T, Terada K, Oyadomari S, Mori M. hsp70-DnaJ chaperone pair prevents nitric oxide- and CHOP-induced apoptosis by inhibiting translocation of Bax to mitochondria. Cell Death Differ. 2004;11(4):390–402. doi:10.1038/sj.cdd.4401369.
25. Stankiewicz AR, Lachapelle G, Foo CP, Radicioni SM, Mosser DD. Hsp70 inhibits heat-induced apoptosis upstream of mitochondria by preventing Bax translocation. J Biol Chem. 2005;280(46):38729–39.
26. Guo F, Sigua C, Bali P, George P, Fiskus W, Scuto A, et al. Mechanistic role of heat shock protein 70 in Bcr-Abl-mediated resistance to apoptosis in human acute leukemia cells. Blood. 2005;105(3):1246–55. doi:10.1182/blood-2004-05-2041.
27. Gehrmann M, Marienhagen J, Eichholtz-Wirth H, Fritz E, Ellwart J, Jäättelä M, et al. Dual function of membrane-bound heat shock protein 70 (Hsp70), Bag-4, and Hsp40: protection against radiation-induced effects and target structure for natural killer cells. Cell Death Differ. 2005;12(1):38–51. doi:10.1038/sj.cdd.4401510.
28. Multhoff G, Botzler C, Jennen L, Schmidt J, Ellwart J, Issels R. Heat shock protein 72 on tumor cells: a recognition structure for natural killer cells. J Immunol. 1997;158(9):4341–50.
29. Zaarur N, Gabai V, Porco J, Calderwood S, Sherman M. Targeting heat shock response to sensitize cancer cells to proteasome and Hsp90 inhibitors. Cancer Res. 2006;66(3):1783–91.
30. Pulaski BA, Terman DS, Khan S, Muller E, Ostrand-Rosenberg S. Cooperativity of Staphylococcal aureus enterotoxin B superantigen, major histocompatibility complex class II, and CD80 for immunotherapy of advanced spontaneous metastases in a clinically relevant postoperative mouse breast cancer model. Cancer Res. 2000;60(10):2710–5.
31. Jinek M, Chylinski K, Fonfara I, Hauer M, Doudna JA, Charpentier E. A programmable dual-RNA-guided DNA endonuclease in adaptive bacterial immunity. Science. 2012;337(6096):816–21. doi:10.1126/science.1225829.
32. Pouget JP, Mather SJ. General aspects of the cellular response to low- and high-LET radiation. Eur J Nucl Med. 2001;28(4):541–61.
33. Ran FA, Hsu PD, Lin CY, Gootenberg JS, Konermann S, Trevino AE, et al. Double nicking by RNA-guided CRISPR Cas9 for enhanced genome editing specificity. Cell. 2013;154(6):1380–9. doi:10.1016/j.cell.2013.08.021.
34. Laemmli UK. Cleavage of structural proteins during the assembly of the head of bacteriophage T4. Nature. 1970;227(259):680–5. doi:10.1038/227680a0.
35. Schilling D, Gehrmann M, Steinem C, De MA, Pockley AG, Abend M, et al. Binding of heat shock protein 70 to extracellular phosphatidylserine promotes killing of normoxic and hypoxic tumor cells. FASEB J. 2009;23(8):2467–77. doi:10.1096/fj.08-125229.
36. Towbin H, Staehelin T, Gordon J. Electrophoretic transfer of proteins from polyacrylamide gels to nitrocellulose sheets: procedure and some applications. Proc Natl Acad Sci U S A. 1979;76(9):4350–4. doi:10.1073/pnas.76.9.4350.
37. Murakami N, Mori T, Yoshimoto S, Ito Y, Kobayashi K, Ken H, et al. Expression of EpCAM and prognosis in early-stage glottic cancer treated by radiotherapy. Laryngoscope. 2014;124(11):E431–6. doi:10.1002/lary.24839.
38. Lee JM, Bernstein A. p53 mutations increase resistance to ionizing radiation. Proc Natl Acad Sci U S A. 1993;90(12):5742–6.

Murakami *et al. Radiation Oncology* (2015) 10:149

Page 13 of 13

39. Wu H, Schiff DS, Lin Y, Neboori HJ, Goyal S, Feng Z, et al. Ionizing radiation sensitizes breast cancer cells to Bcl-2 inhibitor, ABT-737, through regulating Mcl-1. Radiat Res. 2014;182(6):618–25. doi:10.1667/RR13856.1.

40. Zhang P, Leu JI, Murphy ME, George DL, Marmorstein R. Crystal structure of the stress-inducible human heat shock protein 70 substrate-binding domain in complex with peptide substrate. PLoS ONE. 2014;9(7):e103518. doi:10.1371/journal.pone.0103518.

41. Daugaard M, Rohde M, Jäättelä M. The heat shock protein 70 family: Highly homologous proteins with overlapping and distinct functions. FEBS Lett. 2007;581(19):3702–10. doi:10.1016/j.febslet.2007.05.039.

42. Daugaard M, Jäättelä M, Rohde M. Hsp70-2 is required for tumor cell growth and survival. Cell Cycle. 2005;4(7):877–80.

43. Zorzi E, Bonvini P. Inducible hsp70 in the regulation of cancer cell survival: analysis of chaperone induction, expression and activity. Cancer. 2011;3(4):3921–56. doi:10.3390/cancers3043921.

44. Beere HM, Wolf BB, Cain K, Mosser DD, Mahboubi A, Kuwana T, et al. Heat-shock protein 70 inhibits apoptosis by preventing recruitment of procaspase-9 to the Apaf-1 apoptosome. Nat Cell Biol. 2000;2(8):469–75.

45. Pandey P, Saleh A, Nakazawa A, Kumar S, Srinivasula SM, Kumar V, et al. Negative regulation of cytochrome c-mediated oligomerization of Apaf-1 and activation of procaspase-9 by heat shock protein 90. EMBO J. 2000;19(16):4310–22.

46. Park HS, Cho SG, Kim CK, Hwang HS, Noh KT, Kim MS, et al. Heat shock protein hsp72 is a negative regulator of apoptosis signal-regulating kinase 1. Mol Cell Biol. 2002;22(22):7721–30.

47. Petersen NH, Kirkegaard T, Olsen OD, Jäättelä M. Connecting Hsp70, sphingolipid metabolism and lysosomal stability. Cell Cycle. 2010;9(12):2305–9.

48. Hightower LE, Guidon PT. Selective release from cultured mammalian cells of heat-shock (stress) proteins that resemble glia-axon transfer proetisn. J Cell Physiol. 1989;138(2):257–66.

49. Nickel W, Seedorf M. Unconventional mechansims of proetein transport to the cell surface of eukaryotic cells. Annu Rev Cell Dev Biol. 2008;24:287–308. doi:10.1146/annurev.cellbio.24.110707.175320.

50. Multhoff G. Heat shock protein 70 (Hsp70): membrane location, export and immunological relevance. Methods. 2007;43(3):229–37. doi:10.1016/j.ymeth.2007.06.006.

51. Gehrmann M, Liebisch G, Schmitz G, Anderson R, Steinem C, De MA, et al. Tumor-specific Hsp70 plasma membrane localization is enabled by the glycosphingolipid Gb3. PLoS ONE. 2008;3(4):e1925.

52. Komarova EY, Meshalkina DA, Aksenov ND, Pchelin IM, Martynova E, Margulis BA, et al. The discovery of Hsp70 domain with cell-penetrating activity. Cell Stress Chaperones. 2015;20:343–54. doi:10.1007/s12192-014-0554-z.

53. Shevtsov MA, Komarova EY, Meshalkina DA, Bychkova NV, Aksenov ND, Abkin SV, et al. Exogenously delivered Hsp70 displaces its endogenous analogue and sensitizes cenacer cells to lymphyocytes-mediated cytotoxicity. Oncotarget. 2014;5(10):3101–14.

54. Horvath I, Vigh L. Cell biology: Stability in times of stress. Nature. 2010;463(7280):436–8. doi:10.1038/463436a.

55. Olive PL, Banath JP, Sinnott LT. Phosphorylated histone H2AX in spheroids, tumors, and tissues of mice exposed to etoposide and 3-amino-1,2,4-benzotriazine-1,3-dioxide. Cancer Res. 2004;64(15):5363–9. doi:10.1158/0008-5472.CAN-04-0729.

56. Olive PL, Banath JP. Phosphorylation of histone H2AX as a measure of radiosensitivity. Int J Radiat Oncol Biol Phys. 2004;58(2):331–5.

57. Tait SW, Green DR. Mitochondria and cell death: outer membrane permeabilization and beyond. Nat Rev Mol Cell Biol. 2010;11(9):621–32. doi:10.1038/nrm2952.

58. Korsmeyer SJ, Wei MC, Saito M, Weiler S, Oh KJ, Schlesinger PH. Pro-apoptotic cascade activates BID, which oligomerizes BAK or BAX into pores that result in the release of cytochrome c. Cell Death Differ. 2000;7(12):1166–73. doi:10.1038/sj.cdd.4400783.

59. Pfister K, Radons J, Busch R, Tidball JG, Pfeifer M, Freitag L, et al. Patient survival by Hsp70 membrane phenotype: association with different routes of metastasis. Cancer. 2007;110(4):926–35. doi:10.1002/cncr.22864.

60. Breuninger S, Ertl J, Bayer C, Knape C, Gunther S, Regel I, et al. Quantative analysis of liposomal Hsp70 in the blood of tumor patients using a novel lipHsp70 ELISA. J Clin Cell Immunol. doi:org/10.4172/2155-9899.1000264.

61. Gehrmann M, Cervello M, Montalto G, Capello F, Gulino A, Knape C, et al. Hsp70 serum levels differ significantly in patients with chronic hepatitis, lievr chirrosis and hepatocellular carcinoma. Front Immunol. 2014;5:307. doi:10.3389/fimmu.2014.00307. eCollection2014.

ORIGINAL ARTICLE

NZ28-induced inhibition of HSF1, SP1 and NF-κB triggers the loss of the natural killer cell-activating ligands MICA/B on human tumor cells

**Daniela Schilling · Annett Kühnel · Fabian Tetzlaff ·
Sarah Konrad · Gabriele Multhoff**

Abstract The activity of natural killer (NK) cells is regulated by activating and inhibiting receptors, whereby the C-type lectin natural killer group 2D (NKG2D) receptor serves as the major activating receptor on NK cells which recognizes major histocompatibility class I chain-related proteins A and B (MICA/B). The MICA/B expression has been described to be regulated by the transcription factor heat shock factor 1 (HSF1). Inhibition of heat shock protein 90 (Hsp90) is known to induce the heat shock response via activation of HSF1 which is associated with tumor development, metastasis and therapy resistance and also with an increased susceptibility to NK cell-mediated lysis. Therefore, we compared the effects of Hsp90 inhibitor NVP-AUY922, HSF1 inhibitor NZ28 and HSF1 knockdown on the sensitivity of lung (H1339) and breast (MDA-MB-231, T47D) cancer cells to NK cell-mediated cytotoxicity and the expression of the NKG2D ligands MICA/B. Although NVP-AUY922 activates HSF1, neither the MICA/B surface density on tumor cells nor their susceptibility to NK cell-mediated lysis was affected. A single knockdown of HSF1 by shRNA decreased the surface expression of MICB but not that of MICA, and thereby, the NK cell-mediated lysis was only partially blocked. In contrast, NZ28 completely blocked the MICA/B membrane expression on tumor cells and thereby strongly inhibited the NK cell-mediated cytotoxicity. This effect might be explained by a simultaneous inhibition of the transcription factors HSF1, Sp1 and NF-κB by NZ28. These findings suggest that new anticancer therapeutics should be investigated with respect to their effects on the innate immune system.

Keywords Heat shock factor 1 (HSF1) · MICA/B ·
Natural killer (NK) cells · NKG2D · NVP-AUY922 · NZ28

D. Schilling · A. Kühnel · F. Tetzlaff · S. Konrad ·
G. Multhoff (✉)
Department of Radiation Oncology, Klinikum rechts der Isar,
Technische Universität München, TUM, Ismaningerstr. 22,
81675 Munich, Germany
e-mail: gabriele.multhoff@lrz.tu-muenchen.de

D. Schilling · G. Multhoff
Helmholtz Center Munich, German Research Center
for Environmental Health – Institute of Biological and Medical
Imaging, Munich, Germany

Abbreviations

BMBF	Bundesministerium für Bildung und Forschung
DFG	Deutsche Forschungsgemeinschaft
DSMZ	Deutsche Sammlung von Mikroorganismen und Zellkulturen
FACS	Fluorescence-activated cell sorting
HSF1	Heat shock factor 1
Hsp	Heat shock protein
ic	Intracellular
IL-2	Interleukin 2
MICA/B	Major histocompatibility class I chain-related proteins A and B
MFI	Mean fluorescence intensity
NKG2D	Natural killer group 2D
NF-κB	Nuclear factor kappa-light-chain-enhancer of activated B cells
NK	Natural killer
PI	Propidium iodide
Sp1	Specificity protein 1

Introduction

Inhibition of heat shock protein 90 (Hsp90) which promotes tumor cell survival and proliferation by stabilizing multiple oncogenic client proteins is a promising concept to overcome resistance of tumor cells to anticancer therapies. Numerous inhibitors of Hsp90 are currently tested in clinical trials. A negative side effect of Hsp90 inhibition is the activation of heat shock factor 1 (HSF1) which induces the expression of other cytoprotective stress proteins including Hsp70. Consequently, inhibition of Hsp70 or HSF1 has been shown to improve the anticancer effectivity of Hsp90 inhibitors [1–5]. With respect to ionizing irradiation, a simultaneous treatment of tumor cells with the HSF1 inhibitor NZ28 [5] and the Hsp90 inhibitor NVP-AUY922 has been shown to potentiate the radiosensitizing effect mediated by NVP-AUY922 alone (unpublished data). Herein, we study how modulators of the heat shock response can affect natural killer (NK) cell-mediated immunity. The cytolytic activity of NK cells is regulated by a fine balance of activating and inhibitory NK cell receptors. Among others, the C-type lectin natural killer group 2D receptor (NKG2D) acts as an activating receptor which recognizes the major histocompatibility class I chain-related proteins A and B (MICA/B). An enhanced sensitivity of tumor cells to NK cell-mediated lysis has been attributed to an increased membrane expression density of the NKG2D ligands MICA and MICB [6–9]. Vice versa, a reduced MICA/B membrane expression on tumor cells impairs the recognition by NK cells and promotes tumor immune escape [10]. The molecular mechanisms that regulate the expression of MICA/B on tumor cells are not completely understood. In the promoter regions of MICA and MICB, heat shock elements (HSE) which are similar to those of the *hsp70* genes have been found [11]. Stress such as heat shock induces the binding of the transcription factor HSF1 to the HSE in the promoter region of MICA/B and thus up-regulates mRNA and protein expression of MICA/B [12, 13]. Inhibitors of Hsp90 which are also known to activate HSF1 increase the expression of MICA/B in a variety of multiple myeloma cells [6].

However, besides HSF1, other factors such as the transcription factor SP1 which binds constitutively to the MICA/B promoter [12] have been described to participate in the transcriptional regulation of MICA/B. Histone deacetylase inhibition (HDAC) can increase the binding of HSF1 and SP1 to the promoter of MICA/B and thus results in an increased membrane MICA/B expression [8, 14]. In endothelial cells, a treatment with TNF-α induces binding of the transcription factor NF-κB to the MICA promoter and thereby causes an up-regulated expression of MICA [15].

In the present study, we were interested to analyze the effects of HSF1 activation (Hsp90 inhibitor NVP-AUY922)

and inhibition (NZ28, HSF1 knockdown) in different human cancer cells on the NK cell ligands MICA/B and its consequences on NK cell-mediated lysis. Our data demonstrate that Hsp90 inhibition alters neither the MICA/B surface density nor the sensitivity of the tumor cells to NK cell-mediated lysis. A knockdown of HSF1 decreases the membrane expression of MICB but not that of MICA, whereas a treatment with NZ28 inhibits the expression of both, MICA and MICB on the surface of the investigated tumor cells. In line with these findings, the loss of MICA and MICB on NZ28-treated tumor cells resulted in a complete inhibition of the NK cell-mediated cytotoxicity, whereas down-regulation of MICB by HSF1 knockdown resulted in a partial reduction in lysis mediated by NK cells. We also could show that NZ28 inhibits not only HSF1 but also other transcription factors such as NF-κB and Sp1 which are responsible for the expression of MICA/B.

Materials and methods

Reagents

10 mM stock solutions of NZ28 (J. Yaglom and M. Sherman; Boston University School of Medicine, USA) and NVP-AUY922 (Novartis) were prepared in 100 % DMSO. Dilutions were performed in PBS. A vehicle control with the respective amount of DMSO diluted in PBS was tested in all experiments to exclude an effect of DMSO itself (maximal 0.2 %).

Cells and cell culture

The human lung (H1339) and breast (MDA-MB-231, T47D) cancer cell lines were cultured as described previously [16, 17]. Cells were routinely checked for mycoplasma contamination. The authenticity of the cell lines was tested by the DSMZ (German collection of microorganisms and cell cultures).

Retroviral vectors and infection

For knockdown of HSF1, RNAi-Ready pSIREN-RetroQ vector with puromycin resistance (BD Biosciences) was used. Target sequence for HSF1 small interfering RNA was 5′-TATGGACTCCAACCTGGATAA-3′ [5]. Retroviruses were produced by transfection of Phoenix cells with pSIREN-RetroQ/HSF1 shRNA (shHSF1) or pSIREN-RetroQ (control) (provided by J. Yaglom and M. Sherman, Boston University School of Medicine, USA) using Ca phosphate. Tumor cells were infected with virus containing supernatants in the presence of 10 μg/ml polybrene. Selection was performed with 2 μg/ml puromycin.

Western blot analysis and ELISA

Cells were lysed in TBST buffer as described previously [18]. The protein content in the cell lysates was determined using the BCA™ Protein Assay Kit (Pierce). On immunoblots, proteins were detected with antibodies against HSF1 (ADI-SPA-901; Enzo Life Sciences), HSF1 phospho S326 (pHSF1) (ab76076; abcam), Hsp70 (ADI-SPA-810; Enzo Life Sciences) and β-actin (A5316; Sigma-Aldrich).

MICA and MICB concentrations in the cell lysates were measured by ELISA (R&D Systems), and the concentrations were calculated relative to the total protein content of each sample.

Luciferase assay

Cells were transfected with an inducible transcription factor-responsive (HSF1, Sp1, NF-κB) firefly luciferase construct (Qiagen). The luciferase activity was measured using the Dual-Glo Luciferase assay system (Promega). A constitutive Renilla luciferase construct served as an internal control for normalizing transfection efficiencies, cell viability and cell numbers.

Flow cytometry

Cells were incubated with the APC-conjugated MICA (clone 159227, FAB1300A, R&D Systems) and MICB antibodies (clone 236511, FAB1599A, R&D Systems) or the corresponding isotype-matched control antibody (clone 133303, IC0041A, R&D Systems) for 30 min at 4 °C. Dead cells were stained with propidium iodide, and only viable cells were analyzed on a FACSCalibur flow cytometer (BD Biosciences).

NK cell isolation

NK cells were generated by a CD3/CD19 depletion of PBMCs from healthy human volunteers using a magnetic separation method (Miltenyi Biotec). The purity of NK cells (89.9 % of lymphocytes) was determined by flow cytometry with antibodies against CD19 (#555413, BD Biosciences), CD3 (#345766, BD Biosciences) and CD56 (#345811, BD Biosciences).

NK cell cytotoxicity

NK cells were stimulated with 100 IU/ml IL-2 (Novartis) for 4 days. Activation of NK cells was checked by flow cytometry with antibodies against CD94 (#555888, BD Biosciences), NKG2D (FAB139P, R&D Systems) and CD56 (#345811, BD Biosciences). Their cytotoxic activity against differentially pre-treated tumor cells was

determined either by europium or by CD107 degranulation assay. During the co-incubation of tumor and NK cells, no drugs were added.

For the europium assay, the tumor cells were labeled with BATDA (Perkin Elmer) and then co-incubated with NK cells at different ratios in a V-bottom 96-well plate in 200 μl-medium. After a 4-h co-incubation period at 37 °C, 25 μl of supernatants were transferred into ELISA plates containing 200 μl europium solution (Perkin Elmer). The time-resolved fluorescence was measured using a Victor X4 plate reader (Perkin Elmer).

In the degranulation assay, the cytotoxicity of NK cells was determined by measuring the cell surface expression of the lysosomal marker, CD107a, which correlates with NK cell cytotoxicity [19]. Tumor cells were mixed with NK cells at a ratio of 1:1 in a U-bottom 96-well tissue culture plate. Anti-CD107a-FITC (#555800, BD Biosciences) or the isotype-matched control antibody (#555748, BD Biosciences) was added. After 1 h, GolgiStop™ (BD Biosciences) was added and after a co-incubation period of 3 h, the cells were stained with anti-CD3-PerCP (#345766, BD Biosciences) and anti-CD56-APC (#555518, BD Biosciences) antibodies. The CD107a expression on the CD3⁻CD56⁺ NK cell population was determined by flow cytometry.

Statistics

Statistical analysis was performed using SPSS 18.0.2 software (IBM). The unpaired Student's t test was used to evaluate significant differences (*$p \leq 0.05$, **$p \leq 0.01$, ***$p \leq 0.001$).

Results

NZ28 impairs susceptibility of tumor cells to NK cell-mediated lysis

To investigate whether inhibitors of the stress response can modulate the sensitivity of human tumor cells to NK cell-mediated cytotoxicity, HSF1 inhibitor NZ28 and/or Hsp90 inhibitor NVP-AUY922-treated tumor cells were used as target cells for IL-2 (100 IU/ml)-activated NK cells. A successful stimulation of purified NK cells was shown by an up-regulated cell surface density of the NK cell markers CD94, CD56 and NKG2D (Fig. 1a) [20]. The cytotoxic activity of NK cells against H1339 (lung) and MDA-MB-231 (breast) cancer cells was determined by measuring the expression of the lysosomal marker CD107a [6, 19]. As shown in Fig. 1b, the NK cell-mediated cytotoxicity against H1339 and MDA-MB-231 tumor cells that were treated with 2 or 20 μM NZ28 was significantly reduced
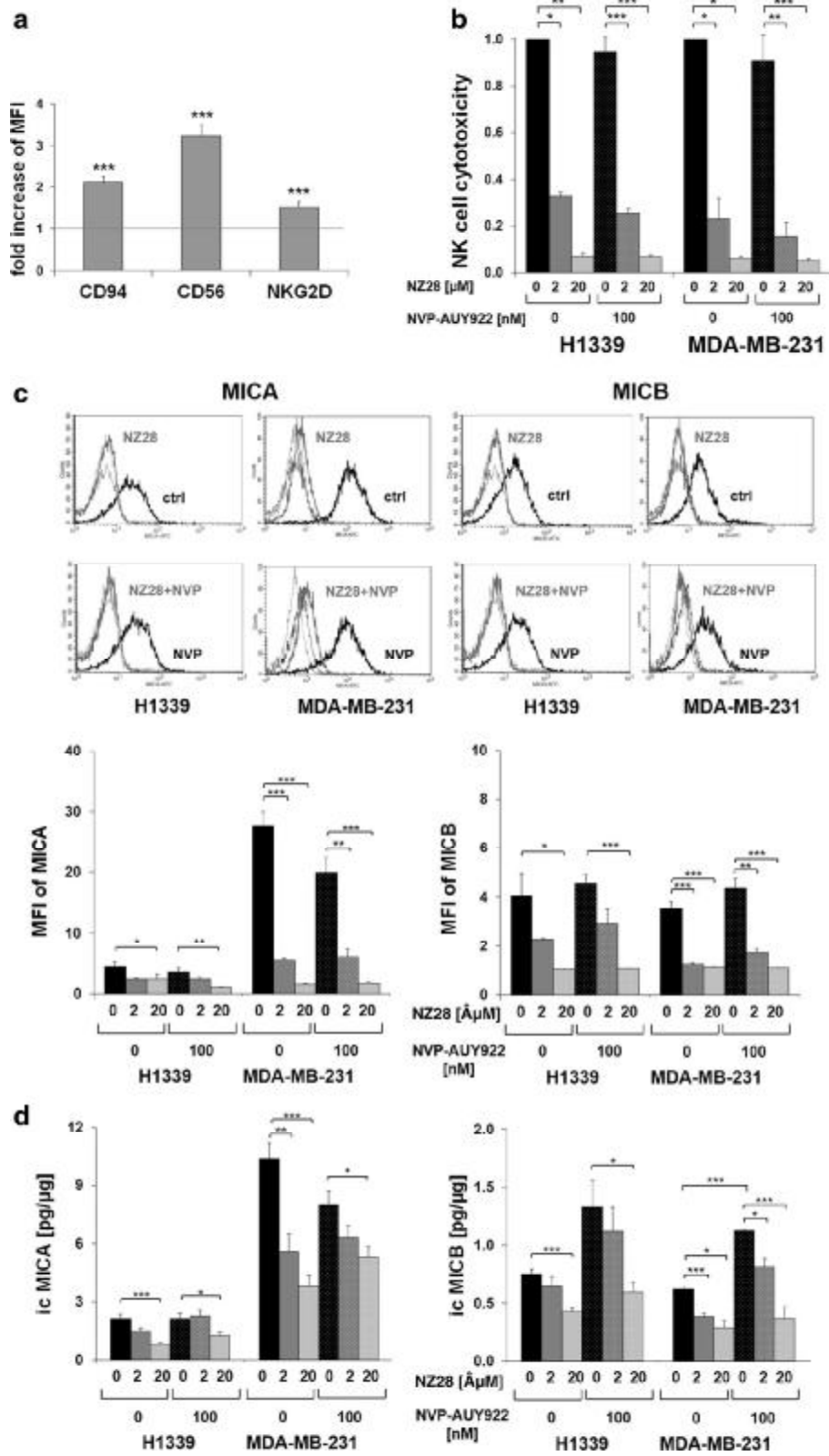
◀ **Fig. 1** NZ28 impairs killing of tumor cells by activated NK cells. Tumor cells were treated with 2 or 20 μM NZ28 and/or 100 nM NVP-AUY922 for 24 h. DMSO (0.2 %)-treated cells served as control. NK cells were stimulated for 4 days with 100 U/ml IL-2. **a** The expression of CD94, CD56 and NKG2D on NK cells was determined by FACS analysis. The fold increase in mean fluorescence intensity (MFI) of cell surface markers on stimulated compared to unstimulated NK cells is shown. *Graphs* represent mean values of seven independent experiments ±SEM. *$p \leq 0.05$, **$p \leq 0.01$, ***$p \leq 0.001$. **b** The cytotoxicity of activated NK cells was measured after a 4-h co-incubation with tumor cells by the CD107a degranulation assay. The relative cytotoxicity of activated NK cells incubated with differentially treated tumor cells compared to control cells is shown. *Graphs* represent mean values of 2–3 independent experiments ±SEM. *White dots* in the *bar graphs* indicate treatment of tumor cells with NVP-AUY922. *$p \leq 0.05$, **$p \leq 0.01$, ***$p \leq 0.001$. **c** Tumor cells were stained with antibodies against MICA/B or the respective isotype control. Representative FACS analysis shows MICA (*left*) and MICB (*right*) surface staining on tumor cells. The *black solid lines* represent MICA or MICB staining of control cells (ctrl; *upper panels*) or cells treated with 100 nM NVP-AUY922 (NVP; *lower panels*). The *gray solid lines* represent MICA or MICB staining of cells treated with 20 μM NZ28 (NZ28; *upper panels*) or with 20 μM NZ28 plus 100 nM NVP-AUY922 (NZ28 + NVP; *lower panels*). *Dotted lines* represent the respective isotype controls. *Graphs* show mean values of at least two independent experiments ±SEM of the mean fluorescence intensity (MFI) of MICA and MICB. *White dots* in the *bar graphs* indicate treatment of tumor cells with NVP-AUY922. *$p \leq 0.05$, **$p \leq 0.01$, ***$p \leq 0.001$. **d** The intracellular levels of MICA (icMICA, *left*) and MICB (icMICB, *right*) in tumor cells were determined by ELISA. The concentrations in the cell lysates were calculated relative to the total protein content of each sample. *Graphs* represent mean values of four independent experiments ±SEM. *White dots* in the *bar graphs* indicate treatment of tumor cells with NVP-AUY922. *$p \leq 0.05$, **$p \leq 0.01$, ***$p \leq 0.001$

compared to untreated tumor cells (Fig. 1b). Treatment of tumor cells with 100 nM NVP-AUY922 alone did not affect the NK cell-mediated cytotoxicity, and a combined treatment with NZ28 and NVP-AUY922 did not reverse the immunosuppressing effect of NZ28. Similar findings were observed in another breast cancer cell line (T47D, supplementary Fig. 1a). A direct drug-induced cytotoxicity could be excluded since the drug concentrations which were used in the cytotoxicity assays did not affect cell viability of the tumor cells (supplementary Figs. 1b, 2).

NZ28 suppresses the expression of activating NK cell ligands MICA and MICB

Hsp90 inhibitors such as NVP-AUY922 are known to activate HSF1, whereas NZ28 has been shown to inhibit the heat shock response by reducing the HSF1 activity [5, 21]. As HSF1 has been described to regulate the transcription of the NK cell ligands MICA and MICB [12, 13], we investigated whether treatment of tumor cells with NZ28 and/or NVP-AUY922 alters the cell surface density [mean fluorescence intensity (MFI)] of the NK cell ligands MICA and MICB on tumor cells.

To test whether detaching adherent tumor cells with trypsin is suitable to measure the MICA/B membrane expression, the surface expression of MICA/B on cells that were detached with trypsin and accutase was compared by FACS analysis. Accutase has been described to perform exceptionally well in detaching cells without altering the membrane expression of MICA/B [22]. As no differences were observed (supplementary Fig. 3), tumor cells treated for 24 h with NZ28 and/or NVP-AUY922 were detached with trypsin and the MICA/B membrane expression was determined by FACS analysis. Representative flow cytometric histograms are shown in Fig. 1c (upper part). Treatment of H1339 and MDA-MB-231 tumor cells with 100 nM NVP-AUY922 did not affect the MICA and MICB cell surface density (MFI) (Fig. 1c, lower part). In contrast, NZ28 significantly reduced the MICA and MICB membrane expression (MFI) in both tumor cell lines. In T47D tumor cells which lack a MICA membrane expression, the MICB expression was found to be strongly reduced upon treatment with NZ28 (supplementary Fig. 4).

In line with the membrane expression, the intracellular (ic) expression of MICA and MICB was significantly reduced in H1339 and MDA-MB-231 cells by NZ28 (Fig. 1d). The Hsp90 inhibitor NVP-AUY922 did not affect the icMICA levels but increased the icMICB levels.

The activation of HSF1 by NVP-AUY922 and the inhibition of HSF1 by NZ28 were proven by immunoblots and HSE-luciferase reporter assays. As expected, NVP-AUY922 increased, whereas NZ28 decreased phosphorylated HSF1 at serine residue 326 (pHSF1 Ser326) and Hsp70 expression as well as HSF1 activity (Fig. 2, supplementary Fig. 5).

HSF1 depletion mimics NZ28 by impairing NK cell-mediated lysis

To investigate whether an inhibition of HSF1 can explain the effects of NZ28 on the NK cell-mediated cytotoxicity and MICA/B expression, we knocked down HSF1 in H1339 tumor cells by RNA interference. H1339 cells were infected either with a retrovirus encoding a specific shRNA against HSF1 (shHSF1) or with a control retrovirus (ctrl). The successful knockdown of HSF1 is shown in Fig. 3a. The HSF1 knockdown also strongly reduced the expression of Hsp70 (Fig. 3a) and of a HSE-luciferase reporter construct (Fig. 3b). Despite the HSF1 knockdown, tumor cell growth under standard cell culture conditions was not impaired (Fig. 3c).

To investigate whether depletion of HSF1 in H1339 tumor cells affects NK cell-mediated cytotoxicity, control and HSF1 knockdown tumor cells were used as target cells for IL-2-activated NK cells. The cytotoxicity of stimulated
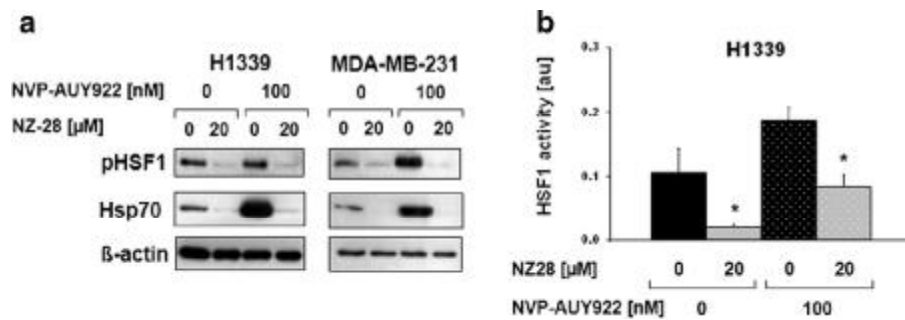
Fig. 2 NZ28 reduces Hsp70 expression and HSF1 activity. **a** Representative HSF1 phospho S326 (pHSF1) and Hsp70 immunoblots of H1339 and MDA-MB-231 tumor cells treated with 20 μM NZ28 and/or 100 nM NVP-AUY922 for 24 h. DMSO (0.2 %) treated cells served as control. **b** Luciferase assay of H1339 cells transfected with a HSF1 responsive firefly luciferase construct and treated with 20 μM

NZ28 and/or 100 nM NVP-AUY922 for 24 h. DMSO (0.2 %)-treated cells served as control. *White dots* in the *bar graphs* indicate treatment with NVP-AUY922. *Graphs* represent mean values ± SEM of at least three independent experiments. Significant differences are indicated (*$p \leq 0.05$, **$p \leq 0.01$)
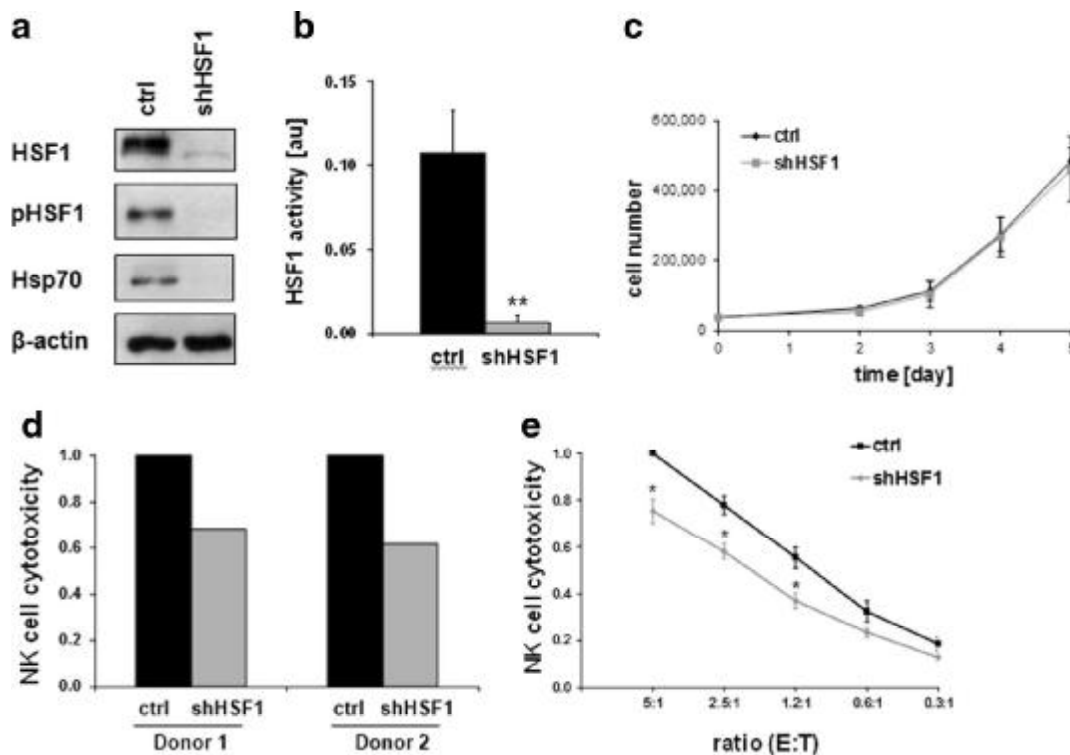
Fig. 3 HSF1 depletion impairs lysis of H1339 tumor cells by activated NK cells. **a** Representative immunoblot showing the expression of HSF1, HSF1 phospho S326 (pHSF1), Hsp70 and ß-actin in H1339 cells transfected with control (ctrl) or HSF1 shRNA (shHSF1). **b** Luciferase assay of H1339 ctrl and shHSF1 cells transfected with a HSF1 responsive firefly luciferase construct. *Graphs* represent mean values ± SEM of five experiments. Significant differences are indicated (*$p \leq 0.05$). **c** Growth curve of H1339 cells transfected with control (ctrl) or HSF1 shRNA (shHSF1). **d** NK cells from two different healthy donors were stimulated for 4 days with 100 U/ml IL-2. The cytotoxicity of IL-2-stimulated NK cells was measured after a 4-h co-incubation with H1339 tumor cells transfected with control

(ctrl) or HSF1 shRNA (shHSF1) by the CD107a degranulation assay. The relative cytotoxicity of NK cells incubated with shHSF1 cells compared to NK cells incubated with control tumor cells is shown for each NK cell donor. **e** NK cells were stimulated for 4 days with 100 U/ml IL-2. The cytotoxicity of IL-2-stimulated NK cells was measured after a 4-h co-incubation with H1339 tumor cells transfected with control (ctrl) or HSF1 shRNA (shHSF1) by europium assay. The cytotoxicity of stimulated NK cells against control tumor cells at an E:T (effector to target) ratio of 5:1 was set to one. *Graphs* represent mean values ± SEM of at least three independent experiments. Significant differences between control and HSF1 knockdown cells are indicated (*$p \leq 0.05$)

NK cells against shHSF1 knockdown tumor cells was strongly reduced compared to control cells as demonstrated by degranulation (Fig. 3d) and europium assay (Fig. 3e). However, the reduction in NK cell-mediated lysis was much more pronounced after treatment of the H1339 tumor cells with NZ28 (Fig. 1b) compared to that of a HSF1 knockdown (Fig. 3d).

HSF1 regulates MICB but not MICA expression

To ascertain whether the HSF1 knockdown has any impact on MICA/B levels, the membrane expression and ic expression of MICA/B were measured by FACS and ELISA, respectively. As shown in Fig. 4a, b, the HSF1 knockdown did not affect the MICA, but reduced the MICB surface
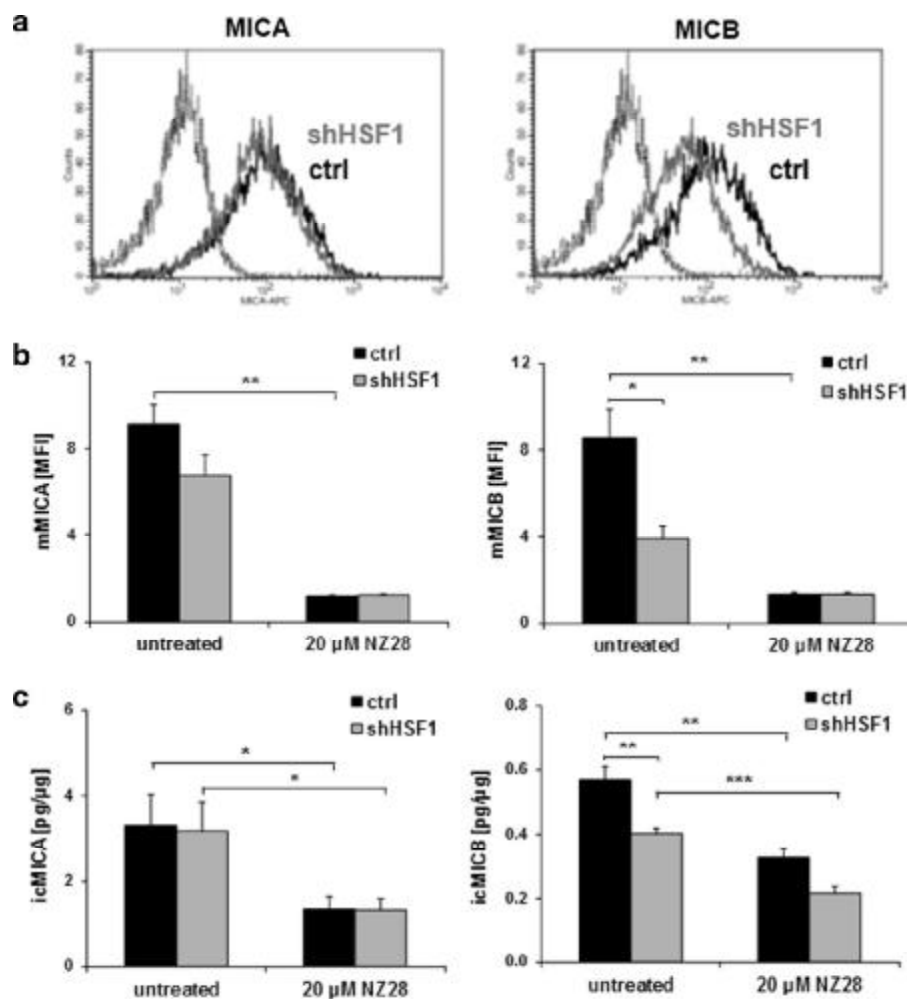
Fig. 4 HSF1 knockdown reduces membrane and intracellular MICB levels. The expression of MICA and MICB on the membrane of H1339 tumor cells transfected with control (ctrl) or HSF1 shRNA (shHSF1) was determined by flow cytometry (**a**, **b**) and the intracellular expression by ELISA (**c**). **a** Representative FACS analysis showing MICA and MICB surface staining. The *black solid lines* represent MICA or MICB staining of control (ctrl) cells. The *gray solid lines* represent MICA or MICB staining of cells transfected with shRNA against HSF1 (shHSF1). *Dotted lines* represent the respective isotype controls. **b** The mean fluorescence intensity (MFI) of MICA and MICB on H1339 cells transfected with control (ctrl) or HSF1 shRNA (shHSF1) and treated with 20 μM NZ28 for 24 h is shown. *Graphs* represent mean values ± SEM of at least three independent experiments. Significant differences are indicated (*$p \leq 0.05$, **$p \leq 0.01$, ***$p \leq 0.001$). **c** The intracellular levels of MICA (icMICA, *left*) and MICB (icMICB, *right*) of H1339 cells transfected with control (ctrl) or HSF1 shRNA (shHSF1) and treated with 20 μM NZ28 for 24 h were determined by ELISA. The concentrations in the cell lysates were calculated relative to the total protein content of each sample. *Graphs* represent mean values ± SEM of at least three independent experiments. Significant differences are indicated (*$p \leq 0.05$, **$p \leq 0.01$, ***$p \leq 0.001$)

density significantly. In line with the membrane expression, the ic MICB levels were significantly down-regulated by HSF1 knockdown, whereas the ic MICA expression remained unaffected (Fig. 4c). These data suggest that HSF1 regulates the transcription of MICB but not that of MICA.

NZ28 inhibits activity of the MICA/B transcription factors NF-κB and Sp1

Although HSF1 knockdown only diminished the MICB expression in H1339 cells, NZ28 strongly reduced the ic and membrane MICA and MICB expression in control as well as in HSF1 knockdown cells (Fig. 4b, c). Therefore, we asked the question whether other transcription factors that have been described to regulate the transcription of MICA/B might also be affected by NZ28. As shown by the luciferase assay, NZ28 inhibited not only the transcriptional activity of HSF1 but also that of NF-κB and Sp1 in H1339 and T47D tumor cells (Fig. 5).
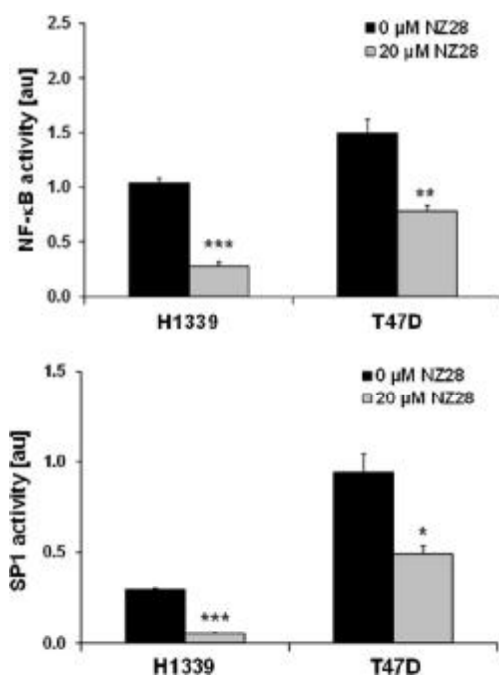
Fig. 5 NZ28 reduces NF-κB and SP1 transcriptional activity in tumor cells. H1339 and T47D cells were transfected with reporter plasmids that contain NF-κB and SP1 responsive firefly luciferase constructs and treated with 20 μM NZ28 for 24 h. DMSO (0.2 %)-treated cells served as control (0 μM NZ28). Mean values ± SEM of two independent experiments (each measured in duplicate) are presented. Significant differences are indicated (*$p \leq 0.05$, **$p \leq 0.01$, ***$p \leq 0.001$)

Discussion

Targeting the heat shock response (Hsp70 or its main transcription factor HSF1) by small molecules or RNA interference has been shown to sensitize tumor cells to Hsp90 inhibition [1–5]. Previous work of our group revealed that HSF1 inhibition by NZ28 increases the radiosensitizing efficiency of the Hsp90 inhibitor NVP-AUY922 in lung and breast cancer cell lines (unpublished data). In recent years, evidence has accumulated that not only the interplay between radio- and chemotherapy, but also the host immune system plays an important role in determining the clinical outcome of cancer patients [23]. Radiochemotherapy has been reported to affect the antigen expression on tumor cells and the secretion of soluble factors that contribute to immune stimulation [24]. Lung and breast tumors are frequently treated with radiotherapy, and NK cells have been documented to be critically involved in anti-tumor immunity against these very common tumor entities [25, 26]. Therefore, in this study, we investigated the effects of this novel combined treatment modality (NZ28 and NVP-AUY922) with respect to NK cell cytotoxicity and NK cell ligand expression on lung and breast tumor cells.
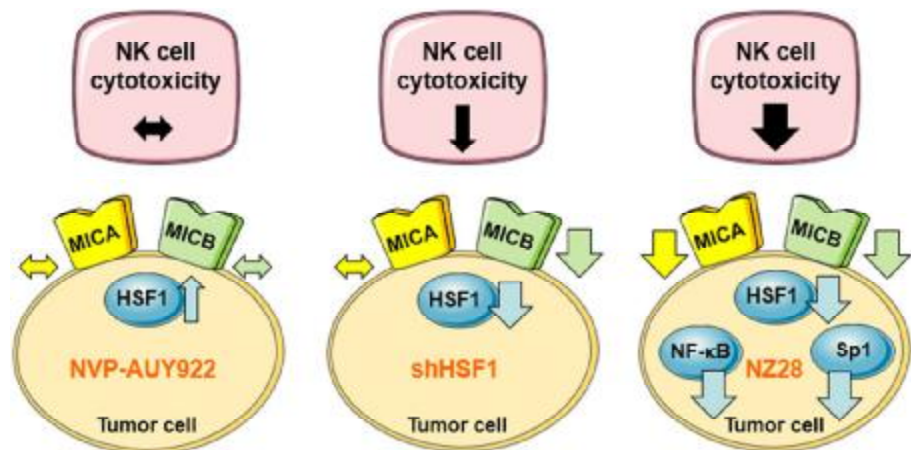
Whereas NVP-AUY922 was shown to increase the activity of HSF1 and the icMICB expression, it did not alter the icMICA expression, suggesting that MICA is not regulated by HSF1 in our investigated cell lines. Indeed, HSF1 knockdown reduced the expression of MICB but not that of MICA. In line with our results, Venkataraman et al. [12] have shown that MICA is less inducible by stress than MICB due to a weaker binding capacity of HSF1 to the HSE.

In contrast to icMICB, the MICB cell surface density was not increased by NVP-AUY922. This might be due to a default in the membrane translocation of MICB. Consistently, the sensitivity of tumor cells toward NK cell-mediated lysis was not improved. Other groups demonstrated that high concentrations of the Hsp90 inhibitor 17-AAG (1 and 6 μM) up-regulate the cell surface density of MICA and MICB on multiple myeloma cells and Hodgkin's lymphoma cells and thereby can enhance NK cell cytotoxicity [6, 7]. The discrepancy to their results might be either explained by differences in the tumor cell lines or by the lower and more physiological concentration of the Hsp90 inhibitor used in our study.

NZ28 down-regulated the HSF1 activity and the MICA/B expression on lung and mammary tumor cells, and this correlated with a reduced sensitivity to NK cell-mediated lysis. As NZ28 treatment also reduced the MICA and MICB expression in HSF1-depleted cells, we assume that NZ28 exerts its effects on MICA/B expression not only via HSF1. Luciferase reporter assays revealed that the activity of other

transcription factors such as Sp1 and NF-κB was also inhibited by NZ28. In line with our results, treatment of Hela cells with a NF-κB inhibitor also reduced the MICA expression [27]. In contrast, in Jurkat cells NF-κB down-regulation by siRNA did not modify the MICA/B expression but silencing of Sp1 reduced the MICA/B expression [14].

Like NZ28, the naturally derived compound triptolide has originally been shown to inhibit the heat shock response [28]. Later on, Banerjee et al. [29] demonstrated that triptolide reduces the activity of Sp1 and this in turn leads to decreased HSF1 and NF-κB activities. By silencing Sp1, they could clearly show that Sp1 is a master regulator for HSF1 and NF-κB. Therefore, we propose that NZ28 might inhibit the transcriptional activity of Sp1 which in turn results in a reduced HSF1 and NF-κB activity. Subsequently, this leads to the down-regulation of both MICA and MICB which causes a complete loss in NK cell-mediated killing.

In summary, our data reveal that HSF1 activation by NVP-AUY922 neither affects MICA/B surface density nor affects the associated NK cell cytotoxicity (Fig. 6). However, HSF1 depletion decreases the MICB but not MICA membrane expression and thereby leads to a reduction in the NK cell-mediated cytotoxicity. In contrast, NZ28 severely blocks NK cell-mediated cytotoxicity by a substantial down-regulation of both NK2D ligands, MICA and MICB. This effect might be explained by the fact that NZ28 impairs not only HSF1 but also Sp1 and NF-κB activities.

Despite these negative effects of NZ28 on the function of NK cells, NZ28 has been shown to be very efficient in sensitizing tumor cells toward radiation (unpublished data) and chemotherapy [5].

References

1. Ma L, Sato F, Sato R, Matsubara T, Hirai K, Yamasaki M, Shin T, Shimada T, Nomura T, Mori K, Sumino Y, Mimata H (2014) Dual targeting of heat shock proteins 90 and 70 promotes cell death and enhances the anticancer effect of chemotherapeutic agents in bladder cancer. Oncol Rep 31(6):2482–2492. doi:10.3892/or.2014.3132

2. Massey A, Williamson D, Browne H, Murray J, Dokurno P, Shaw T, Macias A, Daniels Z, Geoffroy S, Dopson M, Lavan P, Matassova N, Francis G, Graham C, Parsons R, Wang Y, Padfield A, Comer M, Drysdale M, Wood M (2010) A novel, small molecule inhibitor of Hsc70/Hsp70 potentiates Hsp90 inhibitor induced apoptosis in HCT116 colon carcinoma cells. Cancer Chemother Pharmacol 66(3):535–545. doi:10.1007/s00280-009-1194-3

3. Powers M, Clarke P, Workman P (2008) Dual targeting of HSC70 and HSP72 inhibits HSP90 function and induces tumor-specific apoptosis. Cancer Cell 14(3):250–262. doi:10.1016/j.ccr.2008.08.002

4. Chen Y, Chen J, Loo A, Jaeger S, Bagdasarian L, Yu J, Chung F, Korn J, Ruddy D, Guo R, McLaughlin ME, Feng F, Zhu P, Stegmeier F, Pagliarini R, Porter D, Zhou W (2013) Targeting HSF1 sensitizes cancer cells to HSP90 inhibition. Oncotarget 4(6):816–829

5. Zaarur N, Gabai V, Porco J, Calderwood S, Sherman M (2006) Targeting heat shock response to sensitize cancer cells to proteasome and Hsp90 inhibitors. Cancer Res 66(3):1783–1791. doi:10.1158/0008-5472.CAN-05-3692

6. Fionda C, Soriani A, Malgarini G, Iannitto M, Santoni A, Cippitelli M (2009) Heat shock protein-90 inhibitors increase MHC class I-related chain A and B ligand expression on multiple myeloma cells and their ability to trigger NK cell degranulation. J Immunol 183(7):4385–4394. doi:10.4049/jimmunol.0901797

7. Böll B, Eltaib F, Reiners K, von Tresckow B, Tawadros S, Simhadri V, Burrows F, Lundgren K, Hansen H, Engert A, von Strandmann E (2009) Heat shock protein 90 inhibitor BIIB021 (CNF2024) depletes NF-kappaB and sensitizes Hodgkin's lymphoma cells for natural killer cell-mediated cytotoxicity. Clin Cancer Res 15(16):5108–5116. doi:10.1158/1078-0432.CCR-09-0213

8. Zhang C, Wang Y, Zhou Z, Zhang J, Tian Z (2009) Sodium butyrate upregulates expression of NKG2D ligand MICA/B in HeLa and HepG2 cell lines and increases their susceptibility to NK lysis. Cancer Immunol Immunother 58(8):1275–1285. doi:10.1007/s00262-008-0645-8

9. Armeanu S, Bitzer M, Lauer U, Venturelli S, Pathil A, Krusch M, Kaiser S, Jobst J, Smirnow I, Wagner A, Steinle A, Salih H (2005) Natural killer cell-mediated lysis of hepatoma cells via specific induction of NKG2D ligands by the histone deacetylase inhibitor sodium valproate. Cancer Res 65(14):6321–6329. doi:10.1158/0008-5472.CAN-04-4252

10. Fernandez-Messina L, Reyburn HT, Vales-Gomez M (2012) Human NKG2D-ligands: cell biology strategies to ensure immune recognition. Front Immunol 3:299. doi:10.3389/fimmu.2012.00299

11. Groh V, Bahram S, Bauer S, Herman A, Beauchamp M, Spies T (1996) Cell stress-regulated human major histocompatibility complex class I gene expressed in gastrointestinal epithelium. Proc Natl Acad Sci USA 93(22):12445–12450

12. Venkataraman G, Suciu D, Groh V, Boss J, Spies T (2007) Promoter region architecture and transcriptional regulation of the genes for the MHC class I-related chain A and B ligands of NKG2D. J Immunol 178(2):961–969

13. Groh V, Steinle A, Bauer S, Spies T (1998) Recognition of stress-induced MHC molecules by intestinal epithelial gammadelta T cells. Science 279(5357):1737–1740

14. Andresen L, Jensen H, Pedersen M, Hansen K, Skov S (2007) Molecular regulation of MHC class I chain-related protein A expression after HDAC-inhibitor treatment of Jurkat T cells. J Immunol 179(12):8235–8242

15. Lin D, Lavender H, Soilleux EJ, O'Callaghan CA (2012) NF-kappaB regulates MICA gene transcription in endothelial cell through a genetically inhibitable control site. J Biol Chem 287(6):4299–4310. doi:10.1074/jbc.M111.282152

16. Schilling D, Bayer C, Li W, Molls M, Vaupel P, Multhoff G (2012) Radiosensitization of normoxic and hypoxic H1339 lung tumor cells by heat shock protein 90 inhibition is independent of hypoxia inducible factor-1α. PLoS ONE 7(2):e31110

17. Stangl S, Gehrmann M, Riegger J, Kuhs K, Riederer I, Sievert W, Hube K, Mocikat R, Dressel R, Kremmer E, Pockley AG, Friedrich L, Vigh L, Skerra A, Multhoff G (2011) Targeting membrane heat-shock protein 70 (Hsp70) on tumors by cmHsp70.1 antibody. Proc Natl Acad Sci USA 108(2):733–738

18. Schilling D, Bayer C, Geurts-Moespot A, Sweep F, Pruschy M, Mengele K, Sprague L, Molls M (2007) Induction of plasminogen activator inhibitor type-1 (PAI-1) by hypoxia and irradiation in human head and neck carcinoma cell lines. BMC Cancer 7:143. doi:10.1186/1471-2407-7-143

19. Bryceson YT, March ME, Barber DF, Ljunggren HG, Long EO (2005) Cytolytic granule polarization and degranulation controlled by different receptors in resting NK cells. J Exp Med 202(7):1001–1012. doi:10.1084/jem.200511432222

20. Multhoff G, Pfister K, Gehrmann M, Hantschel M, Gross C, Hafner M, Hiddemann W (2001) A 14-mer Hsp70 peptide stimulates natural killer (NK) cell activity. Cell Stress Chaperones 6(4):337–344

21. Meng L, Gabai V, Sherman M (2010) Heat-shock transcription factor HSF1 has a critical role in human epidermal growth factor receptor-2-induced cellular transformation and tumorigenesis. Oncogene 29(37):5204–5213. doi:10.1038/onc.2010.277

22. Wolpert F, Tritschler I, Steinle A, Weller M, Eisele G (2014) A disintegrin and metalloproteinases 10 and 17 modulate the immunogenicity of glioblastoma-initiating cells. Neuro Oncol 16(3):382–391. doi:10.1093/neuonc/not232

23. Ma Y, Conforti R, Aymeric L, Locher C, Kepp O, Kroemer G, Zitvogel L (2011) How to improve the immunogenicity of chemotherapy and radiotherapy. Cancer Metastasis Rev 30(1):71–82. doi:10.1007/s10555-011-9283-2

24. Frey B, Rubner Y, Kulzer L, Werthmoller N, Weiss EM, Fietkau R, Gaipl US (2014) Antitumor immune responses induced by ionizing irradiation and further immune stimulation. Cancer Immunol Immunother 63(1):29–36. doi:10.1007/s00262-013-1474-y

25. Frese-Schaper M, Keil A, Yagita H, Steiner SK, Falk W, Schmid RA, Frese S (2014) Influence of natural killer cells and perforin-mediated cytolysis on the development of chemically induced lung cancer in A/J mice. Cancer Immunol Immunother 63(6):571–580. doi:10.1007/s00262-014-1535-x

26. Roberti MP, Mordoh J, Levy EM (2012) Biological role of NK cells and immunotherapeutic approaches in breast cancer. Front Immunol 3:375. doi:10.3389/fimmu.2012.00375

27. Molinero LL, Fuertes MB, Girart MV, Fainboim L, Rabinovich GA, Costas MA, Zwirner NW (2004) NF-kappa B regulates expression of the MHC class I-related chain A gene in activated T lymphocytes. J Immunol 173(9):5583–5590

28. Westerheide S, Kawahara T, Orton K, Morimoto R (2006) Triptolide, an inhibitor of the human heat shock response that enhances stress-induced cell death. J Biol Chem 281(14):9616–9622. doi:10.1074/jbc.M512044200

29. Banerjee S, Sangwan V, McGinn O, Chugh R, Dudeja V, Vickers SM, Saluja AK (2013) Triptolide-induced cell death in pancreatic cancer is mediated by O-GlcNAc modification of transcription factor Sp1. J Biol Chem 288(47):33927–33938. doi:10.1074/jbc.M113.500983

Original Articles

Sensitizing tumor cells to radiation by targeting the heat shock response

Daniela Schilling [a,b], Annett Kühnel [a], Sarah Konrad [a], Fabian Tetzlaff [a], Christine Bayer [a,c], Julia Yaglom [d], Gabriele Multhoff [a,b,*]

[a] Department of Radiation Oncology, Technische Universität München, Munich, Germany
[b] Helmholtz Center Munich, German Research Center for Environmental Health, Institute of Biological and Medical Imaging, Munich, Germany
[c] German Cancer Consortium (DKTK) partner site Munich, German Cancer Research Center (DKFZ), Heidelberg, Germany
[d] Department of Biochemistry, Boston University School of Medicine, Boston, MA, USA

ABSTRACT

Elevated levels of heat shock proteins (HSPs) contribute to tumor cell survival and mediate protection against radiation-induced cell death. Hsp90 inhibitors are promising radiosensitizers but also activate heat shock factor 1 (HSF1) and thereby induce the synthesis of cytoprotective Hsp70. In this study the heat shock response inhibitor NZ28 either alone or in combination with the Hsp90 inhibitor NVP-AUY922 was investigated for radiosensitizing effects, alterations in cell cycle distribution and effects on migratory/invasive capacity of radioresistant tumor cells. NZ28 reduced the constitutive and NVP-AUY922-induced Hsp70 expression by inhibition of the HSF1 activity and inhibited migration and invasion in human lung and breast tumor cells. Treatment of tumor cells with NZ28 significantly increased their radiation response. One possible mechanism might be a decrease of the radioresistant S-phase. When combined with the Hsp90 inhibitor NVP-AUY922 the concentration of NZ28 could be significantly reduced (1/10th–1/20th) to achieve the same radiosensitization. Our results demonstrate that a dual targeting of Hsp70 and Hsp90 with NZ28 and NVP-AUY922 potentiates the radiation response of tumor cells that are otherwise resistant to ionizing radiation.

© 2015 The Authors. Published by Elsevier Ireland Ltd. This is an open access article under the CC BY-NC-ND license (http://creativecommons.org/licenses/by-nc-nd/4.0/).

Introduction

The major stress-inducible molecular chaperone, heat shock protein 70 (Hsp70, Hsp70A1A), fulfills a variety of housekeeping and cytoprotective functions. Normal cells constitutively express low amounts of Hsp70. Following a broad variety of different stress stimuli (e.g. heat shock, Hsp90 inhibition) the expression of Hsp70 is strongly increased. The main factor which is involved in the transcription of Hsp70 is heat shock factor 1 (HSF1). After trimerization HSF1 translocates to the nucleus and binds to the heat shock element (HSE) in the promoter region of Hsp70. HSF1 activation is regulated by posttranslational modifications such as phosphorylation, sumoylation and deacetylation [1].

In contrast to normal cells, HSF1 and Hsp70 are highly overexpressed in tumor cells already under physiological conditions and thus contribute to tumor cell survival, migration, invasion and angiogenesis [1–6]. High HSF1 and Hsp70 levels are associated with poor prognosis, metastasis and therapy resistance [1,7,8]. Consequently, a knock-down of HSF1 or Hsp70 results in an increased radiation-induced cell killing [9–12]. The small molecular weight inhibitor NZ28 was found to reduce HSF1 and Hsp70 levels and therefore is meant to exert effects similar to a HSF1 depletion [13,14].

Apart from HSF1/Hsp70, Hsp90 is an attractive anticancer target since Hsp90 chaperones a number of oncogenic client proteins (e.g. HER2, mutant EGFR, AKT, BCR-ABL, survivin, mutant p53, HIF-1α, MMP2, hTERT). Several Hsp90 inhibitors are currently tested in clinical trials. By a simultaneous degradation of multiple oncogenic client proteins, Hsp90 inhibitors reduce tumor cell proliferation and enhance the radiosensitivity of tumor cells [15,16]. However, a negative side effect of Hsp90 inhibition is the activation of HSF1 and subsequently the induction of Hsp70. Therefore, a down-regulation or inhibition of HSF1 or Hsp70 increases the sensitivity of tumor cells toward Hsp90 inhibitors [14,17–20]. Herein, we studied the role of the heat shock response inhibitor NZ28 either alone or in combination with the Hsp90 inhibitor NVP-AUY922 on the activation of HSF1, Hsp70 expression, migration, invasion and radiosensitivity of radioresistant human tumor cell lines.
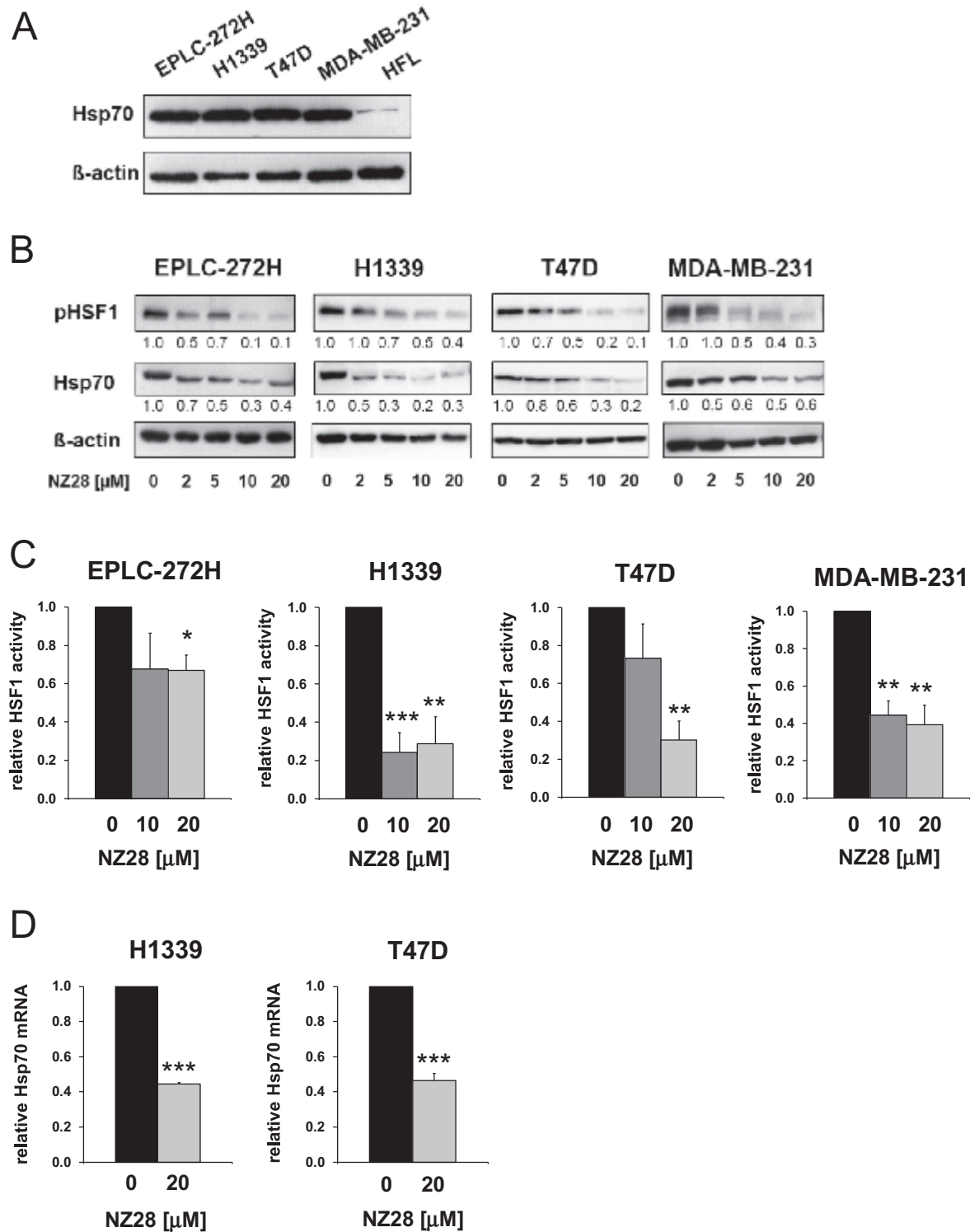
Fig. 1. NZ28 reduces HSF1 activity and Hsp70 expression in tumor cells. (A) Representative immunoblot showing the constitutive expression of Hsp70 in EPLC-272H, H1339, T47D and MDA-MB-231 tumor cells and human fetal lung fibroblasts (HFL). (B) Representative HSF1 phospho S326 (pHSF1) and Hsp70 immunoblots of EPLC-272H, H1339, T47D and MDA-MB-231 tumor cells that were treated for 24 h with different concentrations of NZ28. DMSO (0.2%) treated cells served as control (0 μM NZ28). The protein bands were quantified by densitometry using ImageJ. Numbers under the lanes represent the expression levels of pHSF1 or Hsp70 relative to β-actin. The value of control cells was set to 1 for each cell line. (C) Luciferase assay of EPLC-272H, H1339, T47D and MDA-MB-231 tumor cells transfected with a HSF1 responsive firefly luciferase construct and treated with 10 or 20 μM NZ28 for 24 h. The luciferase activity of vehicle (0.2% DMSO) treated cells (0 μM NZ28) was set to 1. Data are expressed as mean ± SEM of at least 3 independent experiments (**p ≤ 0.01, **p ≤ 0.01, ***p ≤ 0.001). (D) The Hsp70 mRNA expression in H1339 and T47D cells treated with 20 μM NZ28 or 0.2% DMSO (0 μM NZ28) for 24 h was quantified by qRT-PCR. The mRNA levels were normalized to the housekeeping gene β-actin. Data are expressed as mean ± SEM of 3 independent experiments (***p ≤ 0.01).
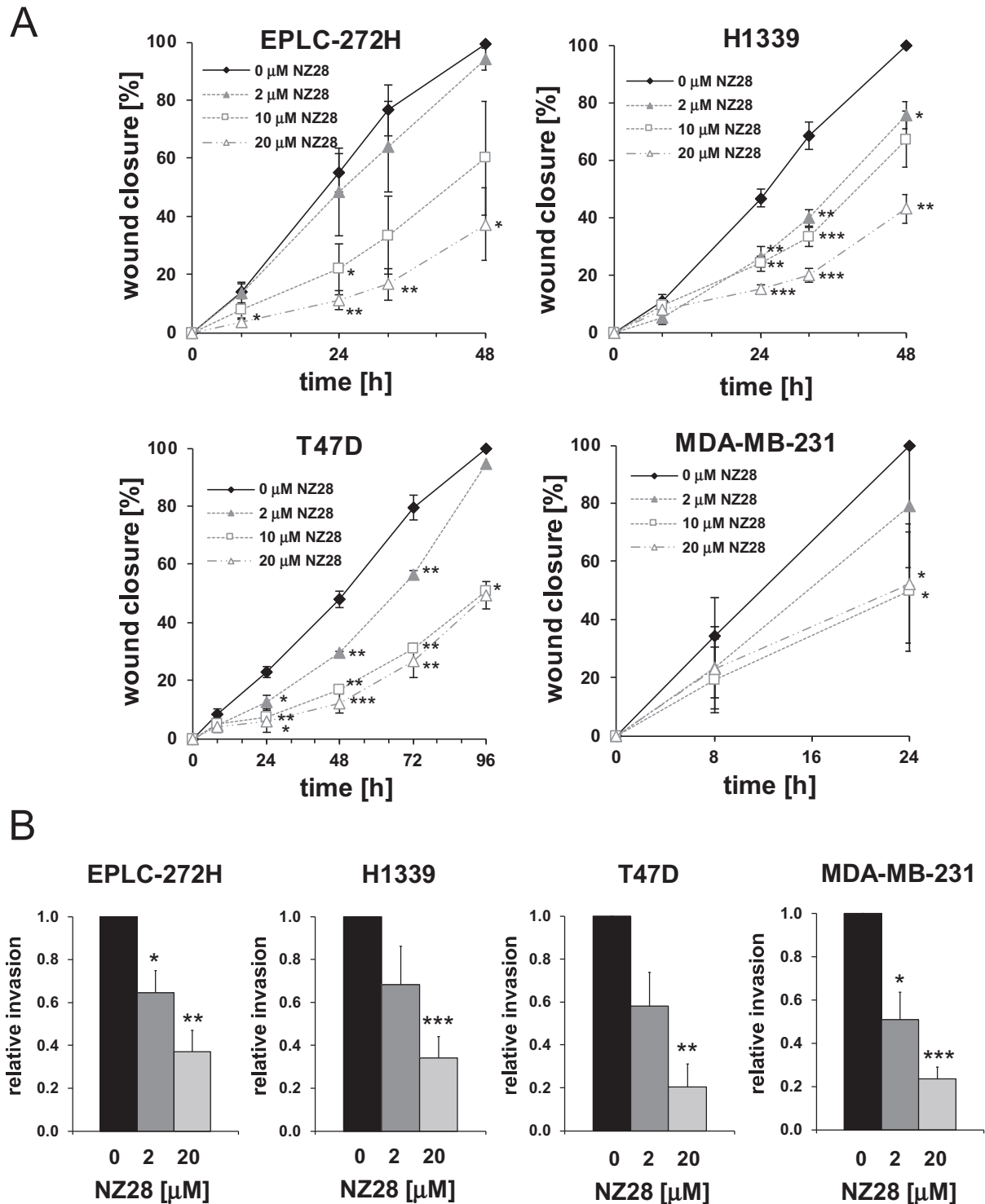
Fig. 2. NZ28 inhibits migration and invasion. (A) Migratory capacity was assessed by a wound healing assay. EPLC-272H, H1339, T47D and MDA-MB-231 tumor cells were plated in culture-inserts and 24 h later, inserts were removed and cells were treated with 2, 10 and 20 µM NZ28 (0 h). 0.2% DMSO diluted in PBS was used as control (0 µM NZ28). The percentage of wound closure was quantified at the indicated time points. Data are expressed as mean ± SEM of 3 independent experiments (*p ≤ 0.05, **p ≤ 0.01, ***p ≤ 0.001). (B) The invasive capacity of EPLC-272H, H1339, T47D and MDA-MB-231 tumor cells treated with 2 and 20 µM NZ28 for 24 h in relation to vehicle (0.2% DMSO) treated cells was determined by a transwell Matrigel invasion assay. Data are expressed as mean ± SEM of 4 independent experiments (*p ≤ 0.05, **p ≤ 0.01***, p ≤ 0.001).

Materials and methods

Reagents and treatment

10 mM stock solutions of NZ28 (M. Sherman; Boston University School of Medicine, USA) and NVP-AUY922 (Novartis) were prepared in 100% DMSO. Dilutions were performed in PBS. A vehicle control with the respective amount of DMSO diluted in PBS (maximal 0.2%) was used in all experiments. If not indicated otherwise, cells were incubated for 24 h with NZ28 and/or NVP-AUY922.

Cells and cell culture

The human lung (H1339 and EPLC-272H) and breast (MDA-MB-231 and T47D) cancer cell lines and human fetal lung fibroblasts (HFL) (kindly provided by Prof. Rodemann) were cultured as described previously [15,21,22]. The authenticity of the tumor cell lines was tested by the DSMZ (German Collection of Microorganisms and Cell Cultures). Cells were routinely checked and determined as negative for mycoplasma contamination.

Western blot analysis

Cells were lysed as described previously [23]. On immunoblots, proteins were detected with antibodies against Hsp70 (ADI-SPA-810, Enzo Life Sciences), HSF1 phospho S326 (pHSF1) (ab76076, abcam) and β-actin (A5316, Sigma-Aldrich). The protein bands were quantified by densitometry using ImageJ. The expression levels of pHSF1 or Hsp70 were calculated relative to β-actin.

HSE luciferase assay

In order to determine the HSF1 activity, cells were transfected with a HSE reporter plasmid that contains a HSF1 responsive firefly luciferase construct (Qiagen). On day one after transfection, cells were treated with NZ28 for 24 h. The luciferase activity was measured using the Dual Glo Luciferase assay system (Promega). A constitutive Renilla luciferase construct served as an internal control.

Quantitative real-time PCR

To investigate the mRNA expression of Hsp70, RNA was isolated with the RNeasy Mini Kit (Qiagen) and reverse transcription of RNA was performed with the QuantiTect Reverse Transcription Kit (Qiagen) according to the manufacturer's instructions. qRT-PCR was performed in a LightCycler 480 (Roche) by using the QuantiTect SYBR Green PCR Kit (Qiagen). Primers used for qRT-PCR were as follows: ACTB-F: GACGACATGGAGAAAATCTG, ACTB-R: ATGATCTGGGTCATCTTCTC, HspA1A-F: AATTTCCTGTGTTTGCAATG, HspA1A-R: AAAATGGCCTGAGTTAAGTG. Each sample was measured in triplicate and the mean Ct was calculated. Relative expression was calculated using the ΔΔCt method. The mRNA expression of β-actin was used as an internal control.

Wound healing assay

To determine the migratory capacity of tumor cells, wound healing assays were performed. Cells were plated in culture-inserts (Ibidi) and 24 h later, inserts were removed and cells treated with 2, 10 and 20 μM NZ28 (0 h). 0.2% DMSO diluted in PBS was used as control (0 μM NZ28). After 24 h the medium was replaced by fresh medium without NZ28 or DMSO. The migration of cells into the cell-free gap was monitored microscopically and quantified using ImageJ's wound healing tool.

Matrigel invasion assay

Invasion of tumor cells was measured by transwell Matrigel assay. Cells were seeded in 6 cm dishes and 24 h later treated with 2 and 20 μM NZ28. 0.2% DMSO diluted in PBS was used as control (0 μM NZ28). After 24 h, cells were trypsinized, counted and plated in Biocoat™Matrigel® Invasion chambers (Corning) in serum-free medium. 10% FCS-containing medium was added as a chemo-attractant to the wells in the bottom. Transmigrated cells were fixed after 24 h, stained with DAPI and counted. The number of NZ28-treated cells that migrated through the matrigel was calculated in relation to vehicle treated (0.2% DMSO) cells (0 μM NZ28).

Clonogenic assay and irradiation

To measure the radiosensitivity, clonogenic assays were performed as described previously [15]. The cells were seeded in 12-well plates, one day later treated with NZ28/NVP-AUY922 and 24 h later irradiated using the RS225A irradiation device (Gulmay Medical Ltd) at a dose rate of 1 Gy/min (70 keV). After irradiation the medium was exchanged by a drug-free medium. On day 9 (H1339) or 16 (T47D) after seeding, colonies were fixed, stained and counted. Survival curves were fitted to the linear quadratic model using Sigmaplot (Systat Software Inc).
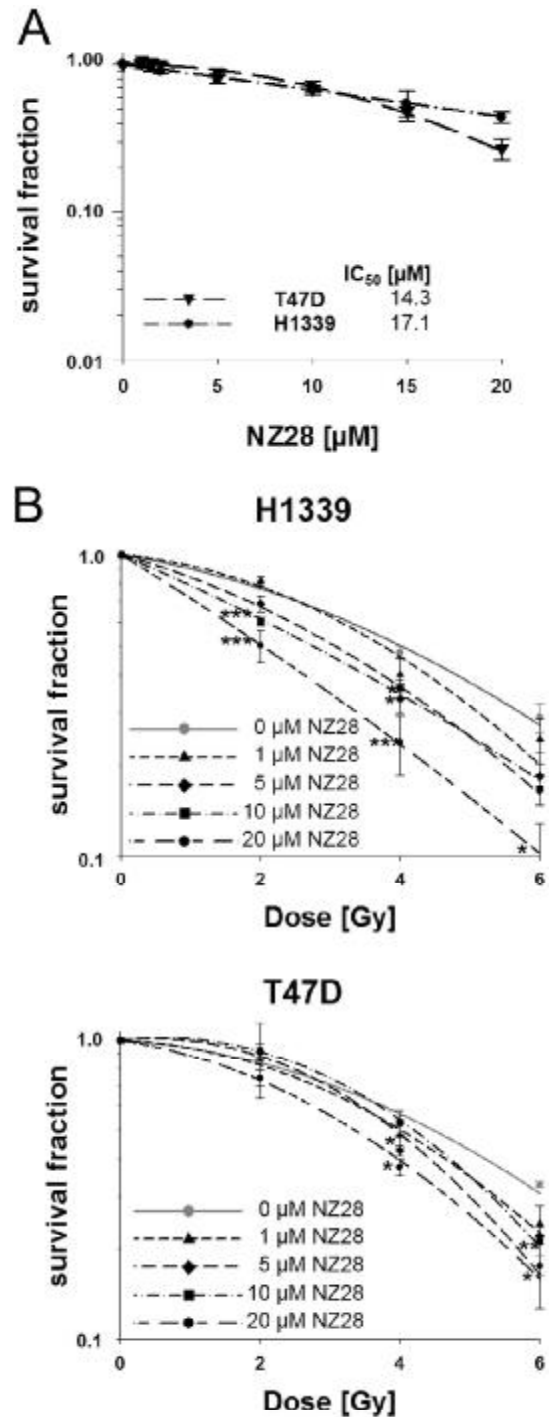

Fig. 3. NZ28 increases radiosensitivity of tumor cells. Clonogenic survival of cells treated with NZ28 (A) or with NZ28 and irradiation (B). (A) One day after seeding H1339 and T47D cells were treated with different concentrations of NZ28. DMSO (0.2%) treated cells served as control. After 24 h the medium was replaced by a drug-free medium. Colonies were fixed either 9 (H1339) or 16 (T47D) days after seeding. The survival fractions were calculated relative to the DMSO-treated control. IC_{50} (half maximal inhibitory concentration) values are indicated. (B) One day after seeding H1339 and T47D cells were treated with NZ28 for 24 h, then irradiated and immediately after irradiation fresh medium without NZ28 was added. DMSO treated cells served as control (0 μM NZ28). Colonies were fixed either 9 (H1339) or 16 (T47D) days after seeding. The survival fractions were calculated after normalization for cell killing by NZ28 alone. Data are expressed as mean ± SEM of at least 3 independent experiments ($^{*}p \leq 0.05$, $^{**}p \leq 0.01$, $^{***}p \leq 0.001$).

Cell cycle analysis

To analyze the cell cycle distribution, cells were fixed, stained with propidium iodide in the presence of RNase and analyzed on a FACSCalibur flow cytometer (BD Biosciences) as described previously [24]. The cell cycle distribution was calculated using Modfit software (Verity Software House Inc).

Statistics

Statistical analysis was performed using SPSS 18.0.2 software (IBM). The Student's t-test was used to evaluate significant differences (*$p \leq 0.05$, **$p \leq 0.01$, ***$p \leq 0.001$). All experiments were independently performed at least 3 times.

Results

NZ28 decreases Hsp70 levels and inhibits activation of HSF1

As shown in Fig. 1A, lung (EPLC-272H, H1339) and breast (T47D, MDA-MB-231) cancer cell lines exhibited high constitutive Hsp70 levels in comparison to normal human fetal lung fibroblasts (HFL). Knock-down of HSF1 revealed that the high constitutive Hsp70 expression levels in H1339 tumor cells depend on HSF1 [25].

Following treatment with different concentrations of the small molecule inhibitor NZ28 [13,14] the Hsp70 levels decreased in all 4 cancer cell lines (Fig. 1B). In parallel, the amount of HSF1 phosphorylated at serine 326 (pHSF1 Ser326) was down-regulated, which indicates that the HSF1 activation was reduced by NZ28 (Fig. 1B) [26]. The inhibitory effect of 10 and 20 μM NZ28 on the HSF1 activity was confirmed in EPLC-272H, H1339, T47D and MDA-MB-231 tumor cells transfected with a HSE reporter luciferase gene (Fig. 1C). Quantitative RT-PCR was performed to address the question of whether inhibition of HSF1 by NZ28 affects the transcription of Hsp70. In line with the reduced HSF1 activity, NZ28 significantly down-regulated Hsp70 mRNA expression in H1339 and T47D tumor cells (Fig. 1D). These data suggest that NZ28 inhibits the basal HSF1 activity and down-regulates constitutive Hsp70 transcription in tumor cells.

NZ28 inhibits tumor cell migration and invasion

Hsp70 and HSF1 were found to be associated with the migratory capacity of tumor cells [2,4,6,11]. Therefore, we examined whether NZ28 affects tumor cell migration. In wound healing assays we could show that NZ28 significantly inhibited the migration of lung and breast cancer cell lines in a concentration-dependent manner (Fig. 2A, Supplementary Fig. S1). In addition to migration, the invasive capacity through Matrigel was also significantly inhibited by NZ28 in all 4 cell lines (Fig. 2B).

NZ28 increases the radiosensitivity

A comparison of the intrinsic radiosensitivity of the 4 different tumor cell lines revealed that H1339 and T47D cells are the two most radioresistant tumor cell lines (indicated by the highest D_{50} values) (D_{50}: EPLC-272H, 3.7 Gy; H1339, 4.0 Gy; T47D, 4.5 Gy; MDA-MB-231, 3.2 Gy). Therefore, H1339 and T47D cells were chosen to test the radiosensitizing effect of NZ28. NZ28 alone similarly affected the clonogenic survival of T47D and H1339 cells with IC_{50} (half maximal inhibitory concentration) values of 14.3 and 17.1 μM, respectively (Fig. 3A). When combined with irradiation, concentrations above 5 μM NZ28 significantly reduced the survival fraction of both cell lines (Fig. 3B, Table 1). The radiosensitizing effect of NZ28 was confirmed by calculating the sensitizing enhancement ratios (SER) which were 1.99 in H1339 and 1.34 in T47D cells treated with 20 μM NZ28 (Table 1).

For a better understanding of the mechanisms that result in the NZ28-mediated radiosensitization, apoptosis, DNA double strand breaks and cell cycle distribution were analyzed. Neither radiation-induced apoptosis (Caspase-3, 24 h post irradiation) nor the amount of residual DNA double strand breaks (γH2AX/p53BP1 foci, 24 h post irradiation) were significantly affected by a treatment with 20 μM NZ28 (data not shown). In contrast, NZ28 significantly reduced the fraction of tumor cells in the radioresistant S-phase from 33.8% to 25.5% in H1339 and from 10.5% to 4.0% in T47D cells (Fig. 4).

A combined treatment with low doses of NZ28 and NVP-AUY922 potentiates the radiosensitivity of tumor cells

We have previously shown that a continuous treatment of H1339 cells with the Hsp90 inhibitor NVP-AUY922 can enhance the radiosensitivity but also increases the expression of Hsp70 [15]. Herein, we investigated whether NZ28 can inhibit the NVP-AUY922-induced activation of HSF1 and the expression of Hsp70 to increase the NVP-AUY922-mediated radiosensitization. As shown in Fig. 5, NZ28 reduced the NVP-AUY922-induced activation of HSF1 (as determined by a phosphorylation of serine 326) and the expression of Hsp70. As a consequence, a combined treatment of tumor cells with low concentrations of NZ28 (1 μM) and NVP-AUY922 (2 nM)

Table 1
Summary of radiobiological parameters depicted in Figs. 3B and 6.

	SF_2[a]	SF_4[a]	SF_6[a]	α [Gy^{-1}][b]	β [Gy^{-2}][b]	D_{50} [Gy][c]	SER[d]
H1339							
Control	0.79 ± 0.03	0.47 ± 0.02	0.29 ± 0.03	0.085	0.022	4.01	1.00
1 μM NZ28	0.82 ± 0.03	0.40 ± 0.05	0.24 ± 0.04	0.049	0.037	3.74	1.07
5 μM NZ28	0.69 ± 0.04	0.33 ± 0.04**	0.18 ± 0.04	0.103	0.026	3.18	1.18
10 μM NZ28	0.60 ± 0.02***	0.36 ± 0.02*	0.17 ± 0.02	0.179	0.013	2.73	**1.47**
20 μM NZ28	0.50 ± 0.06***	0.24 ± 0.05***	0.10 ± 0.03*	0.225	0.010	2.01	**1.99**
2 nM NVP-AUY922	0.75 ± 0.06	0.42 ± 0.02	0.22 ± 0.03	0.101	0.026	3.56	1.12
1 μM NZ28 + 2 nM NVP-AUY922	0.64 ± 0.04*	0.32 ± 0.02**	0.17 ± 0.04	0.191	0.019	2.83	**1.41**
T47D							
Control	0.86 ± 0.06	0.53 ± 0.03	0.33 ± 0.01	0.035	0.027	4.46	1.00
1 μM NZ28	0.83 ± 0.04	0.48 ± 0.04	0.24 ± 0.04	0.024	0.037	4.00	1.12
5 μM NZ28	0.91 ± 0.06	0.43 ± 0.02*	0.22 ± 0.06	−0.057	0.060	3.92	1.14
10 μM NZ28	0.92 ± 0.22	0.53 ± 0.05	0.21 ± 0.02**	−0.067	0.055	4.19	1.06
20 μM NZ28	0.74 ± 0.11	0.38 ± 0.02*	0.17 ± 0.05*	0.083	0.037	3.34	**1.34**
2 nM NVP-AUY922	0.81 ± 0.06	0.44 ± 0.02*	0.15 ± 0.02*	−0.001	0.052	3.64	**1.22**
1 μM NZ28 + 2 nM NVP-AUY922	0.78 ± 0.03	0.28 ± 0.01***	0.11 ± 0.01***	−0.033	0.082	3.12	**1.43**

[a] SF_2, SF_4, SF_6, survival fraction at 2, 4 and 6 Gy, respectively. Mean values ± SEM are shown. Significant differences between vehicle control and cells treated with NZ28 and/or NVP-AUY922 are indicated (*$p \leq 0.05$, **$p \leq 0.01$, ***$p \leq 0.001$).
[b] α and β values were derived from the linear quadratic equation $SF = \exp [-\alpha \times D - \beta \times D^2]$.
[c] D_{50}, dose [Gy] to reduce survival fraction to 50%.
[d] SER, sensitizing enhancement ratio = D_{50} (irradiation)/D_{50} (irradiation and drug). A SER greater than 1.20 is indicative for radiosensitization (indicated in bold).
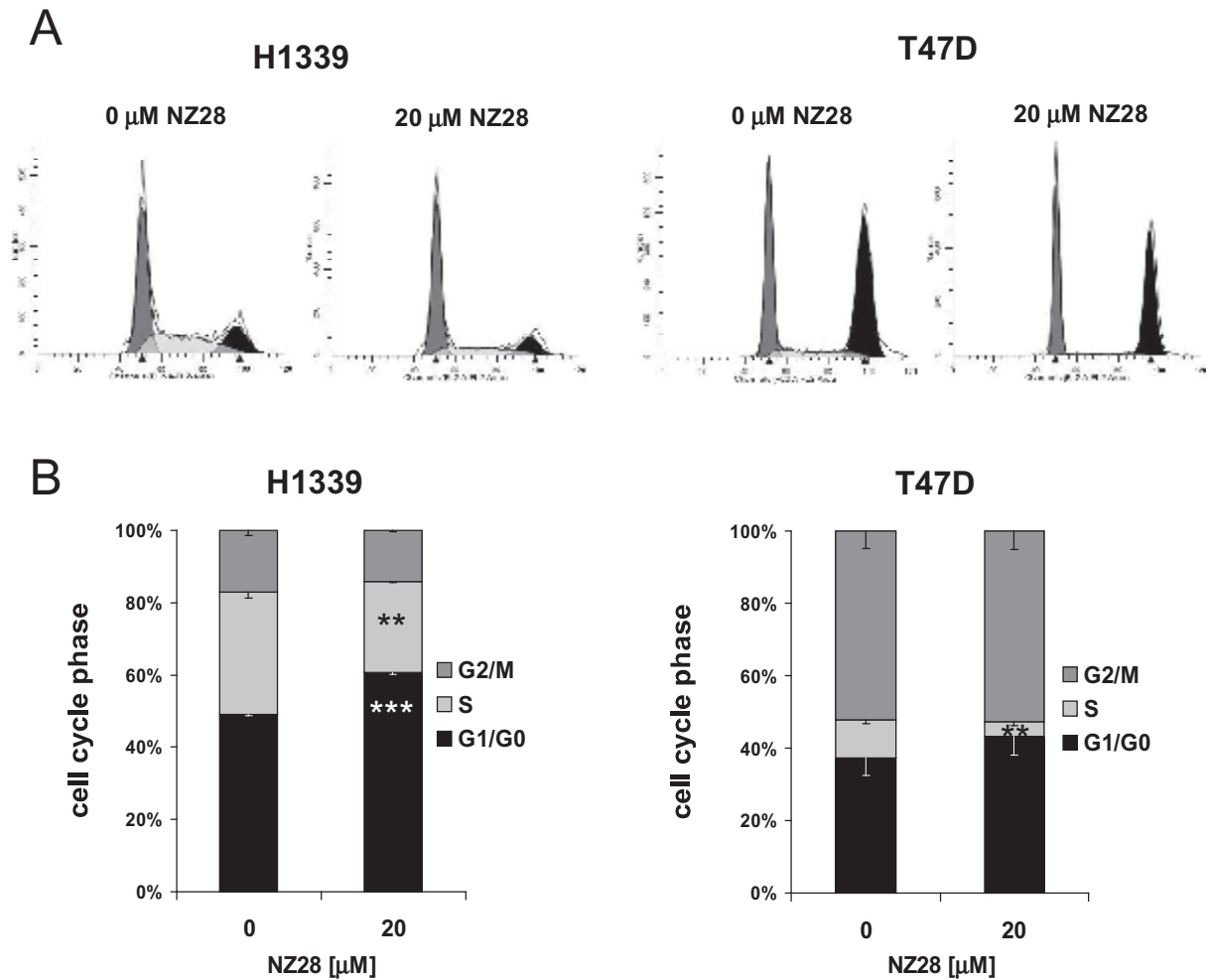
Fig. 4. NZ28 reduces the fraction of tumor cells in the radioresistant S-phase. The cell cycle distribution was determined after a 24 h treatment with 20 μM NZ28. DMSO (0.02%) treated cells served as control (0 μM NZ28). Representative histograms (A) and mean ± SEM (B) of 3 (H1339) and 5 (T47D) independent experiments are shown (*p ≤ 0.05, **p ≤ 0.01, ***p ≤ 0.001).
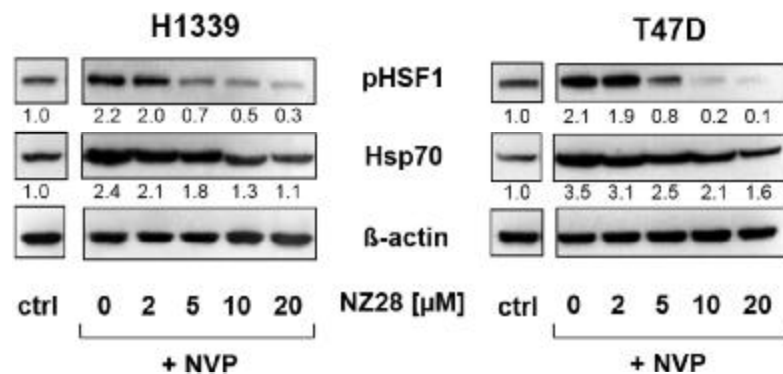

Fig. 5. NZ28 reduces NVP-AUY922-induced pHSF1 and Hsp70 levels. Representative HSF1 phospho S326 (pHSF1) and Hsp70 immunoblots. H1339 and T47D tumor cells were treated with 0, 2, 5, 10 and 20 μM NZ28 and 100 nM NVP-AUY922 (NVP) for 24 h. DMSO (0.2%) treated cells served as control (ctrl). A gap was included between control and treated samples because the lanes were not adjacent but samples were loaded on the same gel and the blot was exposed for the same period of time. The protein bands were quantified by densitometry using ImageJ. Numbers under the lanes represent the expression of pHSF1 or Hsp70 relative to β-actin. The value of control cells was set to 1 for each cell line.
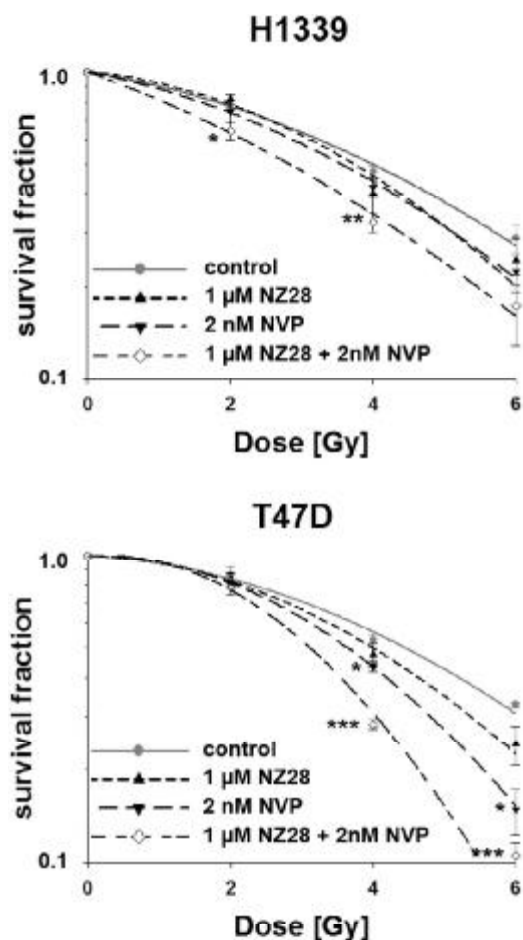
Fig. 6. Treatment with low concentrations of NZ28 and NVP-AUY922 potentiates radiosensitivity of tumor cells. One day after seeding H1339 and T47D cells were treated with 1 μM NZ28 and 2 nM NVP-AUY922 (NVP). 24 h after treatment cells were irradiated and immediately after irradiation fresh medium without NZ28/NVP-AUY922 was added. DMSO (0.01%) treated cells served as control. Colonies were fixed either 9 (H1339) or 16 (T47D) days after seeding. The survival fractions were calculated after normalization for cell kill by NZ28 and/or NVP-AUY922. Data are expressed as mean ± SEM of at least 3 independent experiments (*p ≤ 0.05, **p ≤ 0.01, ***p ≤ 0.001).

significantly enhanced the radiosensitivity with SER values of 1.41 and 1.43 for H1339 and T47D cells, respectively (Fig. 6 and Table 1). The radiosensitization which was achieved by a combined treatment with low concentrations of NZ28 and NVP-AUY922 was comparable to that of a single treatment with NZ28 at 10–20-fold higher concentrations (Fig. 3B, Table 1).

Discussion

Hsp70 is abundantly overexpressed in a variety of human tumor cells and high Hsp70 levels are associated with poor clinical outcome since Hsp70 promotes tumor cell survival and contributes to radioresistance [10,12]. The group of M. Sherman demonstrated that the small molecule inhibitor NZ28 reduces both the stress-induced and basal Hsp70 expression levels in HER2-positive cancer cell lines [13,14]. In line with their data we show that NZ28 down-regulated basal and NVP-AUY922-induced Hsp70 expression in different lung and breast cancer cell lines. Moreover, we could show that NZ28 reduces the phosphorylation of HSF1 at serine 326 and thus inhibits HSF1 transcriptional activity as measured by a luciferase reporter

assay. Concomitantly the Hsp70 mRNA levels were found to be reduced under non-stressed conditions. This suggests that NZ28 down-regulates Hsp70 expression via inhibition of HSF1. Zaarur et al. showed that NZ28 does not alter heat-induced Hsp70 mRNA levels and a weak inhibition of the HSF1 transcriptional activity [14]. Therefore, they propose a post-transcriptional reduction of the stress-induced Hsp70 expression by NZ28. This discrepancy might be explained by the fact that the HSF1 activation and Hsp70 expression is regulated differently by NZ28 under stressed and non-stressed conditions or by the use of different tumor cell lines, incubation times and NZ28 concentrations.

Previous studies demonstrated that knocking-down Hsp70 or HSF1 reduces the invasiveness of tumor cells [3,4,11]. Consistent with these findings, we could show that NZ28 decreases migration and invasion of different human tumor cell lines. Silencing HSF1 or Hsp70 by siRNA is assumed to increase the radiosensitivity of human tumor cell lines [9–12]. However, only few inhibitors targeting HSF1 and/or Hsp70 have been tested with respect to their radiosensitizing capacity and the published data have been controversially discussed. As an example, the small molecule Hsp70 inhibitor VER-155008 has been shown to increase the radiosensitivity of A549 lung cancer cells [27], whereas the HSF1 inhibitor KNK437 exerted an opposite effect in glioblastoma cells [28]. We could demonstrate that NZ28 increases the radiation response of different human lung and breast cancer cells. One possible mechanism might be a decrease of the radioresistant S-phase. In line with our data, the Hsp70 inhibitors, VER–155008 and pifithrin–μ have been found to exert identical effects on the cell cycle distribution [27,29,30].

Hsp90 inhibition is a promising strategy in cancer therapy. However, clinically applied Hsp90 inhibitors induce the synthesis of the cytoprotective chaperone Hsp70 by activation of HSF1. Therefore, it was not astonishing to find that inhibition of HSF1 and/or Hsp70 can sensitize tumor cells toward Hsp90 inhibitors [14,17–19,31–34]. In contrast, knowledge on the effects of HSF1/Hsp70 and Hsp90 inhibition on radiation therapy is limited [35]. Here, we could show that a combined treatment of tumor cells with low, non-toxic concentrations of NZ28 and NVP-AUY922 potentiates the radiosensitization of different tumor cells.

We have demonstrated that NZ28 reduces HSF1 activation and expression of cytoprotective Hsp70, inhibits migration and invasion, decreases the percentage of tumor cells in the radioresistant S-phase and increases their radiosensitivity. In combination with NVP-AUY922, 1/10th–1/20th of the concentration of NZ28 was sufficient to achieve a significant radiosensitization compared to the treatment with a single drug. Therefore, we assume that a simultaneous inhibition of Hsp90 and HSF1/Hsp70 combined with radiotherapy might provide a promising anti-cancer strategy.

Acknowledgments

Conflict of interest

The authors state no conflict of interest.

Appendix: Supplementary material

Supplementary data to this article can be found online at doi:10.1016/j.canlet.2015.02.033.

References

[1] D.R. Ciocca, A.P. Arrigo, S.K. Calderwood, Heat shock proteins and heat shock factor 1 in carcinogenesis and tumor development: an update, Arch. Toxicol. 87 (2013) 19–48.

[2] L.K. Boroughs, M.A. Antonyak, J.L. Johnson, R.A. Cerione, A unique role for heat shock protein 70 and its binding partner tissue transglutaminase in cancer cell migration, J. Biol. Chem. 286 (2011) 37094–37107.

[3] F. Fang, R. Chang, L. Yang, Heat shock factor 1 promotes invasion and metastasis of hepatocellular carcinoma in vitro and in vivo, Cancer 118 (2012) 1782–1794.

[4] Y. Nakamura, M. Fujimoto, S. Fukushima, A. Nakamura, N. Hayashida, R. Takii, et al., Heat shock factor 1 is required for migration and invasion of human melanoma in vitro and in vivo, Cancer Lett. 354 (2014) 329–335.

[5] C. O'Callaghan-Sunol, M.Y. Sherman, Heat shock transcription factor (HSF1) plays a critical role in cell migration via maintaining MAP kinase signaling, Cell Cycle 5 (2006) 1431–1437.

[6] Y. Teng, L. Ngoka, Y. Mei, L. Lesoon, J.K. Cowell, HSP90 and HSP70 proteins are essential for stabilization and activation of WASF3 metastasis-promoting protein, J. Biol. Chem. 287 (2012) 10051–10059.

[7] K. Juhasz, A.M. Lipp, B. Nimmervoll, A. Sonnleitner, J. Hesse, T. Haselgruebler, et al., The complex function of hsp70 in metastatic cancer, Cancers (Basel) 6 (2013) 42–66.

[8] S. Santagata, R. Hu, N. Lin, M. Mendillo, L. Collins, S. Hankinson, et al., High levels of nuclear heat-shock factor 1 (HSF1) are associated with poor prognosis in breast cancer, Proc. Natl. Acad. Sci. U.S.A. 108 (2011) 18378–18383.

[9] E.K. Alexander, V.M. Yana, S.L. David, Hsf1-mediated stress response can transiently enhance cellular radioresistance, Radiat. Res. 165 (2006) 410–423.

[10] R. Bases, Clonogenicity of human leukemic cells protected from cell-lethal agents by heat shock protein 70, Cell Stress Chaperones 10 (2005) 37–45.

[11] X.L. Du, T. Jiang, Z.Q. Wen, R. Gao, M. Cui, F. Wang, Silencing of heat shock protein 70 expression enhances radiotherapy efficacy and inhibits cell invasion in endometrial cancer cell line, Croat. Med. J. 50 (2009) 143–150.

[12] V.L. Gabai, K.R. Budagova, M.Y. Sherman, Increased expression of the major heat shock protein Hsp72 in human prostate carcinoma cells is dispensable for their viability but confers resistance to a variety of anticancer agents, Oncogene 24 (2005) 3328–3338.

[13] L. Meng, V. Gabai, M. Sherman, Heat-shock transcription factor HSF1 has a critical role in human epidermal growth factor receptor-2-induced cellular transformation and tumorigenesis, Oncogene 29 (2010) 5204–5213.

[14] N. Zaarur, V.L. Gabai, J.A. Porco Jr., S. Calderwood, M.Y. Sherman, Targeting heat shock response to sensitize cancer cells to proteasome and Hsp90 inhibitors, Cancer Res. 66 (2006) 1783–1791.

[15] D. Schilling, C. Bayer, W. Li, M. Molls, P. Vaupel, G. Multhoff, Radiosensitization of normoxic and hypoxic H1339 lung tumor cells by heat shock protein 90 inhibition is independent of hypoxia inducible factor-1α, PLoS ONE 7 (2012) e31110.

[16] S. Zaidi, M. McLaughlin, S.A. Bhide, S.A. Eccles, P. Workman, C.M. Nutting, et al., The HSP90 inhibitor NVP-AUY922 radiosensitizes by abrogation of homologous recombination resulting in mitotic entry with unresolved DNA damage, PLoS ONE 7 (2012) e35436.

[17] Y. Chen, J. Chen, A. Loo, S. Jaeger, L. Bagdasarian, J. Yu, et al., Targeting HSF1 sensitizes cancer cells to HSP90 inhibition, Oncotarget 4 (2013) 816–829.

[18] A.J. Massey, D.S. Williamson, H. Browne, J.B. Murray, P. Dokurno, T. Shaw, et al., A novel, small molecule inhibitor of Hsc70/Hsp70 potentiates Hsp90 inhibitor induced apoptosis in HCT116 colon carcinoma cells, Cancer Chemother. Pharmacol. 66 (2010) 535–545.

[19] M.V. Powers, P.A. Clarke, P. Workman, Dual targeting of HSC70 and HSP72 inhibits HSP90 function and induces tumor-specific apoptosis, Cancer Cell 14 (2008) 250–262.

[20] B. Samarasinghe, C. Wales, F. Taylor, A. Jacobs, Heat shock factor 1 confers resistance to Hsp90 inhibitors through p62/SQSTM1 expression and promotion of autophagic flux, Biochem. Pharmacol. 87 (2014) 445–455.

[21] S. Stangl, M. Gehrmann, J. Riegger, K. Kuhs, I. Riederer, W. Sievert, et al., Targeting membrane heat-shock protein 70 (Hsp70) on tumors by cmHsp70.1 antibody, Proc. Natl. Acad. Sci. U.S.A. 108 (2011) 733–738.

[22] J. Wiskirchen, E.F. Groenewaeller, R. Kehlbach, F. Heinzelmann, M. Wittau, H.P. Rodemann, et al., Long-term effects of repetitive exposure to a static magnetic field (1.5 T) on proliferation of human fetal lung fibroblasts, Magn. Reson. Med. 41 (1999) 464–468.

[23] D. Schilling, C. Bayer, A. Geurts-Moespot, F.C. Sweep, M. Pruschy, K. Mengele, et al., Induction of plasminogen activator inhibitor type-1 (PAI-1) by hypoxia and irradiation in human head and neck carcinoma cell lines, BMC Cancer 7 (2007) 143.

[24] D. Schilling, M. Duwel, M. Molls, G. Multhoff, Radiosensitization of wildtype p53 cancer cells by the MDM2-inhibitor PXN727 is associated with altered heat shock protein 70 (Hsp70) levels, Cell Stress Chaperones 18 (2013) 183–191.

[25] D. Schilling, A. Kühnel, F. Tetzlaff, S. Konrad, G. Multhoff, NZ28-induced inhibition of HSF1, SP1 and NF-kB triggers the loss of the NK cell activating ligands MICA/B on tumor cells, Cancer Immunol. Immunother. (2015), published online 18 February 2015.

[26] L. Whitesell, S. Lindquist, Inhibiting the transcription factor HSF1 as an anticancer strategy, Expert Opin. Ther. Targets 13 (2009) 469–478.

[27] W. Wen, W. Liu, Y. Shao, L. Chen, VER-155008, a small molecule inhibitor of HSP70 with potent anti-cancer activity on lung cancer cell lines, Exp. Biol. Med. (Maywood) 239 (2014) 638–645.

[28] K. Ohnishi, S. Yokota, A. Takahashi, T. Ohnishi, Induction of radiation resistance by a heat shock protein inhibitor, KNK437, in human glioblastoma cells, Int. J. Radiat. Biol. 82 (2006) 569–575.

[29] H. Monma, N. Harashima, T. Inao, S. Okano, Y. Tajima, M. Harada, The HSP70 and autophagy inhibitor pifithrin-mu enhances the antitumor effects of TRAIL on human pancreatic cancer, Mol. Cancer Ther. 12 (2013) 341–351.

[30] K. Sekihara, N. Harashima, M. Tongu, Y. Tamaki, N. Uchida, T. Inomata, et al., Pifithrin-mu, an inhibitor of heat-shock protein 70, can increase the antitumor effects of hyperthermia against human prostate cancer cells, PLoS ONE 8 (2013) e78772.

[31] E.L. Davenport, A. Zeisig, L.I. Aronson, H.E. Moore, S. Hockley, D. Gonzalez, et al., Targeting heat shock protein 72 enhances Hsp90 inhibitor-induced apoptosis in myeloma, Leukemia 24 (2010) 1804–1807.

[32] F. Guo, K. Rocha, P. Bali, M. Pranpat, W. Fiskus, S. Boyapalle, et al., Abrogation of heat shock protein 70 induction as a strategy to increase antileukemia activity of heat shock protein 90 inhibitor 17-allylamino-demethoxy geldanamycin, Cancer Res. 65 (2005) 10536–10544.

[33] H. Reikvam, I. Nepstad, A. Sulen, B.T. Gjertsen, K.J. Hatfield, O. Bruserud, Increased antileukemic effects in human acute myeloid leukemia by combining HSP70 and HSP90 inhibitors, Expert Opin. Investig. Drugs 22 (2013) 551–563.

[34] E. Schmitt, L. Maingret, P.E. Puig, A.L. Rerole, F. Ghiringhelli, A. Hammann, et al., Heat shock protein 70 neutralization exerts potent antitumor effects in animal models of colon cancer and melanoma, Cancer Res. 66 (2006) 4191–4197.

[35] A.E. Kabakov, V.A. Kudryavtsev, V.L. Gabai, Hsp90 inhibitors as promising agents for radiotherapy, J. Mol. Med. 88 (2010) 241–247.